CONVERSION OF PALM OIL MILL WASTES TO USEFUL CHEMICALS OVER IRON OXIDE BASED CATALYSTS

RATANAPORN YUANGSAWAD

A THESIS SUBMITTED IN PARTIAL FULFILLMENT

OF THE REQUIRMENT FOR THE DEGREE OF

DOCTOR OF ENGINEERING IN CHEMICAL ENGINEERING

FACULTY OF ENGINEERING

KING MONGKUT'S INSTITUTE OF TECHNOLOGY LADKRABANG

2010

KMITL – 2010 – EN – D – 228 - 096

หัวข้อวิทยานิพนธ์	การเปลี่ยนของเสียโรงงานหีบน้ำมันปาล์มเป็นสารเคมีที่มีคุณค่าโดยใช้ตัวเร่งปฏิกิริยาเหล็กออกไซด์
นักศึกษา	รัตนาภร ยวงสวัสดิ์
รหัสประจำตัว	49061701
ปริญญา	วิศวกรรมศาสตรดุษฎีบัณฑิต
สาขา	วิชาวิศวกรรมเคมี
พ.ศ.	2553
อาจารย์ที่ปรึกษาวิทยานิพนธ์	รศ. ดร. ดวงกมล ณ ระนอง

บทคัดย่อ

งานวิจัยนี้ได้เสนอแนวทางใหม่ในการจัดการของเสียจากโรงงานหีบน้ำมันปาล์ม โดยใช้วิธีไพโรไลซิสและการปรับปรุงคุณภาพน้ำมันไพโรไลซิสด้วยตัวเร่งปฏิกิริยา เซอร์โคเนีย-เหล็กออกไซด์ ของเสียจากโรงงานหีบน้ำมันปาล์มแบ่งเป็นสองส่วน คือ ของเสียที่เป็นของแข็ง (กะลาปาล์ม เส้นใย และเนื้อในปาล์ม) และน้ำเสีย ของเสียที่เป็นของแข็งถูกนำมาไพโรไลซิสเพื่อผลิตน้ำมันชีวภาพ จากนั้นทำการปรับปรุงคุณภาพน้ำมันที่ได้ด้วยตัวเร่งปฏิกิริยา สำหรับน้ำเสียนำมาผ่านการกรองเพื่อแยกกากตะกอนและน้ำออกจากกันจากนั้นจึงนำกากตะกอนไปไพโรไลซิสเพื่อผลิตน้ำมันชีวภาพและปรับปรุงคุณภาพโดยทำปฏิกิริยากับน้ำที่ได้จากขั้นตอนการกรองน้ำเสีย

น้ำมันที่ได้จากการไพโรไลซิสกะลาปาล์มคิดเป็น 55 เปอร์เซ็นต์โดยน้ำหนักของกะลาปาล์ม ประกอบด้วย เมทานอล 5%C, กรดอะซีติก 22%C, อะซีโตน 0.6%C และ ฟีนอล 36%C หลังปรับปรุงคุณภาพที่อุณหภูมิ เท่ากับ 623 เคลวิน และอัตราส่วนน้ำหนักตัวเร่งปฏิกิริยาต่ออัตราการป้อนสารตั้งต้น เท่ากับ 6 ชั่วโมง สามารถนำกลับสารเคมี ได้แก่ เมทานอล กรดอะซีติก อะซีโตน และ ฟีนอล ในปริมาณ 6%C, 24%C, 3%C และ 36%C ตามลำดับ ส่วนน้ำมันชีวภาพที่ได้จากการไพโรไลซิสกากตะกอนน้ำเสียจะแยกเป็นสองชั้น คือ ชั้นน้ำและชั้นน้ำมัน คิดเป็น 30 และ 15 เปอร์เซ็นต์โดยน้ำหนักของสารตั้งต้น ตามลำดับ นำน้ำมันชีวภาพมาปรับปรุงคุณภาพโดยใช้ตัวเร่งปฏิกิริยาเซอร์โคเนีย-เหล็กออกไซด์ ที่ได้รับการพัฒนาโดยการเปลี่ยนชนิดเกลือที่ใช้เป็นสารตั้งต้นในการเตรียมตัวเร่งปฏิกิริยาจากเกลือคลอไรด์เป็นเกลือไนเตรต พบว่าสภาวะที่เหมาะสมในการทำปฏิกิริยาของชั้นน้ำ คือ อุณหภูมิเท่ากับ 593 เคลวิน และอัตราส่วนน้ำหนักตัวเร่งปฏิกิริยาต่ออัตราการป้อนสารตั้งต้น เท่ากับ 2 ชั่วโมง ผลิตภัณฑ์ที่ได้ คือ เมทานอล (7 %C) อะซีโตน (25 %C) และกรดอะซีติก (2.3%C) ในขณะที่สภาวะที่เหมาะสมในการทำปฏิกิริยาของชั้นน้ำมัน คือ อุณหภูมิเท่ากับ 593 เคลวิน และอัตราส่วนน้ำหนักตัวเร่งปฏิกิริยาต่ออัตราการป้อนสารตั้งต้น เท่ากับ 6 ชั่วโมง ผลิตภัณฑ์ที่ได้ คือ อะซีโตน (5 %C) ฟีนอล (12 %C) และเอ็ม-เครซอล (1.2 %C)

Thesis	Conversion of palm oil mill wastes to useful chemicals over iron oxide based catalysts
Student	Ms. Ratanaporn Yuangsawad
Student ID	49061701
Degree	Doctor of Engineering
Programme	Chemical Engineering
Year	2010
Thesis Advisor	Assoc. Prof. Dr. Duangkamol Na – Ranong

ABSTRACT

A new approach to utilize palm oil mill wastes which consists of pyrolysis and chemical upgrading over iron oxide catalysts was proposed. The palm oil mill wastes considered in this study were solid wastes (shell, fiber and kernel) and liquid wastewater. The solid waste was pyrolysed to produce bio-oil and the obtained bio-oil was upgraded over a zirconia supporting iron oxide catalyst. The liquid wastewater was filtrated to obtain solid cake and brown liquid. The obtained cake was dried and so called dried sludge. The dried sludge was pyrolysed to produce bio-oil and the bio-oil was upgraded by the reaction with the brown liquid over the iron oxide catalyst. Pyrolysis of the solid palm shell at 773 K yielded 55% of liquid oil consisting of methanol 5%C, acetic acid 22%C, acetone 0.6 %C and phenol 36%C as the main compositions. The highest yield of useful chemicals from catalytic upgrading over ZrO_2·Al·FeO_x was achieved at the temperature of 623 K and W/F of 6 h. Under this condition, a mixture of methanol 6%C, acetic acid 24%C, acetone 3%C and phenol 36%C was obtained. By changing the metal salts from chloride to nitrate in the preparation of ZrO_2·FeO_x, the activity on upgrading palm shell oil was improved. Pyrolysis of dried sludge at 773 K yielded liquid product which contains oil (15%wt) and aqueous phase (30%wt). ZrO_2·FeO_x was employed to upgrade each phase separately. Under the optimum condition to convert oil phase (T = 593 K, W/F = 6 h), a mixture of acetone 5%C, phenol 12%C and m-cresol 1.2 %C was obtained. Under the optimum condition to convert aqueous phase (T = 593 K, W/F = 2 h), a mixture of methanol 7%C, acetone 25%C and acetic acid 2.3 %C was obtained.

Acknowledgements

I sincerely thank Assoc. Prof. Dr Duangkamol Na-Ranong for her valuable suggestion and encouragement.

I would like to thank Prof. Dr Takao Masuda and Assoc. Prof. Dr. Teriuki Tago for giving the opportunity to do the partial experiment at Hokkaido University.

I would like to acknowledge Suksomboon Palm Oil Co., Ltd. for supplying the oil palm wastes. I also like to extend an appreciation to Ms. Anchana Kampilo for her help and guidance in connection with the manager of palm oil mill.

I wish to thank the officers of chemical engineering department, Mr. Pisan Polpoh and Mrs. Pimjai Phuuchanakij for their support.

Finally, I really want to thank from my heart to my parent for their morale and all support.

Ratanaporn Yuangsawad

Table of Contents

Page

Table of Contents (cont.)

Table of Contents (cont.)

Page

Table of Contents (cont.)

List of Tables

List of Tables

Table Page

List of Figures

Figure Page

List of Figures (cont.)

Figure Page

Nomenclatures

A	pre-exponential factor (s^{-1})
E	Activation energy (kJ/mol)
F	flow rate of reactant (g/h)
f_i	weight fraction of species i (-)
k_i	reaction rate constant of step i (s^{-1})
n	order of reaction (-)
R	gas constant (kJ/mol K)
T	temperature (K)
W	weight of catalyst or actual weight of sample in section 5.1 (g)
W_0	initial weight of sample (g)
W_∞	final weight of sample (g)

Greek letters

β	heating rate (K/min)
α	$(W_0 - W)/(W_0 - W_\infty)$

Subscript

hem	hemicellulose
cel	cellulose
oil	bio-oil

Chapter 1

Introduction

1.1 Motivation

A significant reduction in the petroleum source has taken place during the past decade due to the rapidly population growth and the expansion of industries. Therefore, the effort to develop alternative and renewable energy is in progress in a number of countries. Biodiesel which is a renewable and environmental-friendly is one of promising fuel energies. Several oily plants such as rapeseed, soy bean, palm oil can be used to produce the biodiesel. Among these plants, palm oil is the most important agricultural product and widely used as a feed stock for biodiesel production in South East Asian countries. Thailand produced crude palm oil (CPO) 1.1 million tones per year and trend has been growing up. During palm oil production, a large amount of wastes are produced. These wastes include solid wastes (empty fruit bunches : EFB, shell, fiber and kernel) and wastewater. Although some solid wastes are used as the fertilizer or burn for boiler but a lot of palm oil wastes still remain and cause the environmental problems.

Beside the solid wastes, every 1 ton of crude palm oil produce 2.5 - 4 tones of wastewater and are discharged from the process. Wastewater from palm oil mill is a brown liquid, high suspended solid and high level of COD and BOD. Therefore, the direct discharge this wastewater into the environmental without being treated is not allowed.

The main components of wastes from palm oil mill are high molecular weight compound. Lignocellulosic compound (hemicellulose, cellulose and lignin) is the main composition of the solid wastes. Wastewater consists of carbohydrate, fat and protein which are the long chain hydrocarbon as well.

Pyrolysis is the most promising technology to utilize the high molecular weight hydrocarbon, which converts this component to the lower molecules called pyrolysis oil or bio oil. The obtained pyrolysis oil is of interest due to the composing of various useful chemicals, therefore, the recovery of these chemicals from the pyrolysis oil to utilize alternative chemicals feedstock is desirable.

The upgrading of pyrolysis oil has been studied over wide range catalysts such as zeolites, supported noble metal or metal oxide catalyst. The high yield of useful chemical and less undesirable compounds were obtained. However, these catalysts seem not promising due to the high cost and poor physical properties. The advantage catalyst chosen to upgrade the pyrolysis oil should have high activity, stability and resist to the water and extreme condition.

In this work, the feasibility of the combined chemical process (pyrolysis and catalytic cracking) to utilize the wastes from palm oil mill was investigated. In the pyrolysis process, the thermal characteristic of biomass was determined. The effects of operating conditions on the efficiency of process and the optimum condition for upgrading of pyrolysis oil were studied. The catalyst which has high potential for upgrading of pyrolysis oil was improved and focused on the effect of deactivation – regeneration on the stability and activity of catalyst.

1.2 Objectives

1.2.1 To investigate the decomposition of the palm oil solid wastes in nitrogen atmosphere and estimate kinetic parameters.

1.2.2 To improve and modify the catalyst for upgrading of pyrolysis oil.

1.2.3 To determine the optimum condition for recovery useful chemicals from pyrolysis oil over the zirconia supporting iron oxide catalyst.

1.2.4 To propose the reaction pathway with its kinetic parameters of pyrolysis oil over the zirconia supporting iron oxide catalyst

1.2.5 To obtain an alternative method which enables to utilize the wastes from palm oil mill.

1.3 Hypothesis

The thermal degradation process such as pyrolysis can be used to convert the wastes from palm oil mill to liquid which consist of many useful chemical compounds. The obtained pyrolysis liquid is considered as the chemical sources and these chemicals are recovered by the catalytic upgrading. The utilization of wastes from palm oil mill as the chemical production is an alternative method to handle a large amount of wastes produced during the palm oil production.

1.4 Scopes of the study

1.3.1 Study the background theories and review the involved literatures.

1.3.2 Determine the thermal degradation of palm oil solid wastes under the different operation conditions using Thermogravimetric Analysis (TGA).

1.3.3 Pyrolyse the palm oil mill wastes in order to produce the pyrolysis oil and analyze its composition.

1.3.4 Synthesize the zirconia supporting iron oxide as the catalyst for upgrading pyrolysis oil.

1.3.5 Test the reaction of pyrolysis oil over the zirconia supporting iron oxide catalyst under the different conditions.

1.3.6 Study the reaction of model compound in order to obtain the data to propose the reaction pathway.

1.3.7 Study the deactivation/regeneration of zirconia supporting iron oxide catalyst and investigate the suitable condition for regeneration the used catalyst.

Chapter 2

Theory

2.1 Palm oil production

Oil palm is a tropical palm tree, it can be cultivated in the South East Asian countries such as Malaysia, Indonesia and Thailand, almost 80% of the world's palm oil is produced from these countries as shown in Table 2.1. The oil palm (*Elaeis guineensis*) is single-stemmed, mature palm tree up to 20 m tall (see Figure 2.1). The palm oil fruit comprises an oily, fleshy outer layer with a single seed, rich in oil.

Table 2.1 Statistics for palm oil production [1]

Production (1000T)	2008	2007	2006	2005	2004
World	42711	38510	37122	33519	30892
Indonesia	19000	17100	16050	13800	12350
Malaysia	17350	15823	15881	14960	13970
Thailand	1123	1020	860	685	668
Nigeria	850	830	815	800	790
Columbia	832	738	713	655	6632

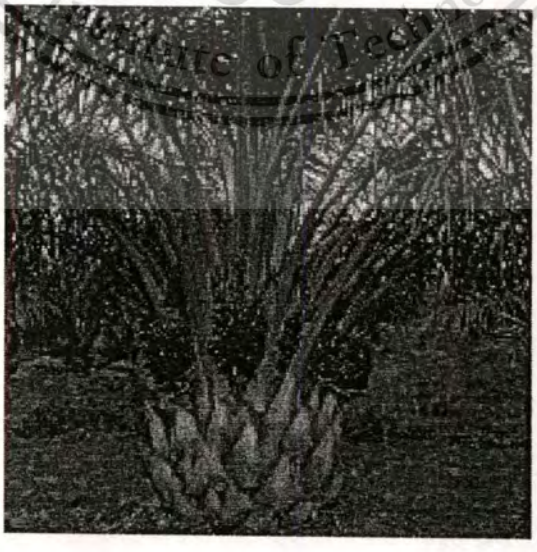

Figure 2.1 Palm oil tree

2.1.1 Process for palm oil production [2]

The palm oil fruit consists of a seed inside a shell, which is surrounded by a mesocarp as shown in Figure 2.2. Oil is extracted from the pulp and the kernel. Figure 2.3 shows the overall process for palm oil production and the key steps for palm oil production used in the standard palm oil mill are described below;

1. Sterilization

The fresh fruit bunches (FFB) of palm oil are transferred to the mill after harvesting. The FFB is sterilized in the autoclave with the capacity 20 – 30 tons depend on the size of the mill. The sterilization is usually operated under the following conditions;

Temperature	393 - 403 K	
Pressure	2	bar
Total sterilizing time per batch	2	h (approximately)
Retention time	45 – 60	min
Total steam consumption	200	kg/t FFB
Steam loss into air	75	kg/t FFB
Liquid residue	150	kg/t FFB (approximately)
Initial oil content	180	kg/t FFB (approximately)
Loss of oil	0.5	kg/t FFB (approximately)

2. Bunch stripping

The palm fruit after sterilizing is loosen from the FFB and easily to separate. The retained empty fruit bunches (EFB) are stored for further incineration to reduce the mass of residue and also used as the fertilizer. The residues produced from this step compose of ;

EFB (solid residues)	200 – 230	kg/t FFB
Moisture content	150	kg/t FFB
Oil loss	4.5	kg/t FFB
Moisture evaporation	30	kg/t FFB
Liquid residues	-	

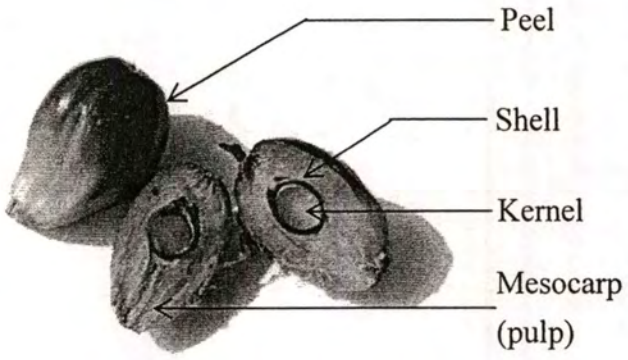

Figure 2.2 Longitudinal section of fresh palm oil fruit

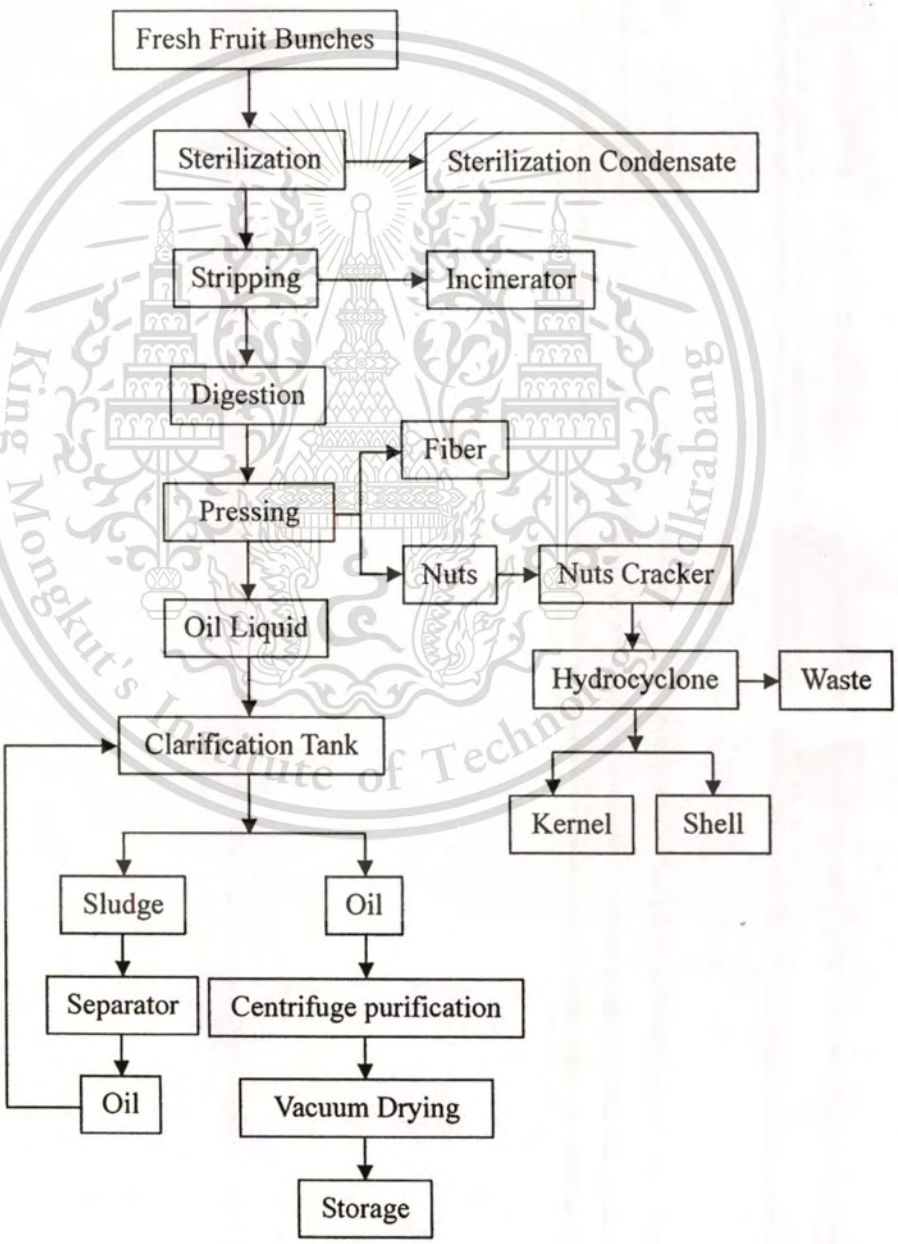

Figure 2.3 The flowchart for palm oil production

3. Digestion

Hot water is fed into the digester where the palm fruit are treated to convert into a homogeneous oily mesh by mechanical. Then, the digested fruit is fed to the extraction process. The energy consumed for this process is listed below;

Steam consumption	20	kg/t FFB
Hot water consumption	65	kg/t FFB
Moisture evaporation	30	kg/t FFB
Solid and liquid residue	-	

4. Oil extraction

The oil is extracted from palm fruit using a continuous screw press and then raw crude oil is obtained. This oil contains a high concentration of suspended matter contribute to the difficulties in the separation of oil - water and a high solid suspension in the wastewater discharged from the palm oil mill. The large amounts of solid wastes are also generated from this step. The cake remained after pressing is transported to a cyclone for recovery nut and fibers. These wastes are used as fuel for the boilers. Kernels which recovered from centrifugal cracker are used to produce fertilizers or feedstuff. The overall products and residues for this process consist of;

Raw crude oil	400	kg/t FFB
Oil content	170	kg/t FFB
Water content	200	kg/t FFB
Non-oil substances	30	kg/t FFB
Moisture evaporation	50	kg/t FFB
Solid residues		
Total	320	kg/t FFB
Kernels	60	kg/t FFB
Shells	60	kg/t FFB
Fibers	145	kg/t FFB
Moisture loss	55	kg/t FFB

5. Oil purification

5.1 Screening of raw crude oil

The crude oil passes through the vibrating screen in order to separate the solid residues. The residues after screening will be turned back to the oil extraction process for pressing again. Therefore, no residues are discharged from this step.

5.2 Separation of suspended solids from oil

The settling tank method is a conventional process to separate the suspended solid from oil. The oil will float to the top of a settling tank and then it is collected by a funnel system in order to transfer to the oil purification system. The product and residue generated from a settling are;

Hot water consumption	320	kg/t FFB
Raw crude oil	~95	kg/t FFB
Liquid watery residues	625	kg/t FFB
Process temperature	>368	K
Surface loading rate	0.5 to 2	m/hr
Retention time	1-5	hr

5.3 Oil drying and cooling

The water contained in purified crude oil is removed by a vacuum evaporation system then the dried crude oil will be obtained. The dried crude oil is stored in the tank and further to transfer to an oil refinery. The product and residues of drying step are;

Steam consumption	~10	kg/t FFB
Cooling water	300	kg/t FFB
Pure crude oil	163	kg/t FFB
Process temperature	368	K
Final oil temperature	313	K
Cooling water effluent	300	kg/t FFB
Cooling water temperature	353	K
Vapors from drying	10	kg/t FFB

6. Treatment of sludge from settling tank

The obtained sludge from the bottom of settling tank contained the 14%wt of oil which is a significant amount and should be recovered. The efficiency for oil separation can be enhanced by the addition of water into sludge. After centrifugation, 78 kg/t FFB of raw crude oil is recovered and less than 742 kg/t FFB of liquid residue is produced.

In the conclusion, the overall material balance of the palm oil production process is shown in Table 2.2.

Table 2.2 Material balance of standard palm oil production

medium	Type of material	individual mass kg/t FFB	individual oil content kg/t FFB	oil loss (%)
Solids	EFB	230	4.5	26
	Fiber	145	5	30
	shell	60	0	0
	kernel	60	0	0
Total		495	9.5	56
Liquids	Raw oil	163	0	0
	Washing/cooling water	150	0.5	3
	Sterilizer effluent under-flow of settling tank	742	7	41
Total		1055	7.5	44
Gas/vapor	Water vapor	250	0	0
Total		250	0	0
Summary total		1800		
Oil loss			17	100

2.2 Wastes from palm oil mill

In the palm oil planting and processing, a large amount of solid wastes such as palm trunks, palm shells, palm fronds, empty fruit bunch (EFB), fiber and kernel are generated. The amount of residue from a palm oil mill is categorized as follow:

Solid residues:

Empty fruit bunches	230	kg/t FFB
Fiber	145	kg/t FFB
Shell	60	kg/t FFB
Sludge cake	30	kg/t FFB

Liquid residues:

Wastewater	~900	kg/t FFB

Air emission from the oil palm mills are from the boilers and incinerators. The gases mainly contain the particulates such as tar and soot droplets of 20 -100 micrometers and a dust load of about 3000 – 4000 mg/Nm^3. Incomplete combustion of the boiler and incinerator produce dark smoke resulting from burning a mixture of solid waste fuels.

Utilization of solid residue

1. Palm oil solid wastes i.e. EFB and sludge cake can be used as the fertilizer in palm plant. However, the utilization is limited by Potassium (K) value.

2. Palm shell can be used as a fuel for boiler because it has high calorific value as compared with EFB or fiber. The calorific value of dried shell is around 17 MJ/kg. Therefore, it is also possible to use for production of activated carbon. On the other hand, the use of EFB as a fuel for boiler is not suitable because it has high moisture content and low heating value.

3. The incineration of solid wastes in order to reduce its volume and to recover ash for fertilizer has the great disadvantage of generating excessive air pollution because of incomplete incineration.

2.3 Waste water treatment

Effluent water is defined as water discharged from industry and contains soluble materials that are harmful to the environment. Palm oil mill effluent (POME) is the effluent from the final stages of palm oil production in the mill. POME includes various liquids, dirties, residual oil and suspended solids. In general, POME contains about 94 - 95% of water, 1 - 2 % of oil and 3 – 4% of solid [3]. Table 2.3 shows the characteristics of POME from several sources.

Table 2.3 Characteristics of POME

Parameters	Concentration (mg/l)			
	Ahmad et al. [4]	Najafpour et al. [5]	Paepatung et al. [6]	Standard limit [2]
pH	4.7	3.8-4.4	4.64	5 - 9
Oil and grease	4,000	4,900-5,700	5,010	<25
BOD_5	25,000	23,000-26,000	29,172	<100
COD	50,000	42,500-55,700	62,035	<1000
Total solids	40,500	n/a	65,674	-
Suspended solids	18,000	16,500-19,500	23,179	<150
Total nitrogen	750	500-700	1,124	<50

The direct discharge of POME into the environment is not allowed because of the high values of COD and BOD as show in Table 2.3. Therefore, the pretreatment method is necessary. There are widely known methods of treating palm oil effluent, include the following;

2.3.1 Anaerobic digestion [7]

Anaerobic digestion is the degradation of organic materials in the absence of oxygen. This process is time consuming as bacterial consortia responsible for the degradation process requires time to adapt to the new environment before they start to consume on organic materials to grow.

Methane, carbon dioxide and water are generated from the process due to some

reactions such as hydrolysis, acidogenesis and methanogenesis. Hydrolysis is the process which the high molecular weight materials such as carbohydrates, lipids, proteins are converted to the lower molecule e.g. sugar and amino acid. Acidogenesis is a biological step which the low molecular weight compound will be broken by acidogenic bacteria and produce organic mainly acetic acid, hydrogen and carbon dioxide. For methanogenesis step, hydrogen is consumed and acetates are converted to methane and carbon dioxide simultaneously.

Type of anaerobic treatment methods [3,5,7-10]

1. Conventional treatment system

Ponding system is the most used in palm oil mills. More than 85% if the mills use this method to treat the effluent. The system consists of de-oiling tank, acidification pond, anaerobic ponds and facultative or aerobic pond which are necessary for reduction the BOD value. Number of used pond depends on the capacity of such palm oil mills. Among of the pond in this system, anaerobic pond requires the longest retention time (around 20-200 days).

2. Anaerobic filtration

Anaerobic filtration is used to treat wastewater because it has a lot of strong point such as

I) requires a smaller reactor volume which operates on a shorter hydraulic retention times
II) high substrate removal efficiency
III) has ability to maintain high concentration of biomass in contact with the wastewater without affecting treatment efficiency
IV) tolerance to shock loadings

However, filtration is involved in this process hence the filter clogging is a major problem for continuous operation.

3. Fluidized bed reactor

Fluidized bed reactor is a better method of treating palm oil mill effluent as compared to the anaerobic filtration because it has high surface area for attachment with biomass. Furthermore, it has high ability to tolerate higher OLR, shorter HRT (6 h) and higher methane production. The fluidized bed reactor can be operated without the problem of channeling, plugging or gas hold-up. In order to maintain the fluidized bed, the higher up-flow velocity of

raw palm oil mill effluent is fed through the reactor then the biomass will attach and grow on the support material. The efficiency of the treatment system strongly depends on the type of support material. The previous research showed that the COD could be removed by 94.4% when ovoid saponite was used as support material while about 60% COD removal was obtained using granular activated carbon (GAC).

4. Up-Flow anaerobic blanket (USAB) reactor

The USAB system was developed to treat wastewater in various industries such as pharmaceutical, instant coffee, sugar beet etc. In the USAB system, sludge from organic matter degradation and biomass settles in the reactor. Organic matter from wastewater which contact with sludge will be digested by the biomass granules. USAB has been used successfully for POME treatment and the COD removal efficiency up to 98% is achieved. However, this system requires the long start up time if seeded sludge is not granulated.

5. Up-Flow anaerobic sludge fixed-film (UASFF) reactor

The Up flow anaerobic sludge fixed film (UASF) is an anaerobic hybrid reactor. It is a combination of up flow anaerobic sludge blanket (UASB) and up flow fixed film reactor (UFF). Generally, a fixed film reactor consists of a solid surface where the substrate and oxygen transfer. The UASB portion located at the lower part where flocculants and granular sludge are treated. The upper part is UFF portion which is to separate bio gas and wash out solids from the liquid phase. The UASFF reactor is able to reduce the COD value in a short time.

6. Continuous stirred tank reactor (CSTR)

For the CSTR, the mechanical agitator provides more area of contact with the sludge then the gas production is improved. The application of CSTR in palm oil mill has COD removal efficiency of approximately 83-97% depended on the operating condition. Furthermore, the treatment POME by CSTR can generate bio gas up to 62.5% efficiency.

7. Anaerobic contact digestion

Contact process involves a digester and a sedimentation tank. The sludge from digester effluent settle in this sedimentation tank and the effluent is recycled back into the digester. The wastewater with high concentration is suitable to be treated by anaerobic contact

digestion because the high quality effluent can be achieved. This system has high ability to remove COD by 80% efficiency.

The list of the advantages and disadvantages of various anaerobic treatment methods shows in Table 2.4.

2.3.2 Aerobic digestion [3,8]

Aerobic digestion is one of methods of treating the organic sludge. As the supply of available substrate food is depleted, the bacteria begin to consume their own protoplasm to obtain energy for cell maintenance reactions. Aerobic digesters can be used to treat

(1) only waste-activated or trickling-filter sludge

(2) mixtures of waste-activated or trickling-filter sludge and primary sludge

(3) waste sludge from activated-sludge treatment plants designed without primary settling

The conventional and pure oxygen are the type of aerobic digestion which commonly used. In the conventional aerobic digestion, the sludge is aerated for an extended period of time in an open, unheated tank using conventional air diffusers or surface aeration equipment. The process can operate in both of batch and continuous mode. In batch systems, the sludge is aerated and completely mixed for an extended period of time follow by inactive settling and decantation for smaller plants. In continuous systems, the tanks for decantation and concentration are separated. The important factor which should be considered in designing conventional aerobic digestion system is the temperature. Due to the open tank system of aerobic digester, the liquid temperatures are depended on the surrounding temperature which extensively fluctuates. Beside the temperature, solid reduction, tank volume (hydraulic retention time), oxygen requirements, energy requirements for mixing and process operation also affect on the efficiency of aerobic digester.

Pure oxygen aerobic digestion is a modification of the aerobic digestion process in which high-purity oxygen is used instead of air. The obtained sludge is similar to that from conventional aerobically digestion. Beside the conventional and pure oxygen digestions, the thermophilic aerobic digestion has also been used. The thermophilic bacteria are carried out at temperature ranging from 298 to 323 K above the ambient air temperature. This process can achieve high removals of the biodegradable fraction by 80% at very short retention times (3 – 4 days).

The advantages of aerobic digestion when compared to the anaerobic digestion are as

follows: (1) volatile solids reduction is approximately equal to that obtained anaerobically (2) lower BOD concentration in supernatant liquid (3) production of an odorless, humus-like, biologically stable end product (4) recovery the more of basic fertilizer values in the sludge (5) operation is relatively easy (6) lower capital cost. However, this method presents the several disadvantages such as (1) a high power cost is associated with supplying the required oxygen (2) a digested sludge is produced with poor mechanical dewatering characteristics (3) the process is affected significantly by temperature, location and type of tank material (4) methane which is a useful by-product can not be recovered.

2.3.3 Membrane Technology [4,11]

Membrane separation technology has been used to handle the palm oil mill effluent in recent years. Membrane can be used to separate the suspended solid, inorganic or organic compounds from waste water. This technology has several advantage such as requires low energy because of the separation involves in liquid phase and no vaporization or phase transformation is required, its wide applicability across a wide range of industries, the quality of the treated water is more uniform, it can be used in-process to allow recycling of selected waste stream within a plant and the plant can be highly automated. However, the efficiency of membrane is limited by the fouling and degradation. Therefore, the system is specifically designed in order to apply this method.

The comparison of the method for wastewater treatment was shown in Table 2.5.

Table 2.4 Advantages and disadvantages of various anaerobic treatment methods [12]

Method	Advantage	Disadvantage
Conventional anaerobic digestion	- Low cost - Low operating and maintenance cost - Recovery sludge cake can be used as fertilizer	- Requires large volume - Requires long retention time - No facilities to capture biogas - Lower methane emission
Anaerobic filtration	- Small reactor volume - Producing high quality effluent - Short hydraulic retention times - Able to shock loading - High concentration of biomass retain	- Clogging at high OLRs - High media and support cost - Unsuitable for high suspended solid wastewater
Fluidized bed	- Most compact of all high-rate process - Very well mixed conditions in the rector - Large surface area for biomass attachment - No channeling, plugging or gas hold-up	- High power requirements - High cost of carrier media - Unsuitable for high suspended solid wastewater - Normally does not capture generated biogas

Table 2.4 (cont.) Advantages and disadvantages of various anaerobic treatment methods

Method	Advantage	Disadvantage
UASB	- Faster start-up - Suitable for treatment of high suspended solid wastewater - Producing high quality effluent - Less cost - High concentration of biomass retain - High methane production	- Performance depend on sludge settleability - Foaming and sludge floatation at high OLRs - Long start up period - Granulation inhibition at high volatile fatty acid concentration
UASFF	- Higher OLR achievable - No clogging - Higher biomass retention - More stable operation - Ability to tolerate shock loadings - Suitable for diluted wastewater	- Lower OLR when treating suspended solid wastewaters
CSTR	- Provides more contact of wastewater with biomass through mixing - Increased gas production	- Less efficient gas production at high treatment volume - Less biomass retention
Anaerobic contact process	- Reaches steady state quickly - Short hydraulic retention time - Produces relatively high effluent quality	- Less stable due to oxygen transfer in digesting tank - Settle ability of biomass is critical to successful performance

Table 2.5 The comparison of the method for wastewater treatment

Method	Advantage	Disadvantage
Anaerobic	- Low energy requirements - Producing methane gas as a valuable product - Digested sludge could be used for land applications	- Long retention time - Slow start-up - Large area required for conventional digests
Aerobic	- Short retention - High efficiency to handle the toxic wastes	- High energy requirement - Unsuitable for land application because the rate of pathogen inactive is lower in aerobic sludge
Membrane	- Produce consistent and good water quality - Use a smaller space - Disinfect treated water is obtained	- Short membrane life - Membrane fouling - Expensive

2.4 Biomass

The chemical compositions of biomass are cellulose, hemicellulose, lignin, organic extractives and inorganic minerals. The amount of each constituent is varied in different type of biomass. The typical lignocellulose contents of some biomass are given in Table 2.6.

Table 2.6 Typical lignocellulose content of several type of biomass

Biomass	Lignocellulose content (%)		
	Hemicellulose	Cellulose	Lignin
Rice hull [13]	13	38	16
Peanut hull [14]	7.5	45.5	7.7
Palm shell [15]	45.42	21.74	17.64
Oil palm empty fruit bunches [16]	33.5	44.2	20.4
Sugar cane [17]	26 - 50	30 - 50	20 - 24

The pyrolysis products of biomass are a complex combination of the product from the degradation of cellulose, hemicellulose and lignin which has its individual kinetic characterization as will be described in next chapter.

2.4.1 Major components of biomass [18]

1. Cellulose

Cellulose is a linear polymer of β-(1→4)-D-glucopyranose units in the $^4C_1$ conformation with high molecular weight (more than 10^6) as shown in Figure 2.4. Gluxose anhydride is polymerized into long cellulose chains which contain 5000 – 10000 glucose units. Cellusose is insoluble material and consists of 2000 – 14000 of residues. Furthermore, it has crystalline structure that resists thermal decomposition better than hemicelluloses. The degradation of cellulose takes place around 513 – 623 K to produce anhydrocellulose and levoglucosan.

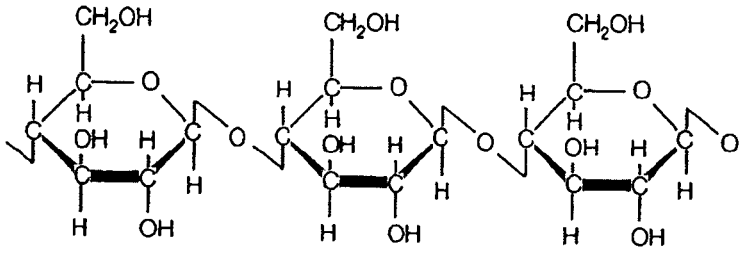

Figure 2.4 Chemical structure of cellulose

2. Hemicellulose

Hemicellulose or polyose is a second major chemical constituent of biomass. Hemicellulose is a mixture of various polymerized monosaccharides such as glucose, mannose, galactose, xylose, arabinose, 4-O-methyl glucuronic acid and galacturonic acid residues. The chemical structure of hemicellulose shows in Figure 2.5. Hemicellulose has a molecular weight about 5000 -1000 g/mol, which is lower than cellulose. Hemicellulose decomposes at temperature of 473 – 533 K. The products from hemicellulose decomposition are more volatiles, less tars and less chars than cellulose. Acetic acid which liberated from the pyrolysis of biomass is attributed to deactylation of the hemicellulse.

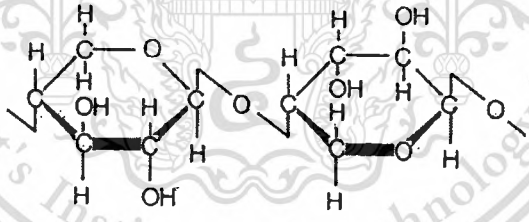

Figure 2.5 Chemical structure of hemicellulose

3. Lignin

Lignin is a high branch and polyphenolic substance. It is an amorphous cross-linked resin with no exact structure as shown in Figure 2.6. In general, softwood contains 23% - 33% of lignin which is mainly Guaiacyl and hardwood contains 16% - 25% of lignin which is mainly Guaiacyl-syringyl lignin. Lignin decomposes at the temperature of 553 – 773 K. Phenol is the main product from the pyrolysis of lignin. The formation of phenol is due to the cleavage of ether and carbon - carbon linkage.

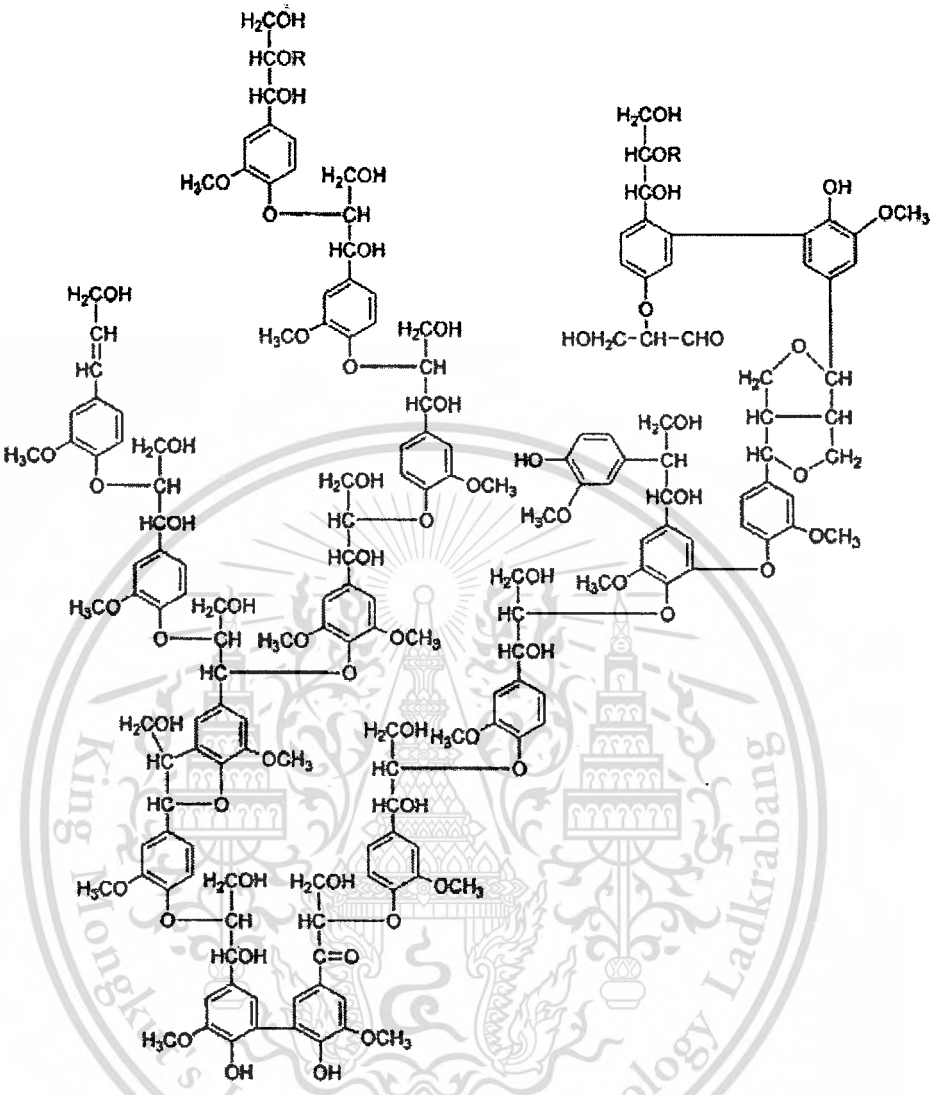

Figure 2.6 Chemical structure of lignin

2.5 Pyrolysis [18]

Pyrolysis can be described as the direct thermal decomposition of the organic material in the absence of oxygen resulting in solid, liquid and gas products. The pyrolysis method has been used for commercial production of fuels, solvent, chemicals and other products from biomass feedstocks.

2.5.1 Types of pyrolysis [18 – 20]

The type of pyrolysis may be categorized by the heating rate or residence. The two main types of pyrolysis are slow and fast pyrolysis as described below;

1. Slow pyrolysis

Slow pyrolysis or conventional pyrolysis, biomass is heated to ~773 K with the very low heating rate and the residence time of vapor is between 5 – 30 min. Because the vapor does not release from the reactor suddenly, components in the vapor phase continue to react with each other. Slow pyrolysis has ordinary been used for the production of charcoal.

2. Fast pyrolysis

Contrast to the slow pyrolysis, fast pyrolysis is characterized by high heating and rapid quenching of the liquid product to prevent the secondary reaction. Fast pyrolysis can be controlled to give a high yield of liquid product. The essential features of a fast pyrolysis process are:

- requires a finely ground biomass feed in order to achieve very high heating and heat transfer rates
- carefully controlled temperature of around 773 K
- rapid cooling of the pyrolysis vapors to give the bio-oil product

Fast pyrolysis process produce 60 – 75 wt% of liquid bio oil, 15 – 25 wt% of solid or char and 10 – 20 wt% of gases. However, the yield of product from pyrolysis strongly depended on the types of feedstock and operating condition and reactor configuration. One advantage of this process is that no waste is generated because the liquid and solid products can be used as a fuel and gas can be recycled back into the process.

In the addition, the other types of pyrolysis are developed by many researchers as listed in Table 2.7.

Table 2.7 Types of pyrolysis [18]

Pyrolysis technology	Residence time	Heating rate	Temperature(K)	products
Carbonization	days	Very low	673	charcoal
Slow	5-30 min	Low	873	oil, gas, char
Fast	0.5-5 s	Very high	923	bio oil
Flash-liquid	<1s	High	<923	bio oil
Flash-gas	<1s	High	<923	chemicals,gas
Ultra	<0.5s	Very high	1273	chemicals,gas
Vacuum	2-30 s	Medium	673	bio oil
Hydro-pyrolysis	<10 s	High	<773	bio oil
Methano-pyrolysis	<10 s	High	>973	chemicals

2.5.2 Pyrolysis Technology [19]

BTG-Biomass Technology Group B.V. Netherlands

The Biomass Technology group B.V has origin in the Chemical Engineering Department of the University of Twente. The several biomass energy technologies such as pyrolysis, carbonation, gasification and combustion are covered.

BTG's fast pyrolysis technology is based on intensive mixing of biomass particles and hot sand particles in a modified rotating cone reactor. A various types of biomass can be used as feedstock in this process. Prior to operation, the feedstock has to be ground in order to reduce the particle size to below 6 mm and its moisture content below 10 %wt.

The products from pyrolysis are up to 75 %wt of pyrolysis oil and only 25 %wt char and gas are produced. Since no "inert" carrier gas is used the pyrolysis prodo ucts are undiluted. The high yield of the oil product is achieved because the gas product is rapidly cooled. The solid residue or charcoal and sand are recycled to a combustor, where charcoal is burned treheat the sand. The permanent gases can be used as the fuel gas to generate electricity or simply flared off. Therefore, no external utilities are required for this process. The diagram of BTG Technology for biomass pyrolysis shows in Figure 2.7.

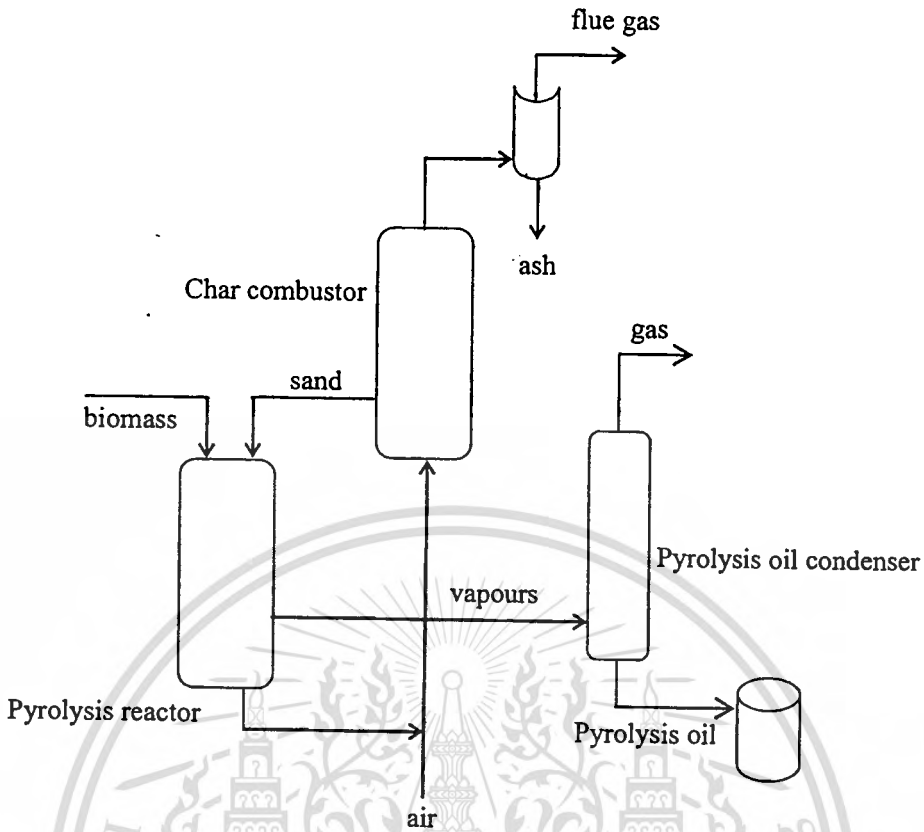

Figure 2.7 Diagram of BTG Technology for biomass pyrolysis [19]

National Renewable Energy Laboratory (NREL), USA

Figure 2.8 shows the configuration of the reactor system of NREL process. The reactor is installed vertically and a hot gas filter, where the char acts as a cracker there by reducing the tar in the gas, equipped after the char cyclone. Biomass which has the particle size around 5 mm is fed into the system and then enter the vortex reactor at speeds of up to 400 m/s in order to force to the reactor wall by high centrifugal forces.

The temperature at the reactor wall is limited at 898 K to ensure that production of a liquid film between the reactor wall and the biomass particle can vaporizes and leaves the reactor. The product is passed to the char cyclone and the char is removed. The cyclone diameter is 10 cm and the temperature is in the range of 748 - 773 K. The vapors pass to the heat exchanger equipped with a 38 cm diameter cyclone. The condensable vapor is condensed in the receiver.

The 67 %wt (including moisture on a dry basis) or 55 %wt (dry oil on dry feed basis) of oil yield and 13 %wt (on a dry feed basis) of char is obtained. The liquid product contained an

oxygenated compound, dark brown in colors and acidic with a pH range of 2 – 3. The phenol fraction has been successfully extracted and polymerized with formaldehyde to form resins. The analytical data when poplar is used as feedstock given in Table 2.8

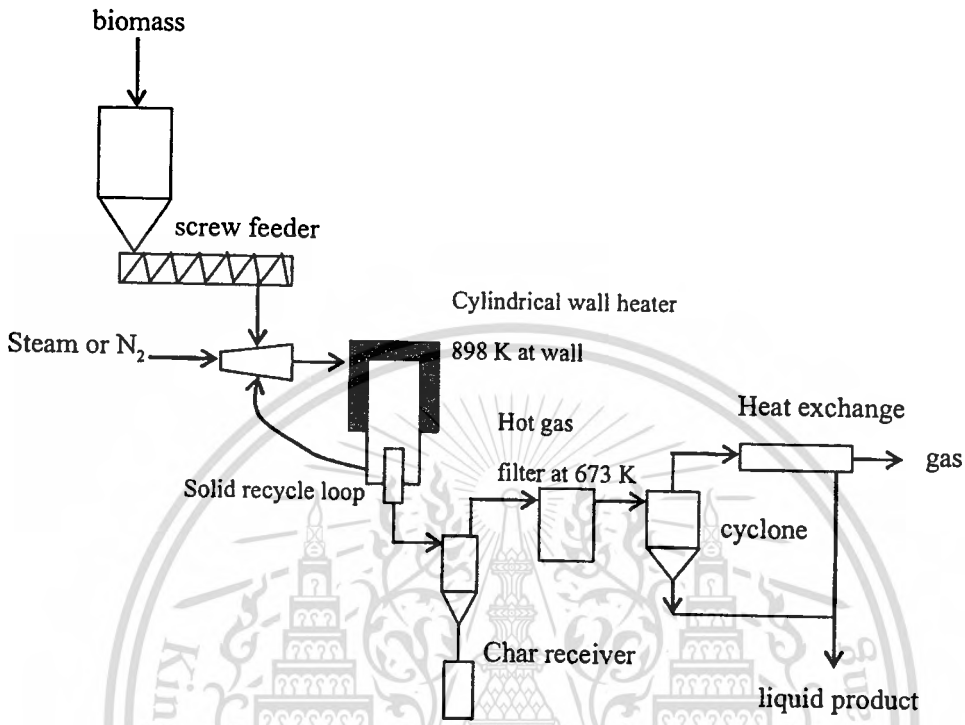

Figure 2.8 Diagram of NREL Technology for biomass pyrolysis [19]

Table 2.8 Analysis of pyrolysis liquids from poplar using the NREL process

	Wet basis	Dry basis
Elemental Composition, wt% on feed	46.5	57.3
Carbon	7.2	6.3
Hydrogen	46.1	6.3
Nitrogen	0.15	0.18
H/C ratio	1.86	1.32
O/C ratio	0.74	0.47
Ash	<0.01	<0.01
Moisture	18.9	0
Viscosity @ 40 °C, cp	18	
Heating value, HHV, MJ/kg	18.6	23

2.6 Bio oil

Definition : Bio oil are the liquid product from pyrolysis of biomass, which is the dark brown, free-flowing organic liquids. Bio oil is often referred to as : pyrolysis oils, pyrolysis liquids, bio-crude oil (BCO), wood liquids, wood oil, liquid smoke, wood distillates, pyroligneous acid, tar, pyrolytic tar and liquid wood [18].

2.6.1 General composition and physicochemical properties [18]

The physical and chemical properties of bio-oil strongly depend on many factors such as biomass feedstock, type of process, operating condition and collecting efficiency. Generally, bio oils are multicomponent mixtures of different size molecules which derived from the fragmentation of cellulose, hemicellulose and lignin. In general, the properties of bio oil and fuel oil are different. The typical properties of bio-oil and heavy fuel oil shows in Table 2.9.

2.6.2 Physical Properties

The basic physical properties of bio oil are described as follows;

1. Water

A large amount of water contained in bio oil as high as 20 -30 wt% depended on the type of feedstock and operating conditions. Water found in bio oil derived from the moisture in feedstock as well as the dehydration during the pyrolysis process. The existing of the water caused the decreasing of the heating value and flame temperature. However, the viscosity of bio oil was decreased by water and the fluidity increased.

2. Viscosity

The viscosity of bio oil is varied in the range of 40 – 100 cP. The viscosity of bio oil from the vacuum pyrolysis of hardwood and softwood was 24 and 62 cSt (at 323 K), respectively. The pyrolysis of wood sawdust in a cyclone reactor had a viscosity of 47cP (at 313 K) and increased to 62 cp after storage for 6 months. The increasing of viscosity resulted from the polymerization reactions.

3. Acidity

In general, bio oil obtained from the pyrolysis of biomass mainly consisted of the carboxylic acid such as acetic acid, butanoic acid and formic acid. Therefore, the pH was low as those compared with fuel oil. Acidity of bio oil leads to the corrosive and extremely severe at higher temperature. The corrosion of the construction materials of the vessel and transport was an important problem, hence the bio oil have to upgrade before using.

4. Heating value

The heating value of bio oil varied around 20 MJ/kg. This property strongly depended on the feedstock. The high heating value (23 MJ/kg) was obtained when spruce bark was used as feedstock. The heating value of bio oil is much lower than fuel oil because it contains a high proportion of water.

Table 2.9 Typical Properties of wood pyrolysis bio oil, light fuel oil and heavy fuel oil [18]

Physical property	Value		
	bio oil	heavy fuel oil	light fuel oil
moisture content (%wt)	20 - 30	0.1	0.025
solids (%wt)	<0.5	0.2-1.0	0
ash	<0.2	0.03	0.01
elementary composition (%wt)			
Carbon	32 - 48	85.6	86
Hydrogen	7 - 8.5	10.3	13.6
Oxygen	44 - 60	0.6	0
Nitrogen	<0.4	0.6	0.2
Sulfur	<0.05	2.5	<0.18
Vanadium, ppm	0.5	100	<0.05
Sodium, ppm	38	20	<0.01
Calcium, ppm	100	1	n.a.
Potassium, ppm	220	1	<0.02
Chloride, ppm	80	3	n.a.
Stability	Unstable	Stable	Stable
Viscosity (cSt)	15-35 at 313 K	351 at 323 K	3.0-7.5 at 313 K
Density (288 K), kg/dm^3	1.1 - 1.3	0.94-0.96	0.89
Flash point (K)	313 - 383	373	333
Pour point (K)	237 to 263	294	258
LHV (MJ/kg)	13 - 18	40.7	40.3
pH	2 - 3	n.a.	Neutral
distillability	Not distillable		433 - 673 K

2.6.3 Application of bio oil [19]

In this section, the applications of bio oil are briefly described. The utilization of crude bio oil was summarized in Table 2.10.

1. Combustion

The heating value of bio oil is lower than fossil fuel as showed in Table 2.10. because the large amount of oxygenated compounds and a high proportion of water. However, bio oil has been successfully replaced heavy and light fuel oils in the industrial boiler applications. The combustion characteristics of bio oil and light fuel oil are similar, although the differences in ignition, viscosity, energy content, stability, pH and emission levels are significantly observed.

2. Electricity production

The applications of bio oil for engine or turbine are widely used in many industrials but the modification of engine is required due to its high acidity. The most important changes involve the fuel pump, the linings and the injection system. Slight modifications of both the bio oil and the diesel engine can render bio oils and acceptable substitute for diesel fuel in stationary engines. Bio oil blends with standard diesel fuels or bio diesel fuel is also possible.

3. Synthesis gas production

The depletion of petroleum source is causing the strong attempt for searching the alternative energy source. Hydrogen has been identified as a very attractive energy because it is a "clean energy". The bio oil derived from biomass is considered as the source of green hydrocarbon and has high potential for H_2 production. The synthesis gas was produced by the gasification of bio oil. The gas products from gasification mainly consisted of H_2, CH_4, CO, CO_2, C_2, C_3 and C_4 - C_n hydrocarbons. The compositions of product gases were contained 16 – 36 %mol of syngas, 19 – 27 %mol of CH_4 and 21 – 31 %mol of C_2H_4.

4. Chemicals production

The composition of bio oil is very complex because there are consist of more than 300 compounds. These compounds have been identified as the fragment of lignocellusic materials. The several functional groups present in bio oil such as acids, sugars, alcohols, ketones, aldehydes, phenols and their derivatives, furans and other oxygenated compounds. A large fraction of composition presented in bio oil is phenolic fraction, consisting of relatively small amounts of phenol, eugenol, cresols and xylenols and much larger quantities of alkylated (poly-)

phenols. These chemicals have exhibited good performance as an adhesive or adhesive extender for waterproof plywood. Furfural and furfruyl alcohol are also detected with the high proportion.

Table 2.10 Summary of applications of pyrolysis liquid products [19]

Combustion ● Once ignited, bio oil burn readily ● Emissions are controllable ● Minor equipment modifications and some handling precautions are needed
Power generation with liquids ● Fuel production is de-coupled from power generation ● Dual fuel diesel engine successful at 250 kW ● Turbine tests successful at 2.5 MW ● Uncertainty over stability and effects of ash and char
Liquid upgrading ● Hydrotreating to naphtha and diesel. Costly, requires hydrogen. Catalyst stability problems ● Zeolite cracking to aromatics. Less costly, no hydrogen, less efficient, less developed ● Costs too high for transport fuels
Chemicals ● Speciality chemicals ● Intermediates e.g. polyphenols, fertilizers, environmental chemicals ● High value of chemicals may improve economics

2.7 Bio oil upgrading

The chemical composition of bio oil is very complicated, comprising mainly of water and oxygenated compounds such as carboxylic acids, carbohydrates and lignin's derivative. The presence of a large amount of carboxylic acids caused the increasing of a corrosive problem. Furthermore, some components in bio oil are chemically reactive and can react with each other. The viscosity of bio oil is increased with the storage time as a result of the undergoing polymerization and the loss of volatiles. Because of the instability of bio oil, the upgrading becomes a necessary process before the bio oil will be used. The samples of the upgrading method are described as follows [18-23].

1. Hydrodeoxygenation

This process consists of two stages, the first is hydro-cracking without catalyst and the second is the catalytic treatment step which operates under lower temperature and the same pressure as compare to the first step. In the second step, the reaction is performed in hydrogen providing solvent with the activation of catalyst. The typical catalysts for hydro-process are Co-Mo, Ni-Mo and their oxides or supported on Al_2O_3. Oxygen is removed in form of H_2O and CO_2, hence this process produce much of water.

2. Catalytic cracking of pyrolysis vapor

In this method, the oxygenated compounds are decomposed to hydrocarbon by the removal of oxygen as H_2O, CO_2 or CO. Several types of catalyst are used for cracking of pyrolysis vapor in order to obtain the higher quality of products which low oxygenated compounds. The porous material or zeolite group such as MCM-41 and HZSM-5 is the effective catalyst to produce the organic distillate fraction and completely eliminate levoglucosan. However, this method is not a promising technique because the obtained fuel has poor quality and high amount of coke is produced.

3. Emulsification

The combination of bio oil and diesel fuel is the simple method to utilize the bio oil as the transportation fuel. However, the separation between bio oil and diesel layer is observed. The addition of surfactant can emulsified the bio oil and diesel and then obtains the more stable bio oil. Furthermore, the viscosity and the corrosiveness of emulsified bio oil is lower than that of pure bio oil.

4. Steam reforming

Hydrogen is considered as an environmentally friendly energy source and its demand as the fuel for the fuel cell technology has been increasing. The production of H_2 can be performed through the steam reforming reaction by using of various hydrocarbons feedstock especially ethanol and methanol [24]. Because the bio oil is typically a complex mixture of hydrocarbon such as carboxylic acid, aldehyde and alcohol, furthermore, high amount of water exist in the bio oil. Therefore, the usage of bio oil as the feedstock for H_2 production has been considered [25]. The steam reforming of bio oil is described by the following reaction:

$$C_nH_mO_k + (2n-k)H_2O \longrightarrow nCO_2 + [2n+m/2-k]H_2 \quad (2.1)$$

5. Chemical extract from bio oil

There are more than hundreds of the component exist in bio oil which have several functional groups such as esters, ethers, aldehydes, ketones, phenols, carboxylic acid and alcohols. These compounds can be extracted and widely used in many applications. Phenol is used to produce resin and plastic. Alcohol is used in clean technology as H_2 production. Moreover, aldehyde and ketone are used in the pharmaceutical, fiber synthesizing, food additive or fertilizing industry.

2.8 Iron oxide [26]

Iron is a reactive element which forms binary compounds with several nonmetallic elements. Iron oxide is widely distributed in nature and as such form huge ore reserves. The most common form of the iron oxide is a rust (or hydrated iron(III)oxide). Other oxides are important in corrosion science and have several applications based on their physical properties such as magnetic, light adsorption and hardness.

The important iron/oxygen system has been extensively studied. The phase diagram of iron/oxygen is shown in Figure 2.10. Several iron oxides and hydroxyl oxides exist as minerals and the more typical minerals are listed in Table 2.11.

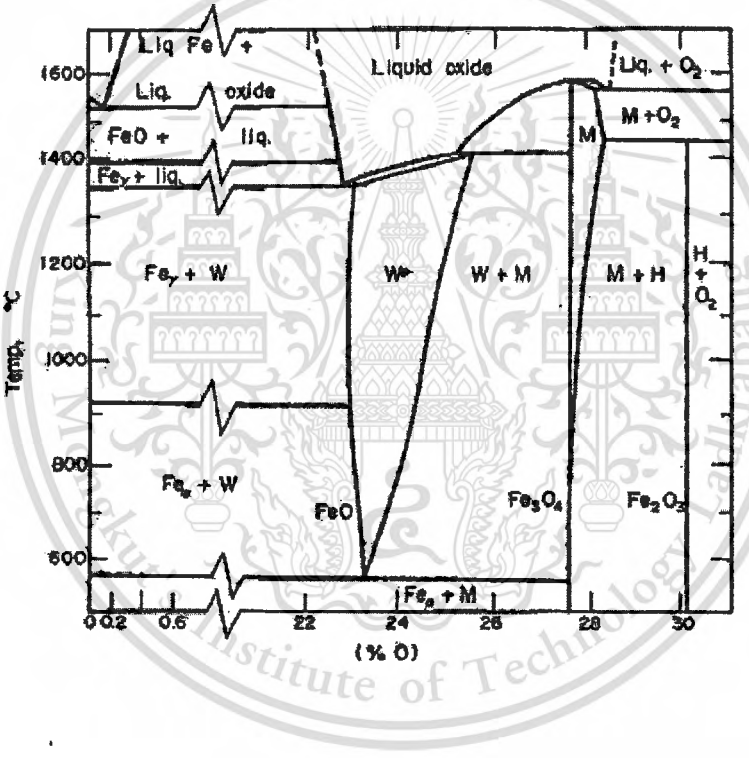

Figure 2.10 Phase diagram for the iron/oxygen system

Table 2.11 Iron oxide and oxyhydroxide minerals

Mineral	Formula	Structure	Density[a]	Color[b]
Goethite	α-FeO(OH)	Orthorhombic	4.26	Yellow brown
Akaganeite	β-FeO(OH)	Tetragonal	3.56	Yellow brown
Lepidocrocite	γ-FeO(OH)	Orthorhombic	4.09	Orange
Feroxyhyte	δ′-FeO(OH)	Hexagonal	4.20	Red brown
Ferrihydrite	$Fe_5HO_8 \cdot 4H_2O$	Trigonal	3.96	Red brown
Magnetite	Fe_3O_4	Cubic	5.18	Black
Hematite	α-Fe_2O_3	Trigonal	5.26	Bright red
Maghemite	γ- Fe_2O_3	Cubic/Tetragonal	4.87	Red brown

[a] $g\ cm^{-3}$

[b] Color depends to a significant extent on particle size and morphology

Three iron oxides are well known i.e. FeO (wusite), Fe_2O_3 (hematite) and Fe_3O_4 (magnetite).

2.8.1 Wüsite (FeO)

Iron (II) oxide has the chemical formula FeO, it is also known as ferrous oxide. The ratio of iron and oxygen is range between $Fe_{0.84}O$ and $Fe_{0.95}O$. Wusite can be prepared by heating of $Fe(OH)_2$ in N_2 atmosphere at 673 K, containing the defect clusters related to the magnetite structure (M, Fe_3O_4) and is an intermediate in the reduction of higher iron oxides. Single crystal XRD and neutron diffraction studies of a quenched sample indicated that the vacancies were not spread statistically over the structure but were arranged in clusters consisting of 13 vacancies and four tetrahedrally coordinated cations as shows in Figure 2.11.

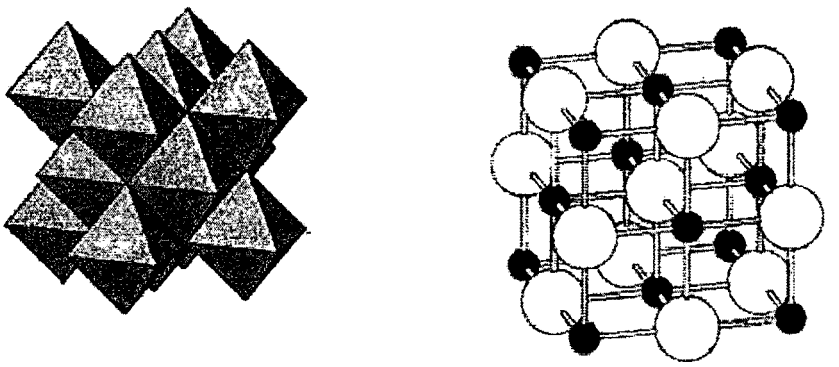

(a) (b)

Figure 2.11 Structure of Wüsite [26]

(a) Arrangement of octahedral (b) Ball-and-stick model

2.8.2 Hematite (α-Fe_2O_3)

Hematite is isostructural with corundum which has the unit cell in hexagonal. Fe_2O_3 is paramagnetic, reddish brown, and readily attacked by acids. The structure of hematite can be described as consisting of hcp arrays of oxygen ions stacked along the [001] direction. Two thirds of the sites are filled with Fe^{3+} which are arranged regularly with two filled sites being followed by one vacant site in the (001) plane thereby forming six fold ring. The structure of hematite demonstrates in Figure 2.12.

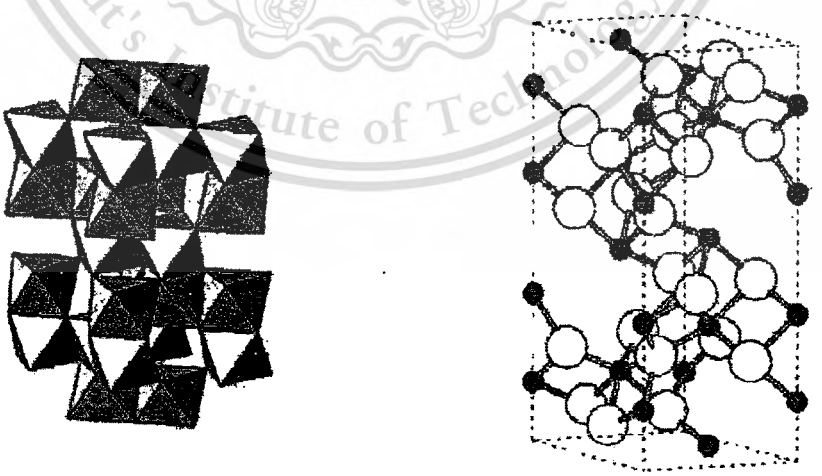

(a) (b)

Figure 2.12 Structure of hematite [26]

(a) Arrangement of octahedral (b) Ball-and-stick model

2.8.3 Magnetite (Fe_3O_4)

Magnetite differs from most other iron oxides since it contains both Fe^{2+} and Fe^{3+} ions and can be written as $Y[XY]O_4$ where $X=Fe^{II}$ $Y= Fe^{III}$. The structure consists of octahedral and mixed tetrahedral/octahedral layers stacked along [111] as shows in Figure 2.13. Magnetite is frequently non-stoichiometric in which case it has a cation deficient Fe^{III} sublattice. In stoichiometric magnetite $Fe^{II}/Fe^{III} = 0.5$. It is most extensive use is as a black pigment which is synthesized rather than being extracted from the naturally occurring mineral as the particle size and shape can be varied by the method of production.

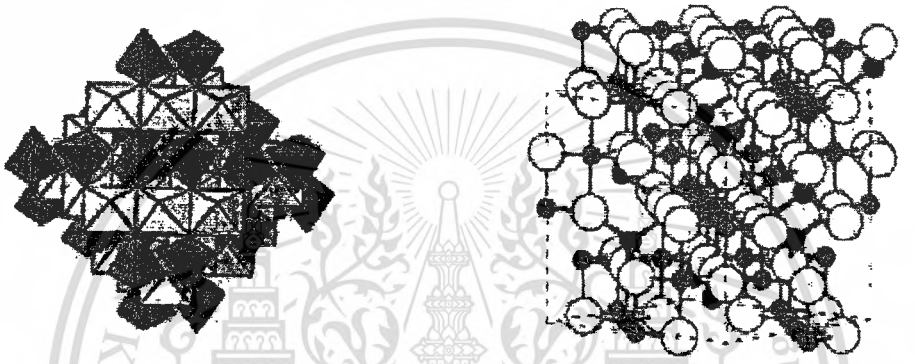

Figure 2.13 Structure of magnetite [26]
(a) Arrangement of octahedral (b) Ball-and-stick model

2.8.4 Iron salts

1. Chloride

Iron (II) chloride, $FeCl_2$ (Ferrous chloride) is a hygroscopic white/pale green solid readily soluble in water and ethanol with a melting point of 950 K and a boiling point of 1347 K. The pale green monoclinic crystals of the tetrahydrate are deposited when a saturated aqueous solution is cooled to 273 K, then further heated to 345.6 K in a partial vacuum a very green dehydrate anhydrous compound will be obtained and a monohydrated is obtained when the temperature reach to 393 K.

$FeCl_3$ is another form of iron chloride, $FeCl_3$ is covalent in nature when anhydrous and gas density measurements indicate that the formula of the gas is Fe_2Cl_6. The iron (III)chloride is mostly used in water treatment where it is used to condition some potable waters.

Furthermore, it is used in other application such as employing in sewage plants to co precipitate and then removing from clarified water, oils, polymers, heavy metals, sulfides and phosphates.

2. Nitrates

Green rhombohedral crystals of iron (II) nitrate hexahydrate, $Fe(NO_3)_2 \cdot 6H_2O$ (ferrous nitrate) are obtained from solutions made by dissolving iron in dilute nitric acid. With more concentrated acid oxidation takes place and monoclinic pale violet iron (III) nitrate nonahydrate, $Fe(NO_3)_3 \cdot 9H_2O$ (ferric nitrate) as cubic crystals. Various basic iron (III) anion $[Fe(NO_3)_4]^-$ has an essentially dodecahedral symmetry with four almost symmetrical bidentate nitrate groups.

Iron and its oxides are applied as a catalytic system; use in the synthesis of ammonia from hydrogen and nitrogen at high pressure as known in "Haber process", and in hydrocarbon synthesis from $CO/CO_2/H_2$ mixtures or Fischer-Tropsch synthesis. Iron oxides also have catalytic activity in mild hydrogenation reactions for example; magnetite has long been used to bring water gas to equilibrium with excess steam. They were also used to absorb sulfur compounds from town gas which obtained by dry distillation of coal.

Chapter 3

Literature Reviews

The utilizations of biomass as the alternative energy or chemical source are widely studied by many researchers. The different routes of biomass upgrading, for example, the catalytic upgrading, themochemical upgrading or biological upgrading are applied in order to achieve the productive and effective process. In this chapter, the research involved in the utilization of the effluent and biomass will be reviewed. The content was divided into 3 parts;

1) Literature reviews on the bio oil production
2) Literature reviews on the bio oil upgrading
3) Literature reviews on the wastewater treatment

3.1 Bio oil production

3.1.1 Bio oil from biomass

The effort for searching the clean source of energy is receiving an increasing attention for the past decade. The many applications of bio oil as mentioned in the latest chapter caused the increasing in the development of the process for bio oil production. Many techniques are applied to increase the yield of product. The common technique that has been widely used to produce bio oil is the thermal degradation process such as liquefaction, gasification and pyrolysis. Among of these techniques, the pyrolysis has seems to be the promising technique and has been developed relatively recently. The agricultural residues are widely used as the feedstock for example cashew nut shell, pine wood, oil palm solid wastes, etc.

Cashew is the mostly produced from India. The pyrolysis oil obtained from the cashew nut shell (CNS) showed the possibility to be a renewable and abundant source of energy [27-28]. The obtained oil after pyrolysis in a fixed-bed reactor was separated into the combustible and non-combustible fractions. The combustible or oil fraction was completely miscible in diesel and had low corrosively while the non-combustible or aqueous fraction mainly contained of ketones, acids and phenols.

Onay [29] investigated the pyrolysis of pistacia khinjuk seed in order to determine the optimum conditions in order to maximize the bio oil yield and to study the product distribution and its chemical compositions. The pyrolysis was carried out in a well-swept fixed bed reactor with the rapidly heating rate (300 K/min) the final temperature were 673 – 973 K. The maximum yield of bio oil was obtained at 873 K. The composition of bio oil was determined by FT-IR, H NMR and GC-MS. It was found that the oil mainly contained aliphatic group such as heptadecene, hexadecene and pentadecane. This oil was further upgraded using the commercial catalyst and the upgrading process would be discussed in the next section.

The high yield of bio oil was obtained (about 74%wt) when using a cyclone which was heated at its walls in the pyrolysis of sawdust wood. Three groups of fractions are recovered at different temperature i.e. heavy oil, light oil and aerosols [30].

Conventional pyrolysis of beech wood was carried out in the range of 1146 - 1446 K in fixed bed reactor. More than 40 species in pyrolysis oil were analyzed by GC-MS such as acetic acid, hydroxyl propanone, hydroxylacetaldehyde, levoglucosan, formic acid, syringol and 2-furaldehyde [31].

One of the most feedstock for bio oil production is palm oil waste such as shell, kernel and empty fruit bunch (EFB) [32-36]. The kinetic model for pyrolysis of palm oil wastes was investigated by many researchers in order to achieve an efficient production of fuel gases, chemicals and energy. Yang et al. [37] studied the pyrolysis of palm oil wastes (shell, kernel and EFB) and reported that the pyrolysis starts as low as 473 K and is complete by 773 K. The decomposition of these wastes could be divided into four stages: i) moisture evaporation ii) hemicellulose decomposition iii) cellulose decomposition iv) lignin decomposition. Futheremore, they also studied the chemical structure of cellulose, hemicellulose and lignin using FT-IR as showed in Table 3.1. It is showed obviously that the components of biomass were mainly consisted of alkene, esters, aromatics, ketone and alcohols.

Islam et al. [36] used the fluidized bed reactor for pyrolysis of palm shell and found the highest oil yield (58 %wt) was obtained at temperature of 773 K. The composition of pyrolysis oil analyzed from FT-IR and GC-MS containing a high fraction of phenol-based compound and acetic acid along with a small concentration of paraffin and no PAH.

Table 3.1 The main functional groups of the lignocellulosic materials [37]

Wave number (cm^{-1})	Functional groups	Compounds
3600 – 3000 (s)	OH stretching	Acid, methanol
2860 – 2970 (m)	C — H_n stretching	Alkyl, aliphatic, aromatic
1510 – 1560 (m)	C═O stretching	Ketone, and carbonyl
1632 (m)	C═C	Benzene stretching ring
1613 (w), 1450 (w)	C═C stretching	Aromatic skeletal mode
1470 – 1430 (s)	O— CH_3	Methoxyl-O-CH_3
1440 – 1400 (s)	OH bending	Acid
1402 (m)	CH bending	
1232 (s)	C— O— C stretching vibration	Aryl-alkyl ether linkage
1215 (s)	C—O stretching	Phenol
1170 (s), 1082 (s)	C— O— C stretching vibration	Pyranose ring skeletal
1108 (m)	OH association	C— OH
1060 (w)	C—O stretching and C— O Deformation	C— OH (ethanol)
700 – 900 (m)	C—H	Aromatic hydrogen
700 – 400 (w)	C— C stretching	

S: strong, m: middle, w: weak

3.1.2 Bio oil from sewage sludge

In general, sewage sludge is a product which retains after wastewater treatment plants. This sewage sludge consists of volatile matter as well as the environmental harmful residues like heavy metals, organic toxins and pathogenic microorganism. The disposal of these wastes by dumping into landfill, ocean or incineration is not suitable due to the inherent of toxic matters. Therefore, many researchers have attempted to address the large amount of sewage sludge.

Pyrolysis of sewage sludge in an inert gas at relatively low-temperature (573 – 1073 K) has successfully generated the liquid oil and lower emissions of NO_x and SO_x as lower operating cost when compared to incineration. The liquid oil obtained from pyrolysis of sewage sludge can be used as diesel fuel. Moreover, the liquid oil is considered as the source of chemicals. In order to implement utilization of this oil, the effect of operating parameters on product distribution has been investigated by many researchers [38-43].

The pyrolysis of sewage sludge obtained from waste water treatment plant in Thailand was studied by Jindarom et al. [38]. The pyrolysis was carried out in a fluidized bed reactor under CO_2 atmosphere at various temperatures. The increasing of CO_2 concentration results in the increased rate of thermal decomposition due to the oxidizing ability of CO_2. The liquid fraction was composed of various types of hydrocarbon and divided into three groups. First group was oxygenated and nitrogenated compounds (e.g. acetic acid, propanoic acid, acetaldehyde, Butanedial, Hydrogencyanide and etc.). The second group was aliphatic and alicyclic compounds (e.g. Hexane, Decane, Cyclohexane, Pentadecane, Hexadecane and etc.). The final group was aromatic compounds (BTXs, Phenol and its derivatives). At low temperature (623 K), the products in the first and second group were markedly observed while the small amount of the compound in the third group was detected. However, the first and second group compounds reached the maximum at 723 K and the yield of aromatic compound continuously increased due to the polymerization and cyclization reactions.

Dominquez et al. [39] investigated the characteristic of oils produced from sewage sludge using microwave heating instead the electric furnace. The effect of types of heating source (multimode and single mode) and types of absorber (graphite and char) on the product yield were studied. The obtained product was analyzed by GC-MS. As a result, monoaromatic compounds such as benzene and toluene were significantly produced when the graphite was used. A high yield of hexadecanoic acid was obtained (24.55 %) with char as absorber.

The usage of graphite as absorber provided the cracking of long chain aliphatic hydrocarbons into lighter hydrocarbons and monoaromatics were also enhanced. Furthermore, cracking and dehydrogenation reaction were promoted when multimode was used. Due to the sewage sludge was heated at high temperature with a few minutes, the secondary reaction to produce polyaromatic hydrocarbons (PAHs) was reduced. Therefore, the applying of microwave for pyrolysis sewage sludge could produce the oil without the harmful compounds.

Kaminsky et al. [40] used the Hamburg process for pyrolysis sewage sludge which obtained from Alfeld Community purification plant, Alfeld/Leine (F.RG.). The pyrolysis was carried out in a fluidized bed reactor at temperatures of 893 K, 963 K and 1023 K. The products from pyrolysis were gas, pyrolysis oil, product water, soot and pyrolysis residue. The yield of gas product increased with the increasing of temperature. CO, CO_2, H_2 and C_1-C_4 hydrocarbons were the main products in gaseous. Contrary to the gaseous, pyrolysis oil

decreased as the increasing of temperature. It was found that the increasing of aromatic compounds was observed, whereas the aliphatic hydrocarbon was cracked into smaller molecule when the temperature increased. Aromatic oil could be used for petrochemical application. The pyrolysis is seem to be a method for utilization the sewage sludge and pyrolysis product could be considered environmental friendly.

3.2 The upgrading of bio oil

It is well known that the bio oil produced by the thermal method such as pyrolysis has high amount of oxygenated compound. The high water content make a problem in the combustion system and the acidity, result from the containing of organic acid, may cause the corrosion of the construction material. Due to the complexity of bio oil, the interaction among the molecules in the oil or the reactivity itself lead to the formation of higher molecule and the condensation result in the increasing of viscosity of the bio oil. Therefore, the upgrading process of pyrolysis oil can not be disregarded in order to stabilize and easy to storage and transportation.

Hydrotreatment or steam reforming and catalytic cracking are mostly performed to improve the quality of the pyrolysis oil for using as the fuel including the purification to used as the chemicals source.

A number reports have been published on the upgrading of biomass over acidic catalyst was reported by many researchers [44-57]. A wide variety of catalysts such as zeolite (HZSM5, MCM, zeolite Y) and supported metal (Rh, Cu, Co over Al_2O_3, CeO) have been used for upgrading of bio oil. Vitolo et al. [44,45] studied the HZSM-5 behavior in the upgrading of wood pyrolysis oil. The upgrading reaction favorable occurred over the Brønsted site via a carbonium ion mechanism. However, the removal of coke deposition by air at 773 K resulted in the dehydroxydation of Brønsted site and then the reducing of activity of catalyst was observed.

Adam et al. [46] studied the different type of mesoporous material which modified by pore enlargement. It was found that the yield of hydrocarbon and phenol increased over all zeolite used in the upgrading pyrolysis vapor but the addition of transition metal such as Cu into the MCM-41 structure could improve the yield of desirable products while the undesirable decreased simultaneously. The other type of mesoporous compounds with the small adding of precious metal such as Ni, Rh and Pt was used as the catalyst for synthesis of clean diesel fuels by

oligomerisation.

The metal oxide catalysts were also used as the catalyst for improve the properties of pyrolysis vapor. Nokkosmäki et al.-[47] used ZnO to improve the stability of the oil obtained from the pyrolysis pine saw dust.

The metal over support i.e. $Ru/MgO/Al_2O_3$ was used in the steaming reforming of aqueous fraction of bio-oil [48]. . The MgO presence in the catalyst structure provided the spillover of oxygen and hydroxyl group to the active metal and the reaction favored at high temperature (>973 K) and low space velocity.

The cracking of biomass - derived oil became an alternative technique to produce hydrogen for using as the clean energy and decreasing on the demand of fossil fuels. The noble metal (Pt and Rh) supported over ceria-zirconia was used as the catalyst for this process. The stable productivity of H_2 with the small production of methane was achieved and the sequential cracking/regeneration could be operated as auto-thermally as well. However, the deactivation of catalyst by carbon deposition was a severe problem especially over the Pt supported catalyst [49]. The iron oxide catalyst was also used as the catalyst for cracking of biomass derived because it is cheaper and non toxic. The usage of iron oxide shows the high stable with cycle use, however, its activity decreased by the repetition [50].

The zirconia supporting iron oxide catalyst prepared by impregnation method was used as the oxidative cracking catalyst. It showed high potential to decompose the petroleum residual oil to gasoline without the solid carbon formation. The adding of Al could improve the stability of zirconia supporting iron oxide [51,52]. Furthermore, the using of this type of catalyst was found to increase ketone (acetone and MEK) production from domestic sludge derived black water as well [53]. Previous work reported that ZrO_2 supporting FeOOH shows high performance for recovery of phenol and acetone from the oil waste obtained from the production of activated carbon [54].

As mentioned earlier, the pyrolysis oil consist of various hydrocarbon compound therefore several reaction such as alkylation, the model compound reaction is necessary to identify the reaction occurred during the reaction of whole oil. Basagiannis [55] studied the reaction of acetic acid, which is one of the major components of pyrolysis oil, over supported nikel catalyst. The strong interaction over Al_2O_3 and the weak interaction over La_2O_3 were observed. The ketonization reaction was observed as the main reaction as followed;

$$2CH_3COOH \longrightarrow (CH_3)_2CO + H_2O + CO_2$$

The model compounds for representative of each chemical group i.e. propanoic acid for acids, 4-methylcyclohexanol for alcohols, cyclopentanone and 2-methylcyclopentanone for ketones, methyl acetate for esters, methoxybenzene and ethoxybenzene for ethers, phenol and 2-methoxy-4-(propenyl) phenol for phenols were selected to study its reaction over HZSM-5 catalyst [56-57]. Furthermore, the mixed model compound in order to study the interaction of each component was performed. From the results, it may be concluded that the reaction during the upgrading of bio oil is complex combination of reaction, consisting mainly of cracking, deoxygenation, aromatization and polymerization.

3.3 Wastewater treatment

Most of palm oil mills use the conventional method mainly based on the chemical and biological treatment such as anaerobic digestion in order to treat the discharged wastewater and produce bio gas as a main product.

In 2006, Thailand had the potential for biogas production about 105 millions m^3 and methane 60 millions m^3 was achieved. Furthermore, the biogas production is expected to increase to 420 millions m^3 in 2029. Yacob et al. [7] studied the emission of methane from open digesting tanks of palm oil mill effluent treatment. The results indicated that an average of 36% of methane composition and biogas flow rate of 5.41 $min^{-1}m^{-2}$ were obtained under normal mill operation and methane was emitted at 518.9 kg/day from the open digesting tank.

Vijayaraghavan et al. [58] investigated the treatment of POME using aerobic oxidation based on an activated sludge process. The results show that the COD value and residual oil could be removed by 98% and 93%, respectively at a hydraulic retention time of 60 h.

The potential of bio gas production is an advantage point for treating by biological method. However, the system for complete treatment of wastewater requires a large area and long retention time. Furthermore, the weather plays the important role in the growth of essential microorganisms and the treated wastewater will be discharged to the environmental without the reuse. In order to recover the water for usesage in the internal process, the other treatment technologies have been developed.

Ahmad et al. [4,11] developed a pilot plant for treatment POME. The integration of pretreatment method and membrane separation were constructed. The overall flow chart shows

in Figure 3.1. The pretreatment processed are the two stages of chemical treatment tank for coagulation, flocculation and sedimentation while activated carbon was used to remove organic matter, colors and odors. UF and RO were used in the stage of membrane separation where the completely treated POME.

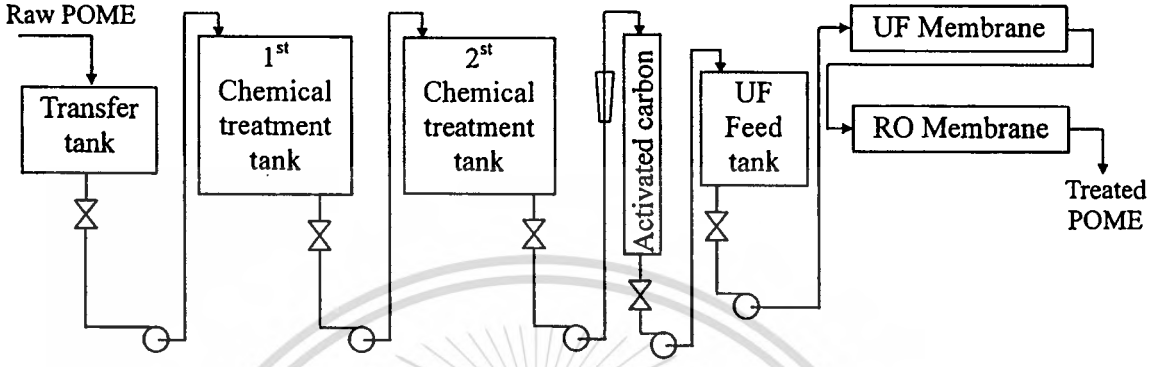

Figure 3.1 Diagram of the pilot plant for POME treatment

By using this method the organic matter and suspended solid were removed by 97.9%. Furthermore, the treated water was used as recycled water in a boiler for the sterilization of fresh fruit bunchs, clarification of the extracted crude palm oil or used in a hydrocyclone separation of the cracked mixture of kernels and shells.

Chapter 4

Experimental

4.1 Process description

Palm oil mill wastes can be categorized into solid and liquid. Figure 4.1 shows the overall process for utilization the palm oil mill wastes proposed in this study. Solid waste (shell, fiber or kernel paste) was directly pyrolysed to obtain bio-oil (BIO1). The bio-oil was then upgraded using an iron based catalyst to obtain useful chemicals. Water leaving from the palm oil mill production contains suspending solid and lipid. This waste was firstly filtrated to obtain sludge and water (W). The sludge was dried and pyrolysed to obtain an aqueous phase of bio-oil (BIO2) and oil phase of bio-oil (BIO3). The bio-oil (BIO2, BIO3) was then upgraded by the reaction with water using an iron-based catalyst. In this chapter, the experimental procedure and apparatus will be explained in detail according to the described utilization process.

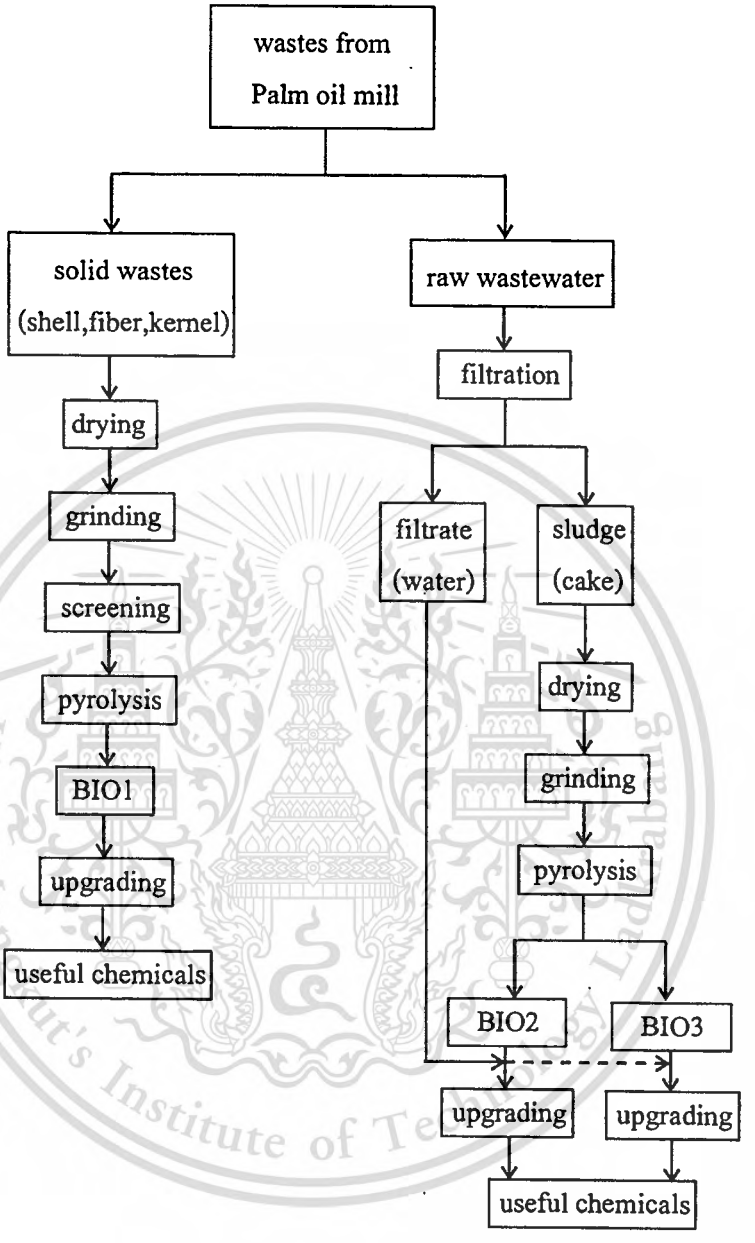

Figure 4.1 The schematic diagram of overall process

4.2 Pyrolysis of biomass

4.2.1 Thermogravimetric analysis

To obtain basic information using for the design of pyrolysis reactor, thermogravimetric analysis of solid waste was performed using a thermogravimetric analyzer (TGA-50H, Shimadzu). The sample was ground and sieved to obtain particle size in the ranges of 0.15-0.3, 0.3-0.5 and 0.5-0.84 mm. These samples were dried in an oven at 373 K overnight before using in the TGA tests. The sample (20 g) was placed in a quartz cell and heated in nitrogen atmosphere from 298 K to 1173 K with the heating rates of 5, 10 and 20 K/min. Volumetric flow rate of nitrogen carrier gas was maintained constant at 50 cm^3/min. The change in the sample weight was measured continuously using a microbalance to investigate the degradation behavior of the solid waste.

4.2.2 Bio-oil preparation

Figure 4.2 shows a schematic diagram of the experimental setup using in the pyrolysis of biomass. The semi-batch quartz reactor had a diameter of 2.2 cm and a bed height of 40 cm. The temperature inside the reactor was measured at the middle of the bed using a thermocouple K type (TC). The thermocouple was connected to a proportional integral-derivative (PID) controller using to control the electrical heater (ARF-50K, ASH). At the bottom of the reactor nitrogen was fed with a constant volumetric flow rate in order to carry the pyrolysed vapor products out from the top of the reactor. The outlet of the reactor was connected with ice traps (273 K) which are used to collect the condensable products. Non-condensable products were collected in a gas pack.

To pyrolyse the biomass, the reactor was heated under nitrogen atmosphere from room temperature (298 K) to a given temperature within 30 min. After the temperature reached the set point, the biomass sample was dropped into a reactor. The weights of the solid char in the reactor and the liquid in the traps were measured. The standard condition was as follow;

weight of sample, W	20	g
temperature, T	773	K
flow rate of nitrogen, v	50	cm^3/min
pyrolysis time, t	1	h

The yields of solid, liquid and gas were calculated from mass balance. Composition of the obtained liquid and gas products were analyzed using GC-MS (6890N, Agilent) equipped with a DB-Wax column and a plot fused silica column, respectively. Concentration of each component in the liquid and gas products were measured using a GC-FID (GC-17A, Shimadzu) equipped with the corresponding columns used in composition analysis. Concentration of inorganic gases was measured using a GC-TCD equipped with an activated charcoal column.

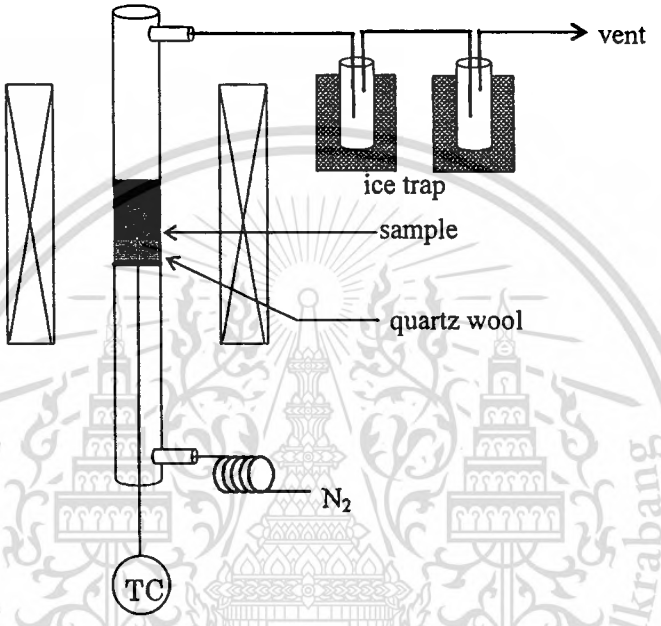

Figure 4.2 Experimental apparatus for pyrolysis

4.3 Bio oil upgrading

4.3.1 Catalyst

Table 4.1 summarized the iron-based catalysts employed in this study. These catalysts were prepared by impregnation or co-precipitation method with different precursors as describes in this section. The chemicals used as precursors to prepare the catalyst were 99% purity except iron (III) hydroxide and Fe_2O_3 were of commercial grade. The symbols "/" and "·" were used to name the impregnated catalyst and the co-precipitated one, respectively.

Table 4.1 The summary of catalysts preparation

catalyst	Preparation method	Precursors		
		FeO_x source	ZrO_2 source	Al_2O_3 source
$ZrO_2/FeO_{x[I]}$	Impregnation	FeOOH	$ZrCl_2O \cdot 8H_2O$	-
$ZrO_2/FeO_{x[II]}$	Impregnation	Fe_2O_3	$ZrCl_2O \cdot 8H_2O$	-
$ZrO_2 \cdot FeO_{x[III]}$	Co-precipitation	$Fe_3Cl_3 \cdot 6H_2O$	$ZrCl_2O \cdot 8H_2O$	-
$ZrO_2 \cdot Al \cdot FeO_{x[IV]}$	Co-precipitation	$Fe_3Cl_3 \cdot 6H_2O$	$ZrCl_2O \cdot 8H_2O$	$Al_2(SO_4)_3 \cdot 14\text{-}18H_2O$
$ZrO_2 \cdot FeO_{x[V]}$	Co-precipitation	$Fe(NO_3)_3 \cdot 9H_2O$	$ZrO(NO_3)_2 \cdot 2H_2O$	-

Impregnation method

Both $ZrO_2/FeO_{x[I]}$ and $ZrO_2/FeO_{x[II]}$ catalysts were impregnated catalysts obtained by the same impregnation procedure with the different FeOx supports. The FeOx support used for $ZrO_2/FeO_{x[I]}$ catalyst was obtained from a commercial grade iron (III) hydroxide (Wako, Japan) whereas the one used for $ZrO_2/FeO_{x[II]}$ catalyst was from a commercial grade Fe_2O_3 (Wako, Japan). These two iron sources were treated with the same manner in steam atmosphere at 773 K for 1 h to obtain iron oxide.

The obtained iron oxide was added into deionized water and stirred continuously. Aqueous solution prepared from $ZrCl_2O \cdot 8H_2O$ (Wako, Japan) with appropriate concentration was added dropwise into the FeO_x mixture. The mixture was continuously stirred for 12 h at room temperature. After that, the mixture was dried in air at 373 K overnight. The obtained solid was packed in a quartz tube reactor and activated in air at 773 K for 4 h. The obtained catalyst was crushed and sieved to the particle sizes between 300-850 μm.

Co-precipitation method

The $ZrO_2 \cdot FeO_{x[III]}$, $ZrO_2 \cdot Al \cdot FeO_{x[IV]}$ and $ZrO_2 \cdot FeO_{x[V]}$ catalysts were all prepared by co-precipitation method but with different compositions and precursors. The precursors of Zr and Fe employed for $ZrO_2 \cdot FeO_{x[III]}$ and $ZrO_2 \cdot Al \cdot FeO_{x[IV]}$ were chloride salts while the ones for $ZrO_2 \cdot FeO_{x[V]}$ were nitrate salts. In the co-precipitation procedure, ammonia solution (NH_3 solution 25%, Merck, Germany) was a precipitating agent. It was diluted to 10 % vol and dropped into the aqueous solution of all precursor salts. During the co-precipitation, the mixture was stirred vigorously and the precipitating agent was added dropwise until the pH of the mixture reached 7.00. After curing by further stirring for 1 h at pH 7.00, the mixture was decantated. The obtained decantated cake was dried in air at 373 K overnight. The solid was activated by calcination at 773 K for 4 h. The obtained catalyst was crushed and sieved to the particle size between 300-850 μm.

Characterization of catalyst

Structure of the obtained catalysts was observed using X-ray diffractometer (D8 Advance, Bruker AXS). Particle size of the catalysts was determined using transmission electron microscopy (TEM, JEOL 2010) and the obtained XRD spectrum. Specific surface area and pore size distribution of the catalysts were measured by nitrogen adsorption (autosorb1C, Quantachrom) according to Brunauer, Emmett, and Teller (BET) method.

4.3.2 Reaction test

Figure 4.3 shows a schematic diagram of the experimental setup using in the bio-oil upgrading reaction test. The reaction was performed in a fixed bed reactor at atmospheric pressure. The reactor was made of stainless steel with an inner diameter of 1.2 cm and a length of 12.0 cm. The catalyst was packed in the middle of reactor. The reactor was placed in an electrical furnace connected with a PID temperature controller. Thermocouple K type was inserted into the reactor to measure the temperature at the middle of the catalyst bed. At the top of the reactor, nitrogen carrier gas and vaporized feed were introduced. The outlet of the reactor was connected with ice traps (273 K) which are used to collect the condensable products. Non-condensable products were collected in a gas pack.

To perform the reaction test, the reactor was heated under nitrogen atmosphere from room temperature (298 K) to a given reaction temperature within 30 min. The mixture of

bio-oil and water was fed into the reactor using a syringe pump (Cole – Parmer). The condition for the reaction was as follow;

Temperature, T	513 – 723	K
Time factor, W/F_{oil}	0.25 – 12	h
Reaction time, t	1	h
Feed flow rate, F_{oil}	0.5	g

After finish the reaction, the catalyst was purged by pure N_2 for 1 h and the carbon residue over the catalyst and reactor wall was determined by the oxidation with air under the following conditions;

Temperature, T	823	K
time, t	1	h
Air flow rate, v_{air}	15	$cm^3 \cdot min^{-1}$

Composition and concentration of the liquid and gas products were measured with the method similar to those explained in section 4.2.2. The obtained results were used to calculate the recovery of each chemical in liquid and gas products. The optimum condition was assigned to be the condition which the highest price of useful chemicals was obtained.

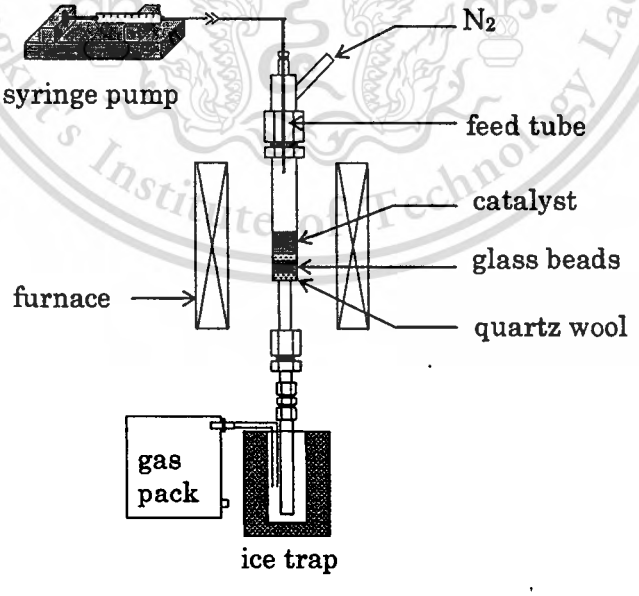

Figure 4.3 Experimental apparatus for reaction test

4.4 Determination of kinetics of bio-oil upgrading

To obtain the kinetic information necessary in the design of the upgrading reactor, the chemicals mainly existing in the bio-oil with large amount were selected and the reaction of these compounds over the iron catalyst was investigated separately. The obtained information was employed in cooperated with the information obtained from the reaction test in section 4.3.2 to determine possible reaction paths and preliminary kinetics of the bio-oil upgrading process.

Reaction of model compound

Methanol, acetic acid, acetone, phenol and ethyl acetate were selected as model compounds. The reaction test of each compound over the iron oxide catalyst was performed using the experimental setup showed in Figure 4.3. Each model compound was diluted with deionized water to obtain the concentration of 10 wt% (carbon basis). The aqueous solution was introduced into the reactor using a syringe pump (Cole – Parmer) with a constant feed flow rate of 0.5 $g \cdot h^{-1}$. The reaction temperature was varied in the range of 573–673 K and the time factor (W/F) was in the range of 0.5–10 h. Composition and concentration of the feed and products were analyzed with the same procedure described in section 4.3.2.

Calculation to determine kinetics of bio-oil upgrading

The reaction of bio oil was performed in fixed bed reactor under the isothermal conditions. The obtained data from the reaction of bio oil and model compounds were used to propose the reaction pathway. An integral reactor model was applied to estimate the kinetic parameters. The yield products could be evaluated from the equation (4.1).

$$r_i = \frac{df_i}{d(W/F)} \tag{4.1}$$

The reactions were assumed to be a first order reaction and then the kinetic parameters were evaluated by non linear regression of the experimental data using POLYMATH software. The rate expression for the reaction of each component based on the reaction pathway is described in the next chapter.

4.5 Deactivation and regeneration of catalyst

Since the used catalyst deactivated during the reaction test, it is necessary to understand deactivation behavior and to establish the regeneration method. The properties of the fresh catalyst and the deactivated one were investigated as described in this section.

4.5.1 Characterization

Crystal structure, particle size, specific surface area and pore size distribution of the used catalyst were analyzed with the method explained in section 4.3.1.

4.5.2 Temperature Program Oxidation (TPO)

In this study, temperature program oxidation of the deactivated catalyst was investigated using home-made experimental setup illustrated in Figure 4.4. Three quartz tubes were connected in series. The first one was packed with the deactivated catalyst and the oxidation of coke occurred in this reactor. Thermocouple K type was placed inside the tube at the middle of the catalyst bed. The temperature of the bed was measured and controlled using a PID temperature program controller (FCR, Shinko). The second one was packed with CO oxidation catalyst and used to perform complete oxidation of CO. The last one was packed with an oxygen adsorbent and used to remove the un-reacted oxygen in the gas stream. Intensity of the TPO spectrum was measured and recorded using TCD connected with data logger.

To measure the TPO spectrum of the deactivated catalyst, mixture of He-O_2 with the concentration of 0.5 vol% was employed. The sample was heated from 298 to 973 K with the heating rate of 10 K/min.

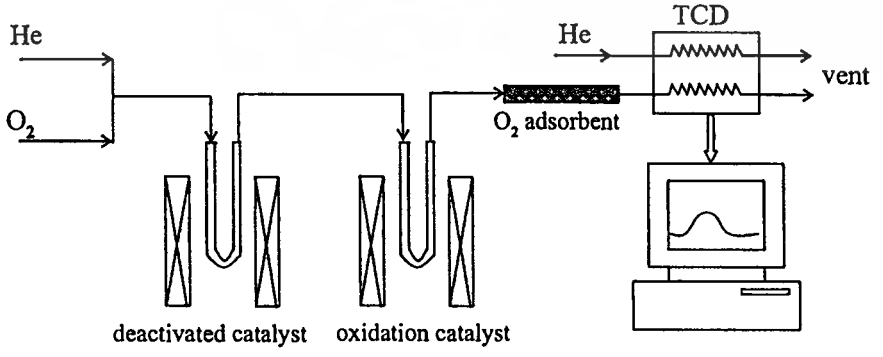

Figure 4.4 Schematic diagram of temperature program oxidation

4.5.3 Reaction-Regeneration cycle

The sequence of reaction and regeneration was conducted using the apparatus shown in Figure 4.3. The reaction was performed under the standard condition (T = 593 K, W/F_{oil} = 2 h and reaction time = 1 h). After the reaction, the catalyst was regenerated in air at 823 K for 1 h. The yield and the composition of the upgraded products were measured for the fresh and the regenerated catalyst. By comparison of catalytic performance for each reaction-regeneration cycle, the durability of the catalyst was discussed.

Chapter 5

Results and Discussions

5.1 Pyrolysis of biomass

5.1.1 Thermogravimetric analysis (TGA)

Figures 5.1 (a) and (b) shows the TG and DTG curves obtained from the temperature programmed pyrolysis of palm oil shell at the heating rate of 20 K/min for various ranges of the particle size. The particle size has insignificant effects on the shape of the TG and DTG curves. It means that the TG results using the particle sizes in the range of 0.15 – 0.85 mm can be used to analyze the kinetics of the pyrolysis in section 5.1.2. All the DTG curves in figure 5.2 show three peaks around 373, 493 – 613 and 613 – 673 K. According to the literature [32, 37], these peaks are assigned to the moisture removal, the decomposition of hemicelluloses and the decomposition of cellulose, respectively. The decomposition of lignin occurs in the range of 433 – 1173 with slow rate [37]. Therefore, the decomposition of lignin is not obviously shown in the DTG spectra. Figure 5.2 shows the DTG curve obtained from the temperature programmed pyrolysis of palm oil fiber compared with the one of palm oil shell obtained under the same condition. It obviously shows that the decomposition behavior of the palm oil fiber is similar to the palm oil shell. There are three peaks with slightly shift to the lower temperatures comparing to the peaks in Figure 5.1 (b). This result agrees well with the fact that the palm oil shell and fiber have three main components; lignin, cellulose and hemicelluloses but with different amount. For this reason, the palm oil shell was selected as a model for further investigation in this study.

Figure 5.3 shows the TG and DTG curves obtained from the temperature programmed pyrolysis of palm oil shell with different heating rates; 5, 10 and 20 K/min. This result shows important characteristics of the TG and DTG curves that the TG and DTG curves shifts to the higher temperatures as the heating rate increases. The two peaks in the temperature ranges of 493 – 590 K and 590 – 650 K shift to 493 – 613 K and 613 – 673 K, respectively.

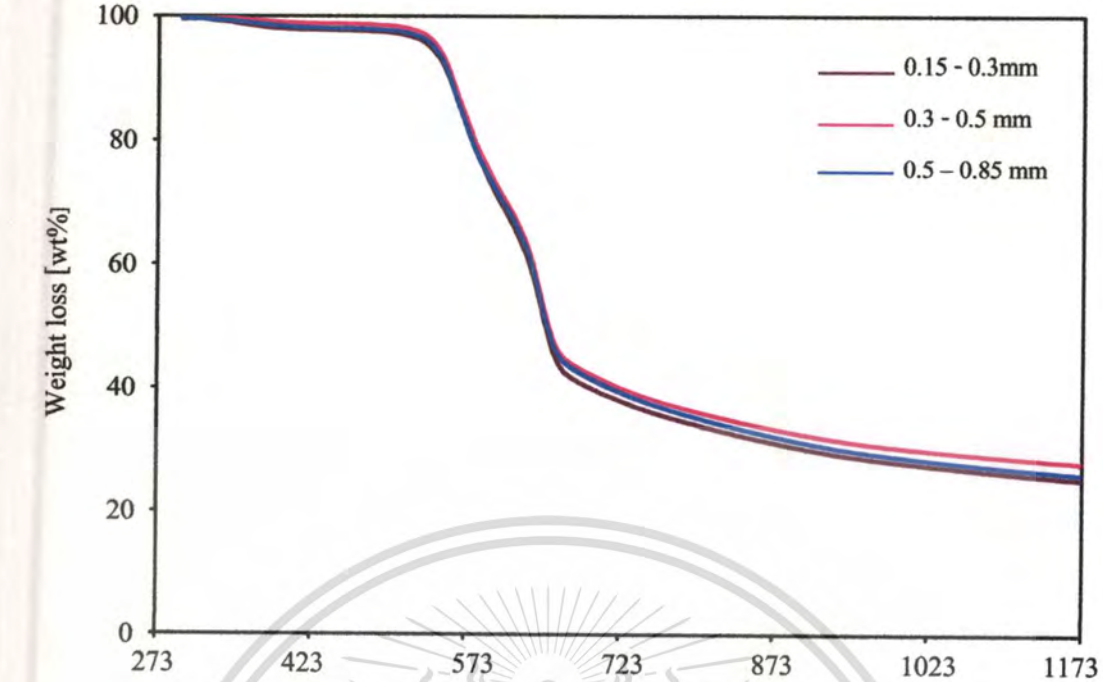

(a)

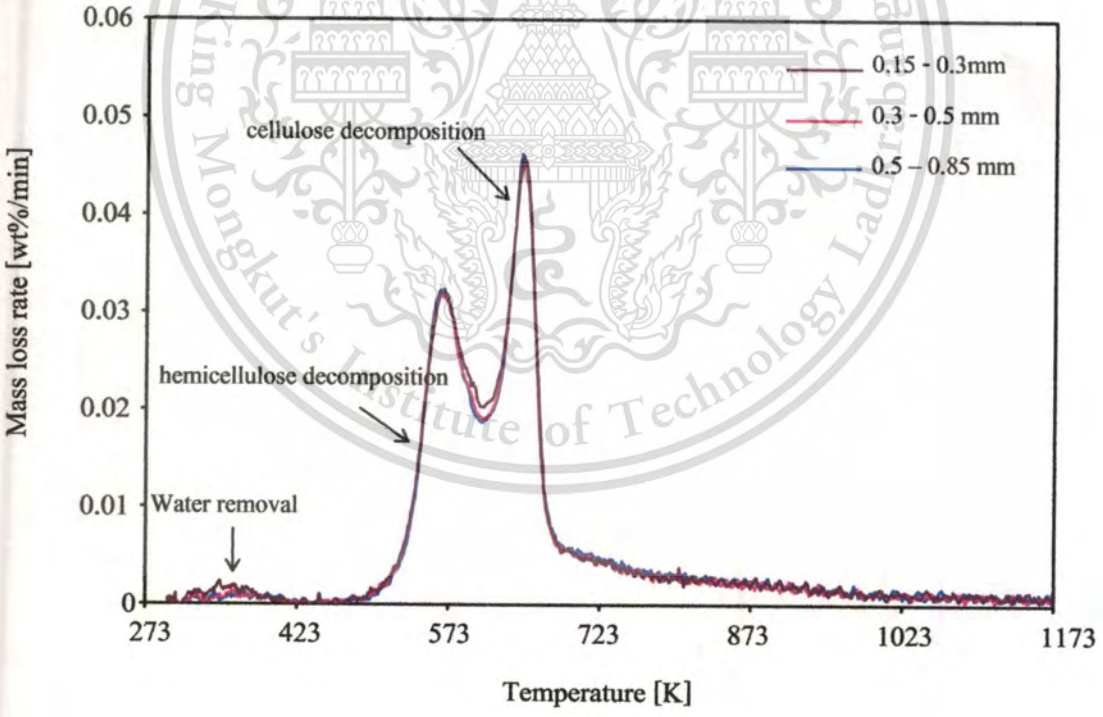

(b)

Figure 5.1 (a) TG curve (b) DTG curve for palm shell decomposition at various particle sizes

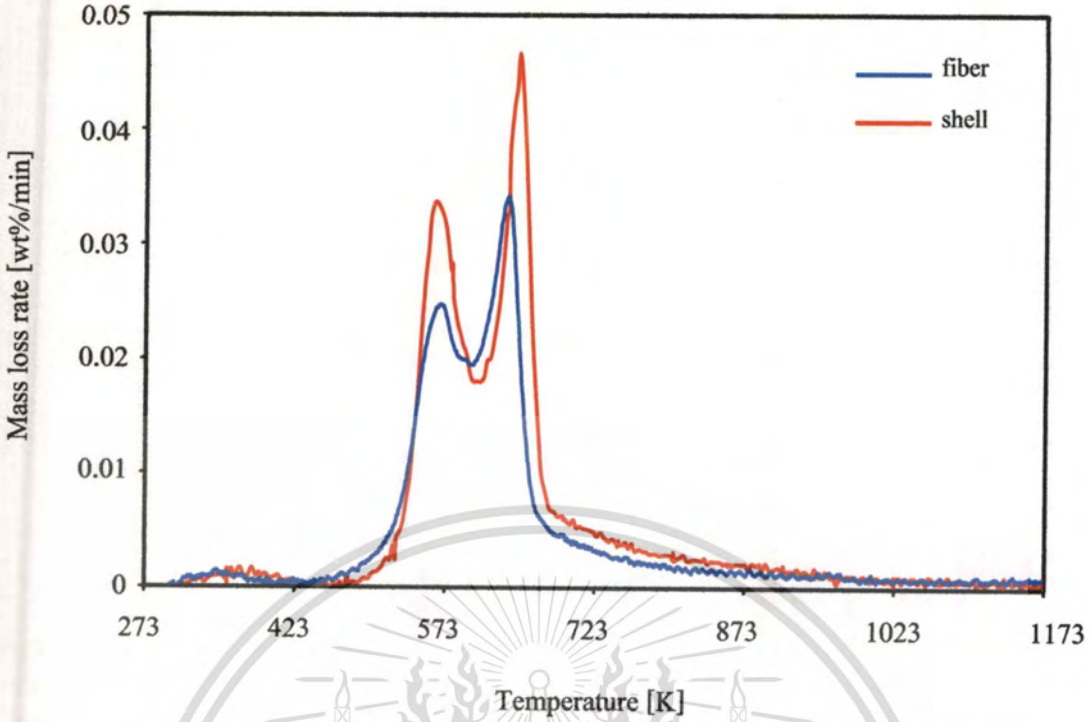

Figure 5.2 DTG curves for fiber and shell decomposition at heating rate of 20 K/min

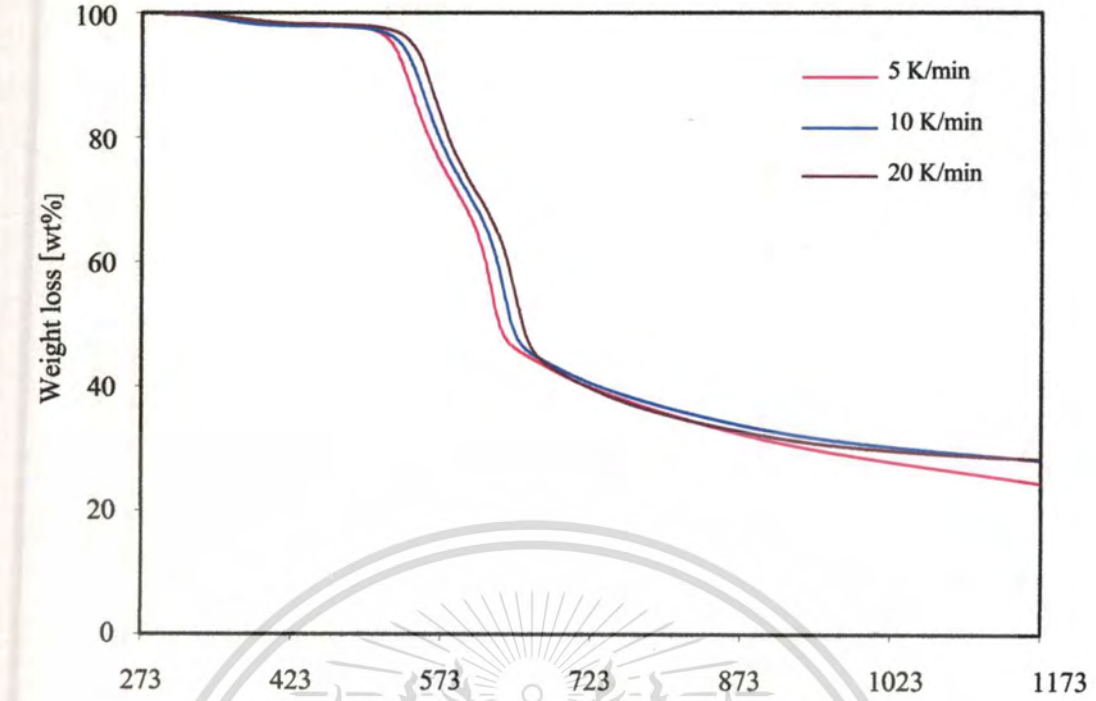

(a)

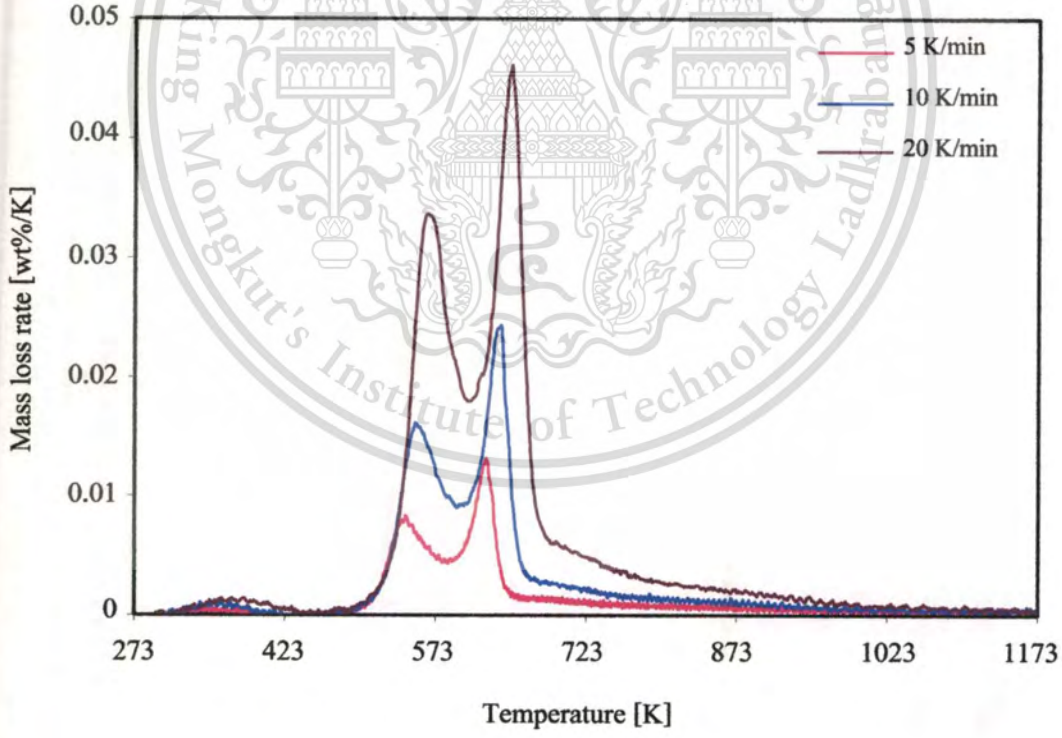

(b)

Figure 5.3 (a) TG curves (b) DTG curves for palm shell decomposition at different heating rates (particle size : 0.5 - 0.84 mm)

5.1.2 Estimation of kinetics parameters

A simply one step decomposition with first order was assumed to establish a simplified kinetic model which can predict the decomposition of palm oil shell. Coats and Redfern method [59] was employed to derive the set of equations as explained in Appendix C. The decomposition of palm shell is expressed in Eq. C.1 and the rate of decomposition is expressed in Eq.C.2.

$$\text{Palm shell} \xrightarrow{k} \text{Char + Volatile} \tag{C.1}$$

$$\frac{d\alpha}{dT} = kf(\alpha) \tag{C.2}$$

$$\ln\left[\frac{g(\alpha)}{T^2}\right] = \ln\left\{\frac{AR}{\beta E}\left[1-\frac{2RT}{E}\right]\right\} - \frac{E}{RT} \tag{C.8}$$

Where

$$\alpha = \frac{W_0 - W}{W_0 - W_\infty} \tag{C.5}$$

$$g(\alpha) = -\ln(1-\alpha) \quad \text{if} \quad n = 1 \tag{C.9}$$

To estimate the frequency factor (A) and the activation energy (E) of the decomposition of palm shell, the experimental results were plotted according to Eq.C.8. Since the DTG curves (Figure 5.3) had two peaks corresponding to the decomposition of different compositions, the kinetic parameters were calculated for each temperature interval: the ones from the 498 – 613 K interval corresponding to the decomposition of hemicelluloses-lignin and the ones from 613 – 673 K interval corresponding to the decomposition of cellulose-lignin. The values of A and E were calculated from the slope and intercept of the straight lines showing the relation between $\ln[g(\alpha)/T^2]$ and 1/T. The parameters obtained in this study were summarized in Table 5.1 comparatively with the literature results. The values of activation energy in this study were the same magnitude with the values reported by Yang H. et al [32] and Gua J. et al [33]. It could be concluded that the activation energy of the decomposition of hemicelluloses-lignin was in the range of 69.32-86.13 kJ/mol and the activation energy of the decomposition of cellulose-lignin was in the range of 49.14-51.08 kJ/mol.

Table 5.1 Kinetic parameters of the decomposition of palm shell

Authors	heating rate	n	T (K)	component	E (kJ/mol)	A (s^{-1})
Yang H. et al	-	1	493-573	hemicellulose	55.64	2.82×10^{1}
[32]	-	1	573-613	cellulose	75.72	2.43×10^{3}
Gua J. et al	5 K/min	1.02	298-873	-	54.1	7.45×10^{3}
[33]	10 K/min	1.07	298-873	-	54.8	9.74×10^{3}
	20 K/min	0.98	298-873	-	55.2	1.12×10^{4}
	30 K/min	1.04	298-873	-	55.3	1.36×10^{4}
This work	5 K/min	1	493-613	hemicellulose-lignin	69.32	2.01×10^{3}
			613-673	cellulose-lignin	49.14	1.6×10^{1}
	10 K/min	1	493-613	hemicellulose-lignin	70.49	2.32×10^{3}
			613-673	cellulose-lignin	50.52	3.87×10^{1}
	20 K/min	1	493-613	hemicellulose-lignin	86.13	2.06×10^{5}
			613-673	cellulose-lignin	51.08	7.2×10^{1}

Figure 5.4 shows the effect of heating rate on the rate constant. It can be seen that the rate constant slightly increased with the increasing of heating rate indicating that at higher heating rate the pyrolysis easier and faster took place.

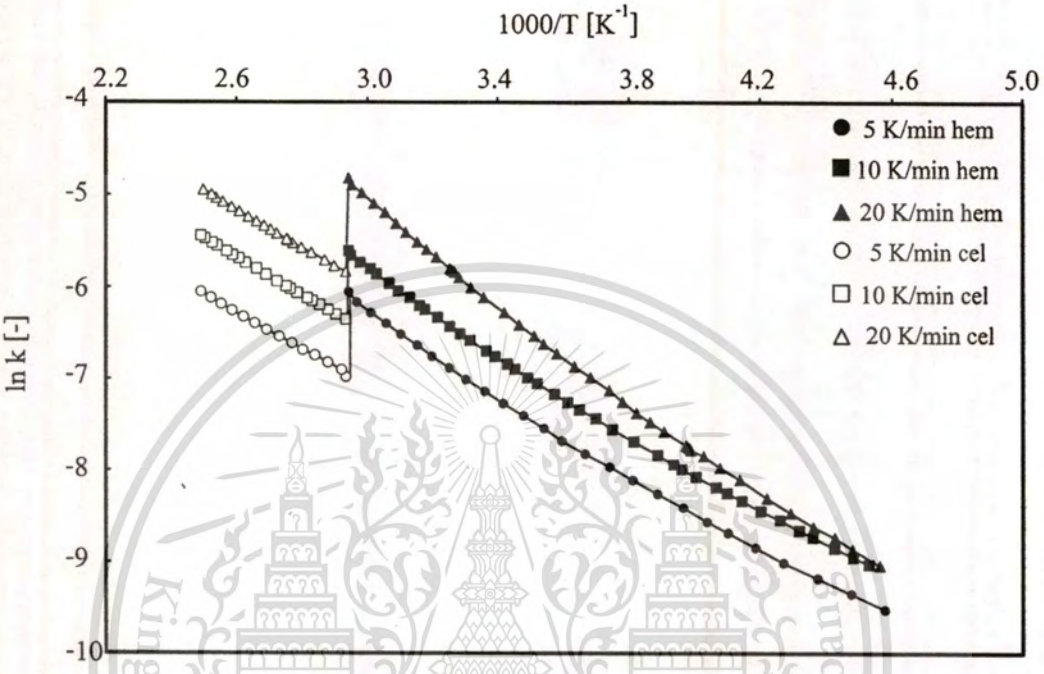

Figure 5.4 The effect of heating rate on the rate constant

5.1.3 Pyrolysis of solid wastes

The products obtained from the pyrolysis of palm shell at 773 K were solid char (34%wt), dark brown liquid oil (56%wt) and gas (10%wt). In this study, the dark brown liquid oil was named as "bio-oil". The composition of bio-oil was analyzed using GC-MS and GC-FID techniques. Figure 5.5 and Table 5.2 showed that the bio-oil contained several kinds of organic compound such as alcohol, ketone, carboxylic acid and phenol derivative. From the quantitative analysis by GC-FID, we found that the bio-oil mainly contained methanol (5%C), acetic acid (22%C), ethylacetate (0.2%C) and phenol (36%C) based on carbon. For further discussion in this study, the term "others" included the hydrocarbons which were not able to identify by GC-MS, the ones existing with trace amount in the bio-oil and the heavy hydrocarbons which contain the fragment of lignocellulosics material such as 2-methoxy-4-methy-phenol, 4-ethyl-2-methoxy-phenol and 2,6-dimethoxy-phenol. Table 5.3 shows the composition of the palm shell derived oil compared with the previous literatures [34,36]. According to these results, the direct utilization of this bio-oil as fuels should be avoided since it contained large amount of oxygenated compounds leading to unstable and low heating value of the bio-oil. Therefore, the bio-oil should be upgraded to improve its stability and/or converted to useful chemicals.

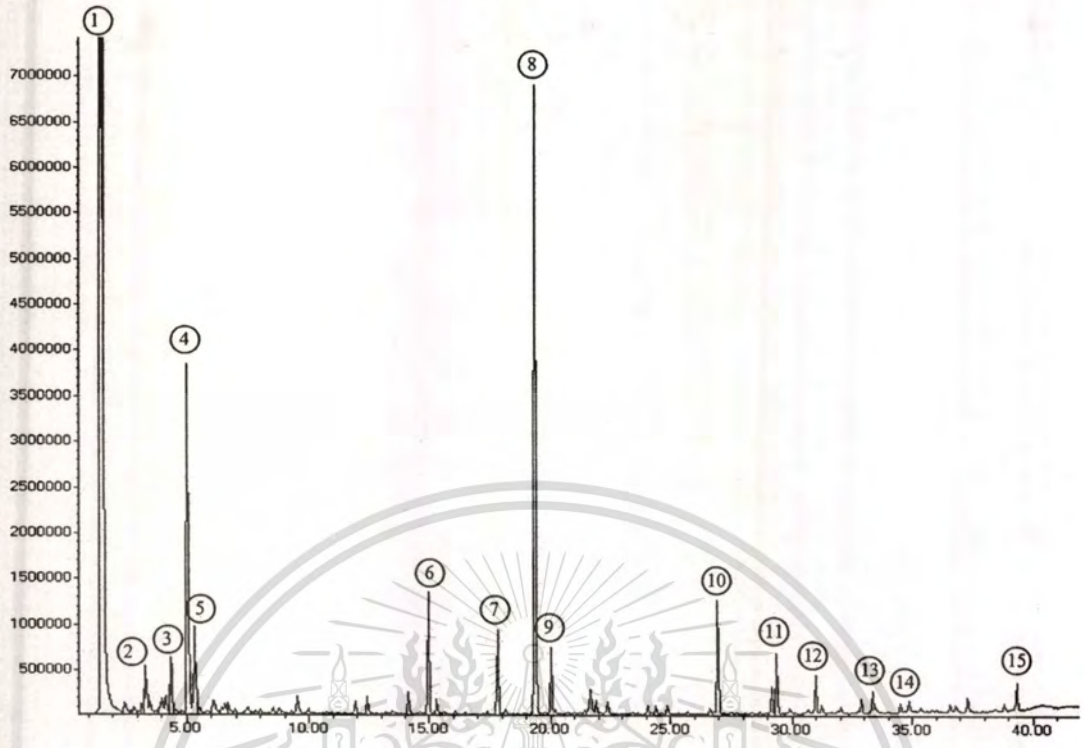

Figure 5.5 GC-MS chromatogram of the bio-oil obtained from pyrolysis of palm shell at 773 K

Table 5.2 Composition of the bio-oil obtained from pyrolysis of palm shell at 773 K

Peak No.	compounds	Peak No.	compounds
1	Methanol	9	4-ethyl-2-methoxy-phenol
2	2-propanone, 1-hydroxy	10	2,6-dimethoxy-phenol
3	4-oxo-5-methoxy-2-penten-5-olide	11	3-hydroxy-4-methoxybenzoic acid
4	Acetic acid	12	2,3,5-trimethoxytoluene
5	2-furaldehyde	13	Dodecanoic acid
6	2-methoxy-phenol	14	4-hydroxy-3-methoxy-benzaldehyde
7	2-methoxy-4-methy-phenol	15	4-allyl-2,6-dimethoxyphenol
8	Phenol		

Table 5.3 Composition of the bio-oil obtained from pyrolysis of palm shell compared with the other works

compounds	This work	Kawser et al. [34]	Islam et al. [36]
Alkanes			
1-octane	-	/	-
Alcohols			
methanol	/	-	-
Aldehydes			
benzaldehyde	-	/	-
2-furaldehyde	/	-	/
4-hydroxy-3-methoxy-benzaldehyde	-	-	-
Carboxylic acids			
acetic acid	/	/	/
butanoic acid	-	/	-
pentanoic acid	-	/	-
dodecanoic acid	/	-	-
3-hydroxy-4-methoxybenzoic acid	/	-	-
Ketones			
acetone	/	-	-
2-propanone, 1-hydroxy	/	/	-
2-propanone, 3-hydroxy	-	-	/
Cyclopentanone	-	-	/
3-methyl-cyclopentanedione	-	-	/
butanedial	-	-	/
Esthers			
4-oxo-5-methoxy-2-penten-5-olide	/	-	-
Allyl-acetate-2-ene	-	-	/
methycrotonate	-	-	/

Table 5.3 (cont.) Composition of the bio-oil obtained from pyrolysis of palm shell compared with the other works

compounds	This work	Kawser et al. [34]	Islam et al. [34]
Phenol and its derivatives			
Phenol	/	/	/
2-methoxy-phenol	/	-	/
4-methy -2-methoxy-phenol	/	-	/
4-ethyl-2-methoxy-phenol	/	-	/
4-propene-2-methoxy-phenol	-	-	/
2,6-dimethoxy-phenol	/	/	/
2,3,5-trimethoxytoluene	/	-	-
4-allyl-2,6-dimethoxyphenol	/	-	-
Ortho-hydroxy phenol	-	/	/
o-cresol	-	/	-
m-cresol	-	/	-
p-cresol	-	/	-
guaiacol	-	/	-
syringol	-	/	-
eugenol	-	/	-

Other solid wastes (fiber and kernel) were pyrolysed to produce bio-oil under the same condition. Figure 5.6 showed that the obtained bio-oils contained the same three main components (methanol, acetic acid and phenol) but with different amounts. The "others" of the bio-oils derived from fiber and kernel were also contained large amount of phenol derivatives liked the "others" in shell derived bio-oil. Furthermore, we found that the amount of "others" was in the order of shell < fiber < kernel. The amount of oils and fatty acids contaminated in fiber and kernel should be the reason for high amount of "others".

These three solid wastes should be considered as a renewable source of useful chemicals if a suitable process was established. In order to investigate the performance of catalysts for conversion of the solid wastes derive bio-oils to useful chemicals, the palm shell derived bio-oil was selected since all the bio-oils contained the same main components and the similar types of hydrocarbon included in the "others".

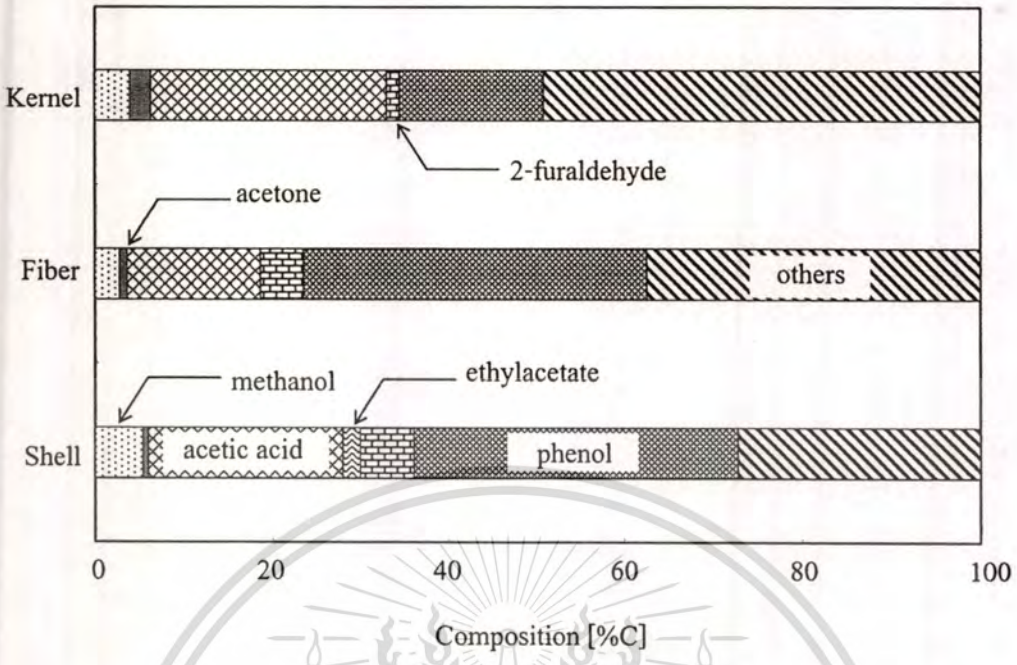

Figure 5.6 Composition of palm oil wastes-derived oil obtained by pyrolysis at 773 K

5.1.4 Pyrolysis of dried sludge

The raw wastewater before entering to the decanter was separated by filtration. The obtained filtrate was analyzed by GC-MS and the chromatogram was shown in Figure 5.7. The main components were fatty acid and ester of fatty acid as listed in Table 5.4. After filtration, the dried sludge with 18.75 %wt of raw wastewater and water with 81.25 %wt were obtained. The elemental composition on a dry basis of sludge was 36.62 %C as shown in Table 5.5. The products obtained from the pyrolysis of dried sludge at 773 K were solid char (34.5%), liquid oil (44.8%) and gas (20.7%). The liquid product was separated into two layers as shown in Figure 5.8. The upper layer with 33.3 %wt of whole oil was named as "oil phase" and the lower layer with 66.7 %wt was named as "aqueous phase". These oils were separated by decantation. Elemental analysis showed that oil phase contained C (77.78%wt), H (8.82%wt), N (0.28%wt) and aqueous phase contained C (16.04%wt), H (9.40%wt), N (0.34%wt) as summarized in Table 5.6. The composition of each phase was analyzed using GC-MS and GC-FID techniques. Figure 5.9 (a) and (b) show chromatogram of oil and aqueous phase, respectively. Table 5.7 shows, in detail, the composition of both bio-oil fractions (oil phase and aqueous). The

difference in the composition between each phase was observed. A large amount of carbon was found in oil phase indicated that this phase mainly consisted of the long chain hydrocarbon whereas the aqueous phase mainly consisted of the oxygenated compounds. It can be seen that the aromatic hydrocarbon such as phenol and m-cresol were the main components in oil phase resulted from the decomposition of the lignin. The smaller molecules found in aqueous phase such as methanol, acetone and acetic acid issued from the holocellulose [21-22]. The components presented in others were significantly different in each phase thus a further reaction testing of these phases should be investigated separately.

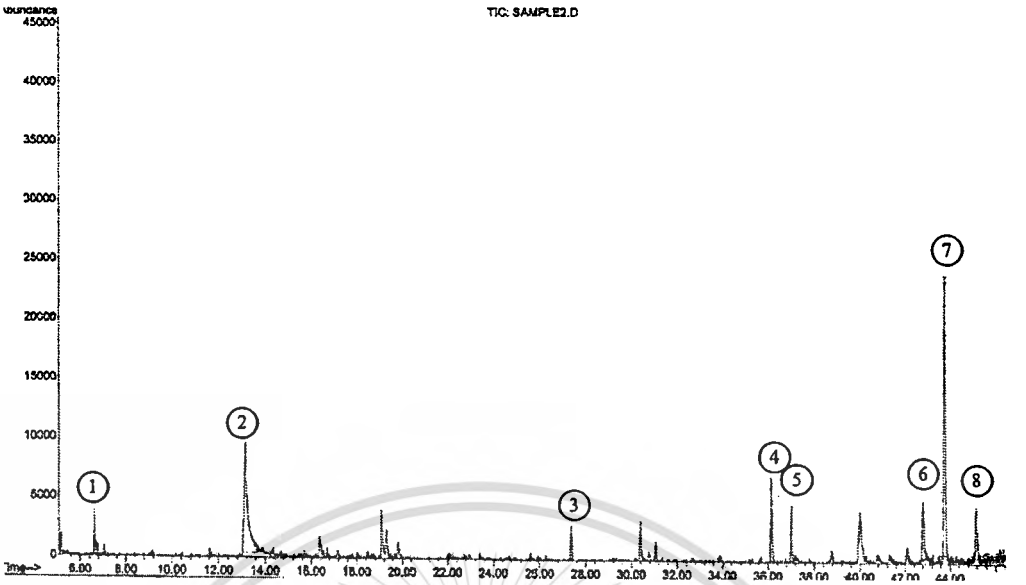

Figure 5.7 GC-MS chromatogram of wastewater

Table 5.4 composition of raw wastewater and its derived oil

Raw wastewater		Oil phase		Aqueous phase	
No.	components	No.	components	No.	components
1	Pyridine	1	Pentadecane	1	Methanol
2	2,5-Dimethyl furan	2	2,5-Dimethyl furan	2	Pyridine
3	Benzeneethanol	3	Phenol	3	Hydroxyacetone
4	4-Vinyl-2-methoxy-phenol	4	m-Cresol	4	Acetic acid
5	Palmitic acid	5	Methyl palmitate	5	Acytoxyacetone
6	4-Hydroxypyridine	6	2-Tridecanone	6	Propanoic acid
7	9-Octadecenoic acid	7	Myristronitrile	7	Butanoic acid
	methyl ester	8	Ketole	8	2-Furalmethanol
8	9,12-octadecadienoic acid			9	Acetamide
	methyl ester			10	Methylcyclopente
				11	Phenol
				12	2-Pyrrolidinone
				13	3-Pyridinol

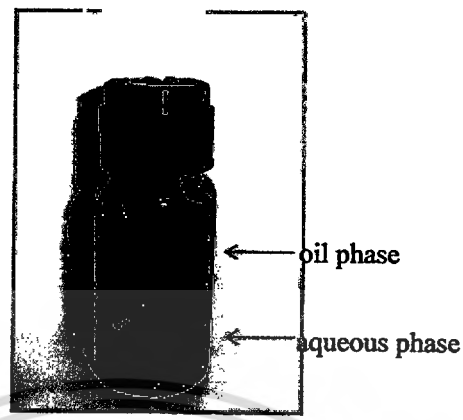

Figure 5.8 The pyolysis oil obtained from the pyrolysis of dried sludge at 773 K

Table 5.5 Elemental analysis from CHNS/O analyzer

material	Elementary composition (%)		
	C	H	N
dried sludge	36.62	-	-
oil phase	72.78	8.82	0.28
aqueous phase	16.04	9.40	0.34

Table 5.6 The yield of pyrolysis product

product	yield (%wt)
solid	34.5
liquid	44.8
oil phase	14.9
aqueous phase	29.9
gas	20.7*

*by difference

Table 5.7 The main components of oil phase and aqueous phase.

Aqueous phase		Oil phase	
Component	%C	Component	%C
methanol	6.32	acetone	0.39
acetic acid	27.24	phenol	6.6
acetone	2.4	m-cresol	1.85
others I	64.04	others II	91.16

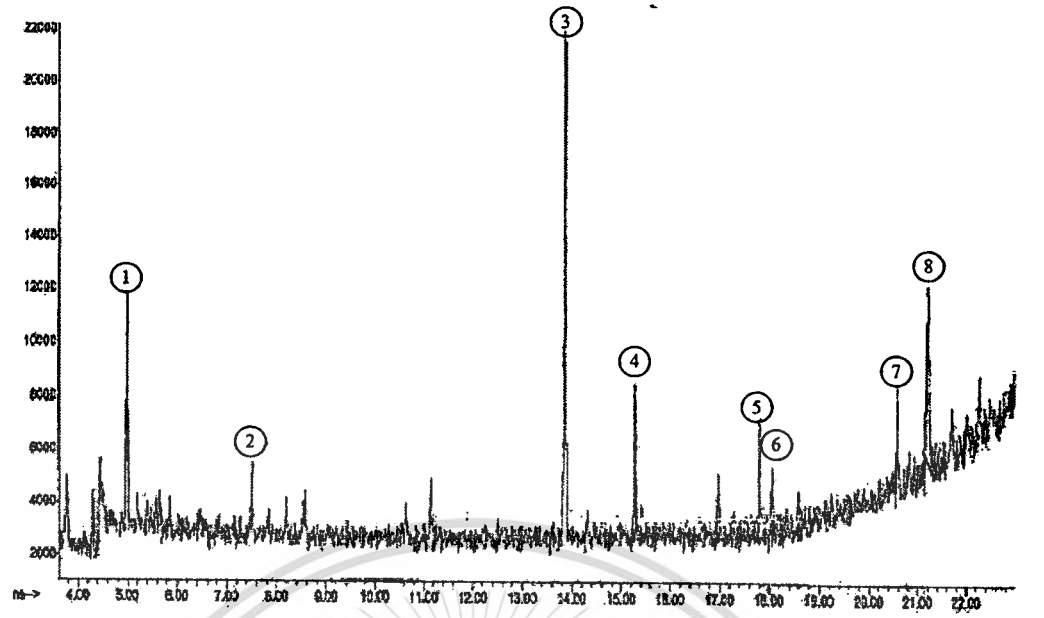

(a)

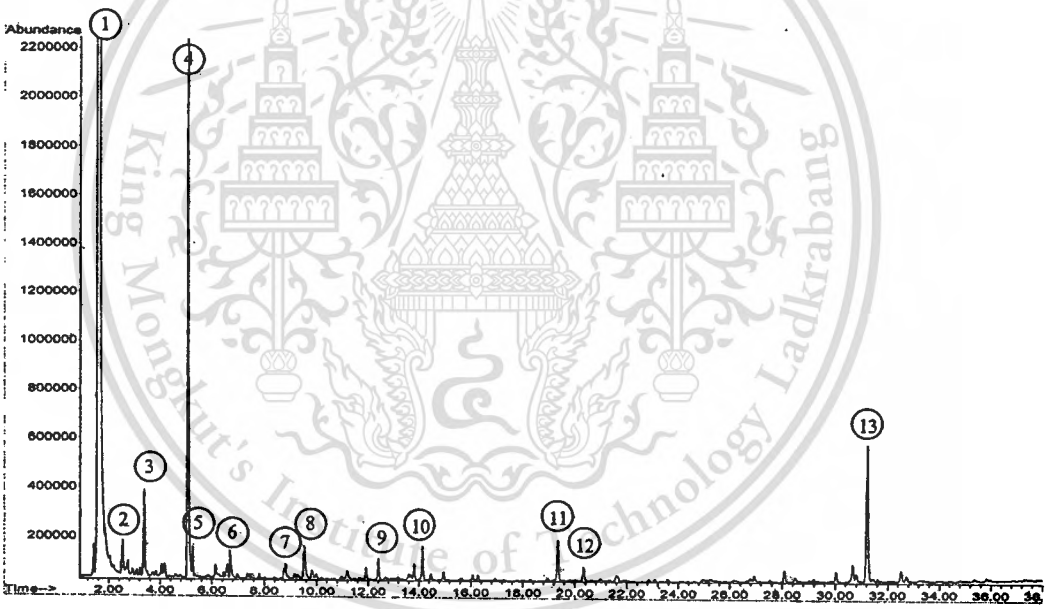

(b)

Figure 5.9 GC-MS chromatogram of the dried sludge derived oil for (a) oil phase (b) aqueous phase

5.2 Upgrading of bio-oils

In section 5.2.1, the performance of several zirconia supporting iron oxide catalysts for palm shell oil upgrading under standard condition was investigated. The most active catalyst was selected and the effect of operating parameters on the conversion of palm shell oil to useful chemicals using this catalyst was further investigated in section 5.2.2. In section 5.2.3, the way to improve the performance of this catalyst by changing its precursors was proposed. In section 5.2.4 the improved zirconia supporting iron oxide catalyst which prepared from nitrate salts was employed for the upgrading of dried sludge derived bio-oil (DSO). Since the DSO consisted of oil and aqueous phases, the catalytic upgrading reaction was tested separately. The optimal condition for upgrading of each phase was investigated.

5.2.1 Selection of catalysts

Figure 5.10 shows the XRD pattern of the fresh ZrO_2 supporting iron oxide catalyst prepared by different methods. All the catalysts showed the same crystalline structure corresponding to hematite without ZrO_2 pattern. This result implied that ZrO_2 was highly dispersed as small particle in the main structure of iron oxide and over the surface of iron oxide particle. The performance of these catalysts on the upgrading of palm shell oil was investigated under the standard condition: reaction temperature = 673 K, W/F_{oil} = 2 h and H_2O to oil molar ratio = 2. Figure 5.11 shows the product distribution obtained from the catalytic upgrading using these catalysts and from the thermal cracking without using catalyst. By comparison the product distribution of the thermal cracking with the ones of catalytic cracking, we concluded that thermal cracking was not suitable for the upgrading of palm shell oil since the thermal cracking increased the amount of hydrocarbon categorized in "others" and produced large amount of solid residue inside the reactor. On the other hand, the catalytic cracking of palm shell oil increased the amount of the target useful chemicals (methanol, acetic acid, acetone and phenol) and reduced the amount of "others" in liquid product without the production of solid residue. Although the yields of methanol, acetic acid and phenol obtained from all the catalysts were almost the same, the $Zr{\cdot}Al{\cdot}FeO_{x\,[IV]}$ was considered as the most suitable catalyst since it reduced the amount of the "others" to the lowest level. For this reason, the $Zr{\cdot}Al{\cdot}FeO_{x\,[IV]}$ was selected as the best catalyst for palm shell oil upgrading for further study.

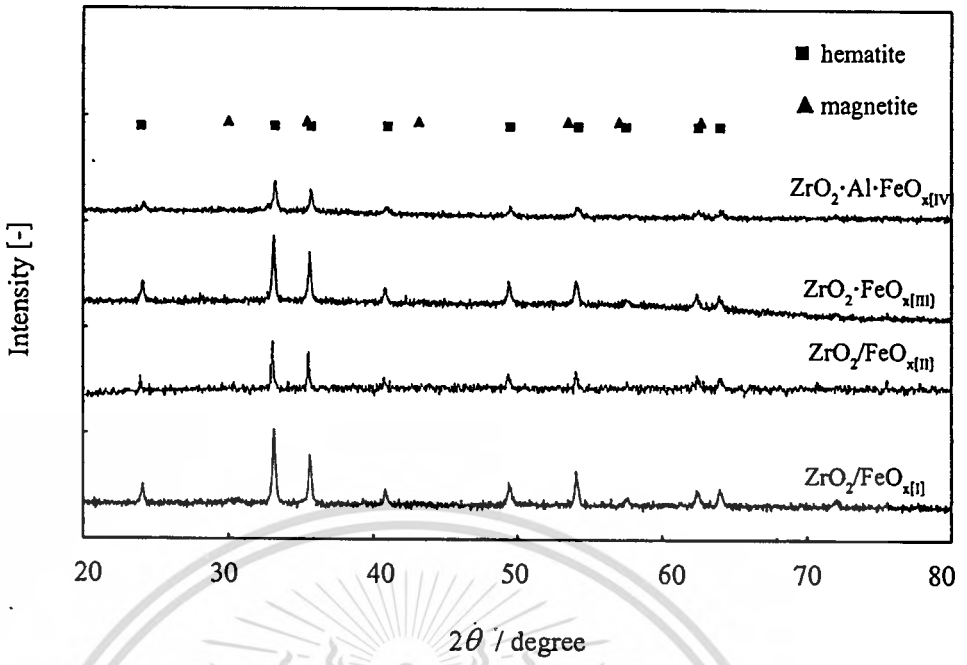

Figure 5.10 XRD pattern of catalyst prior to the reaction

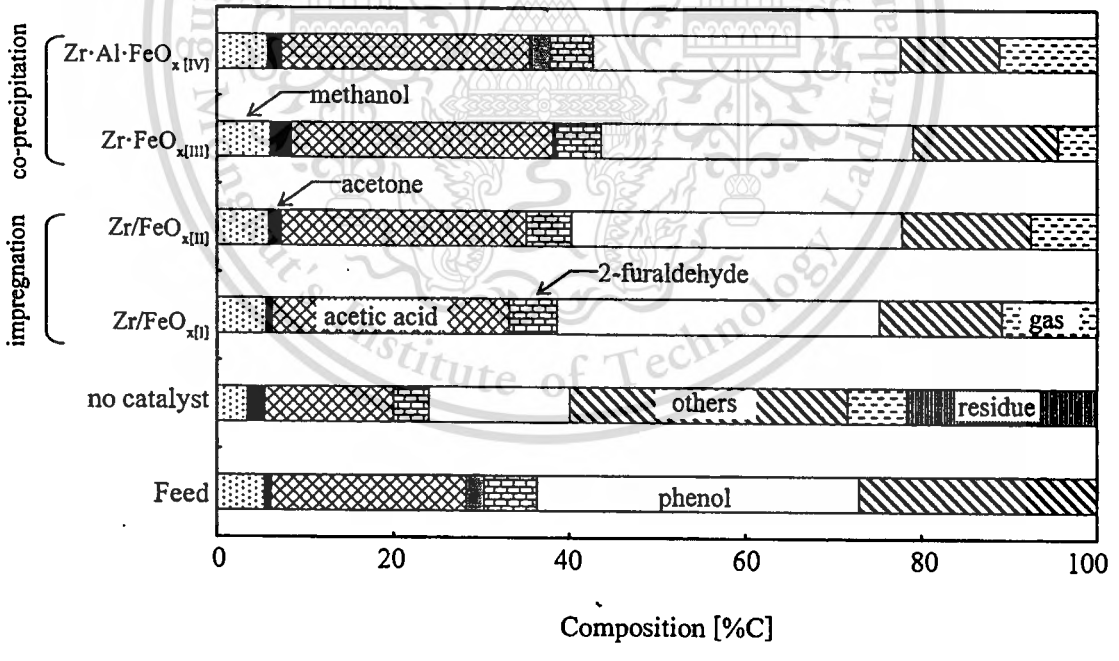

Figure 5.11 Effect of preparation method on product distribution

(T= 673 K, W/F = 2 h, H_2O:F_{oil}= 2:1)

Figure 5.12 shows the roles of each catalytic composition on the oxidative cracking of high molecular weight hydrocarbons over zirconia supporting iron oxide catalyst proposed by Fumoto E. et al [53]. In the first step (step (a)), the high molecular weight hydrocarbons (or palm shell oil in this case) are cracked on the surface of the iron oxide catalyst to produce the small molecule hydrocarbons. The lattice oxygen in hematite structure is consumed and CO_2 is produced. As a result, the catalytic activity decreases due to the loss of lattice oxygen (step (b)). In the case that zirconia exists nearly to the place oxygen were taken, the compensation of oxygen in the lattice can occur and hence the catalytic activity is reactivated as illustrated in steps (c) and (d). The molecule of water in the atmospheric gas is adsorbed on the zirconia and the molecule is cracked to active oxygen and hydrogen species. This active oxygen spills on the surface of iron oxide and moves to the hole that lost the lattice oxygen.

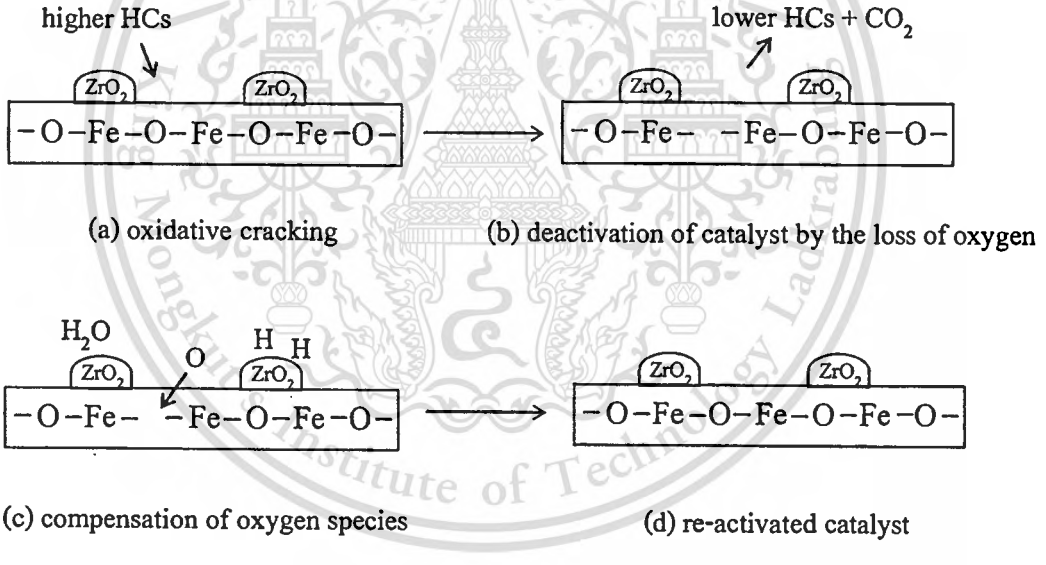

Figure 5.12 Mechanism of the reaction over zirconia supporting iron oxide catalyst

5.2.2 Effect of operating parameters on the Zr·Al·FeO_x performance on palm shell oil upgrading

- Effect of water on product distribution

In order to study the effect of water on the upgrading of palm shell oil, the reaction was carried out for various molar ratios of H_2O to palm shell oil. The reaction test was performed under the standard condition: reaction temperature = 623 K and W/F = 2 h. Figure 5.13 (a) and (b) shows the overall product distribution and the distribution in gas product, respectively. It was found that the addition of water into the bio-oil reduced the methanol decomposition and increased the yield of acetic acid. The gas product mainly consisted of CO_2 due to the oxidative cracking of hydrocarbon in bio-oil and the yield of CO_2 increased by the increasing of H_2O : oil ratio as shown in Figure 5.13 (b). The difference in the product yields was observed when the H_2O to palm shell oil ratio increased from 0 : 1 to 2 : 1 and insignificant when the ratio increased from 2 : 1 to 2.5 : 1. This result indicates that the water existing in the palm shell oil was not enough for the cracking of hydrocarbons. Furthermore, the addition of water into the palm shell oil by the ratio of 2 : 1 could be considered as water in excess condition. Although the performance of Zr·Al·$FeO_{x[IV]}$ for recovering the target chemicals was improved by addition of water, the large excess steam will cause wasteful of energy. Thus, the ratio of 2 : 1 was chosen and set for further investigation.

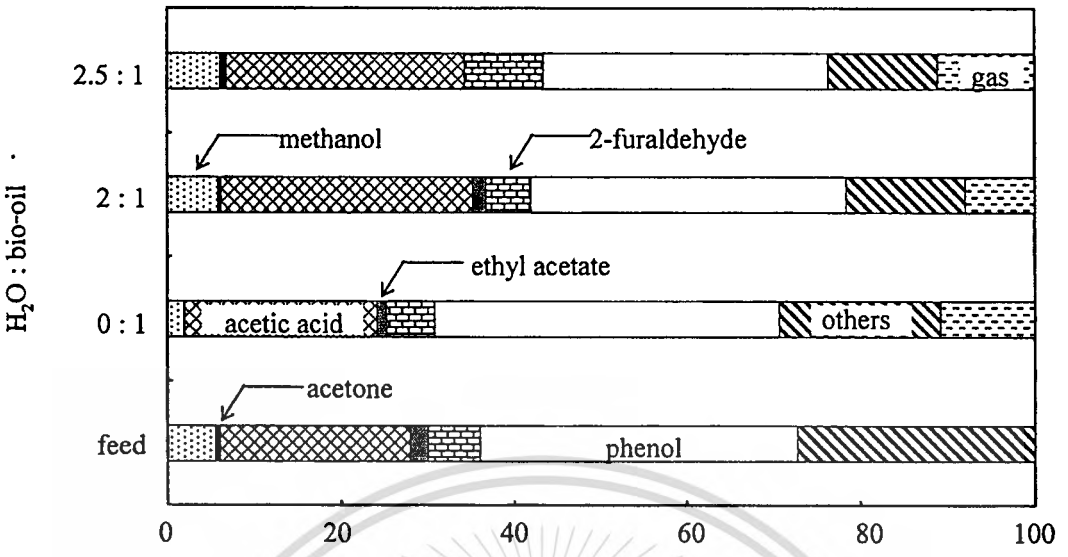

(a)

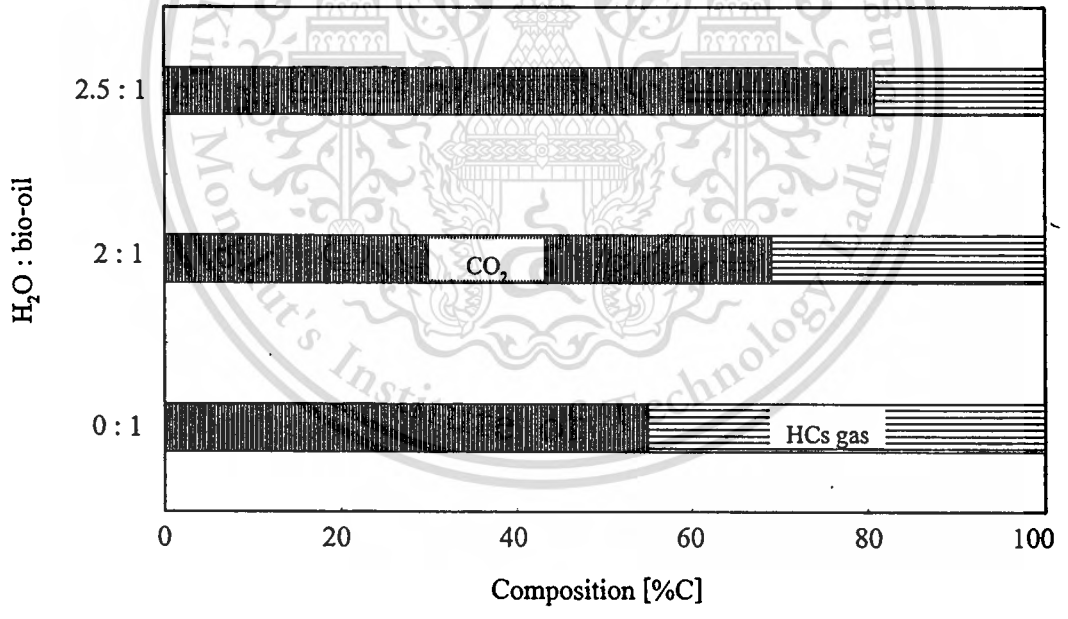

(b)

Figure 5.13 Effect of water on (a) overall product distribution (b) gas product distribution (T = 623 K, W/F = 2 h, $Zr{\cdot}Al{\cdot}FeO_{x[IV]}$ as catalyst)

- Effect of temperature on product distribution

Figure 5.14 shows the effect of reaction temperature on the product distribution at the condition of W/F = 2 h. The increasing of reaction temperature accelerated the complete oxidation of hydrocarbons in the bio-oil to gas mainly CO_2 while the yield of product in liquid product was similarly. At high temperature (723 K) the yield of gaseous product was nearly 50%C so that the recovery of the target compounds in liquid is not efficient. This result indicated that the reaction temperature should not be as high as 723 K. The yield of acetic acid increased by the reaction, whereas, the amount of "others" decreased at lower temperature. This implies that under mild operating condition, some of "others" were converted to acetic acid.

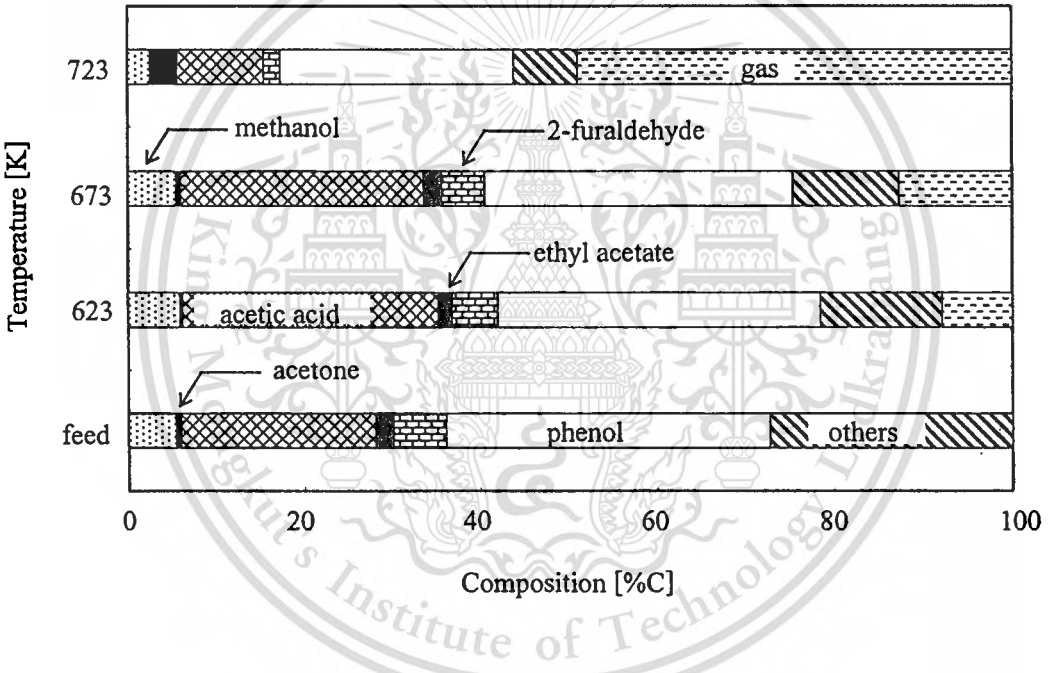

Figure 5.14 Effect of reaction temperature on product distribution

(W/F = 2 h, $Zr{\cdot}Al{\cdot}FeO_{x[IV]}$ as catalyst)

- Effect of time factor (W/F) on product distribution

Figure 5.15 shows effect of time factor on product distribution at 623, 673 and 723 K. The result shows that the yield of "others" decreased with increasing of W/F while the yield of gas increased. This behavior implied that oxidation of "others" finally produced gases. This effect was more obvious when the reaction temperature was high. In the tested range of time factor, the yield of methanol was nearly constant at T = 623 K and decreased with the time factor at higher temperature. This result reveals that the decomposition of methanol over $Zr{\cdot}Al{\cdot}FeO_{x[IV]}$ occurred only when the temperature was high enough. The yield of acetic acid showed the maximum at W/F=2, 2 and 1 h when the temperature was 623, 673 and 723 K, respectively. This result shows the possibility of production of acetic acid from some amount of "others" in the oil and simultaneously decomposition of acetic acid over this catalyst. The trace amount of ethyl acetate was observed and the yield increased by the increasing of W/F at low temperature. The production of ethyl acetate was nearly 0% when W/F increased. This suggested that ethyl acetate was an intermediate of the reaction. At low temperature or W/F, the amount of acetic acid produced from the reaction was higher than that was decomposed. The phenol and methanol yield slightly changed by the time factor.

At the highest temperature (T = 723 K), the amount of all components in liquid product sensitively decreased with increasing of W/F and only gas product was produced. This result reveals that the reaction at 723 K was too severe for recovering all target compounds. From this result, it could be concluded that the optimum condition was T = 623 K and W/F = 6 h which a mixture of methanol 6%C, acetic acid 24%C, acetone 3%C and phenol 36%C was obtained.

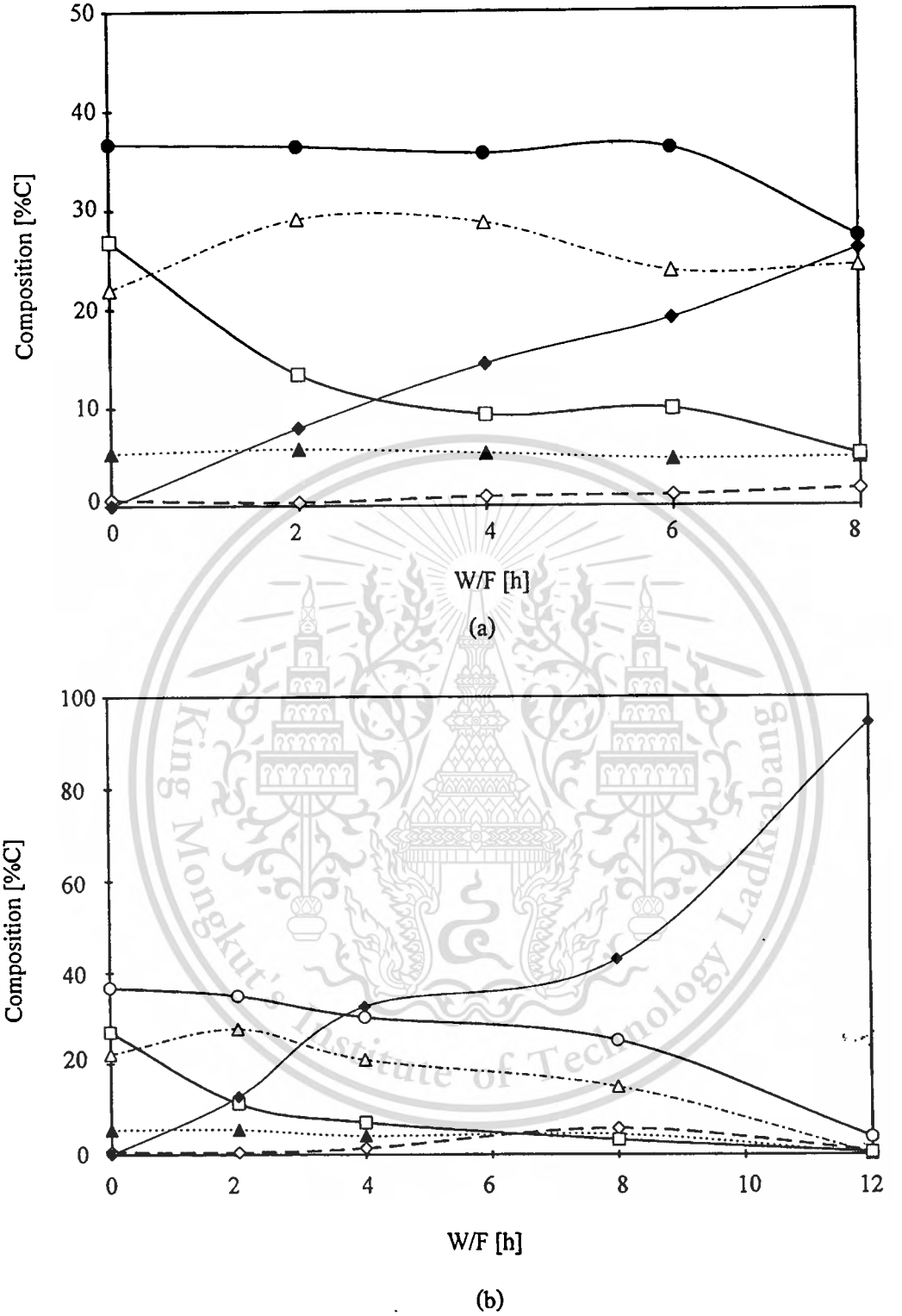

Figure 5.15 Effect of W/F on the product yields obtained from the reaction of palm shell derived oil at (a) 623 K (b) 673 K and (c) 723 K (--▲-- : methanol, —◇— : acetone,--△-- : acetic acid,—○— : phenol, —□— : others in liquid,—◆— : gas)

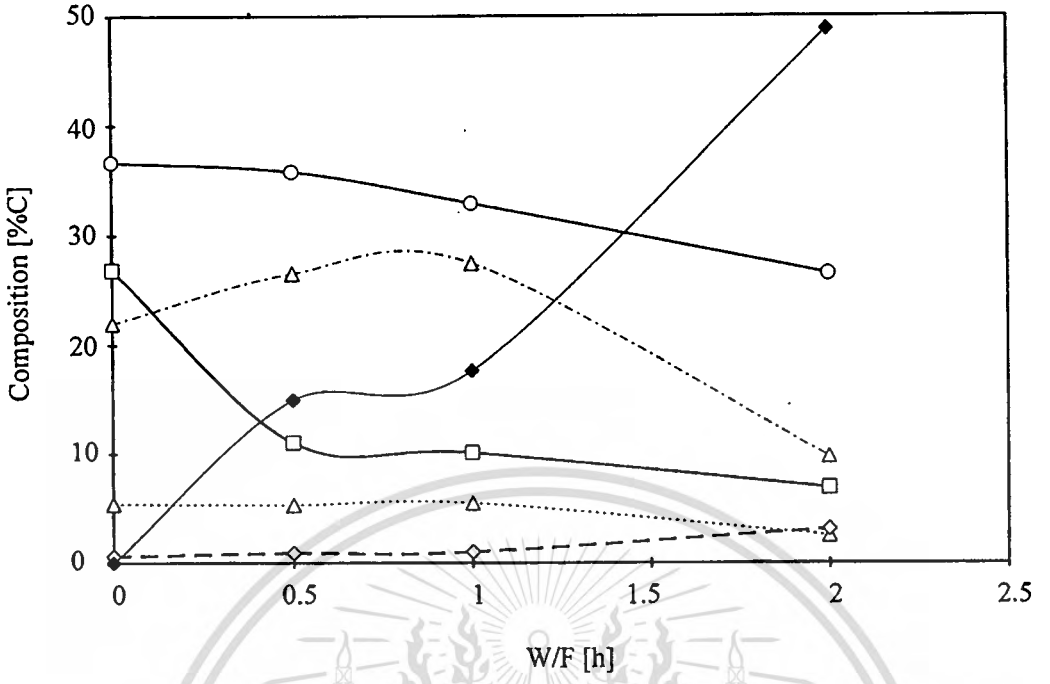

(c)

Figure 5.15 (cont.) Effect of W/F on the product yields obtained from the reaction of palm shell derived oil at (a) 623 K (b) 673 K and (c) 723 K (▲: methanol, ◇: acetone, △: acetic acid, ○: phenol, □: others in liquid, ◆: gas)

5.2.3 Improving of the zirconia supporting iron oxide catalyst

One of the key factors on the activity of catalyst is the surface area of catalyst. Therefore, the improving of catalyst by increasing surface area should be considered. Uddin et al. [50] investigated the effects of iron precursor and precipitating agent on the physical- and chemical properties of iron oxide catalyst. They found that precipitation of nitrate salt with aqueous urea solution gave an iron oxide catalyst with a high surface area. The effect of precursor salts for catalyst preparation on activity of catalyst was also investigated in this research.

Table 5.8 summarizes BET surface area of the modified catalysts. The surface area of the catalyst prepared from nitrate salt was higher than that of the catalyst prepared from chloride salt by 2.3 times and slightly higher than the catalyst obtained from chloride salt with the addition of Al. It can be concluded that the use of nitrate salt as a precursor for the catalyst preparation

should be more effective than the $ZrO_2 \cdot Al \cdot FeO_{x[IV]}$ in terms of the increase in the surface area of catalyst. Figure 5.16 shows the XRD pattern of catalyst prepared from nitrate salts compared with the former catalyst. The XRD pattern of $ZrO_2 \cdot FeO_{x[V]}$ catalyst show hematite structure indicating that the type of precursor salt has no effect on the crystalline structure of catalyst.

Table 5.8 BET surface area of catalyst

Catalyst	Precursor salt	Surface area (m^2/g)
$ZrO_2 \cdot FeO_{x[III]}$	Chloride salt	25.41
$Zr\text{-}Al\text{-}FeO_{x[IV]}$	Chloride salt	54.32
$ZrO_2 \cdot FeO_{x[V]}$	Nitrate salt	56.91

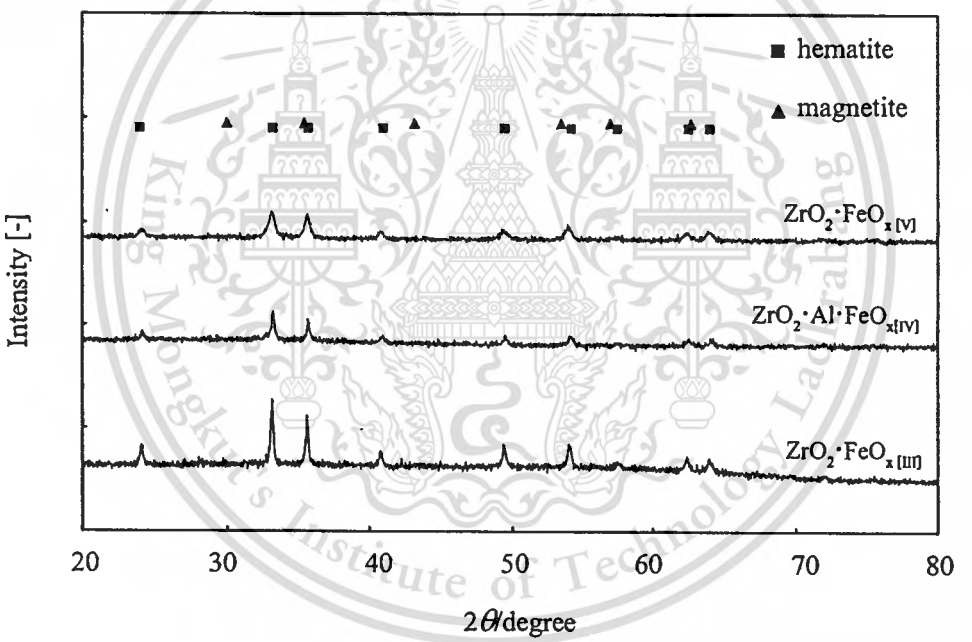

Figure 5.16 XRD pattern of modified catalyst

Figure 5.17 shows the product distribution for the reaction of bio-oil over the modified catalyst at temperature was 673 K and W/F was 2 h. The $ZrO_2 \cdot FeO_{x\,[IV]}$ shows highest activity compared with the catalyst obtained from chloride salt. The large amount of gaseous product was observed while "others" and acetic acid remarkably reduced. It was interesting that acetone was produced as the main product. In order to gain the insight into the reaction route, the reaction of model compound will be examined in section 5.3.

Due to the high surface area and reactivity of $ZrO_2 \cdot FeO_{x[V]}$ catalyst, then $ZrO_2 \cdot FeO_{x[V]}$ will be used as the catalyst for upgrading of dried sludge derived oil in the next section.

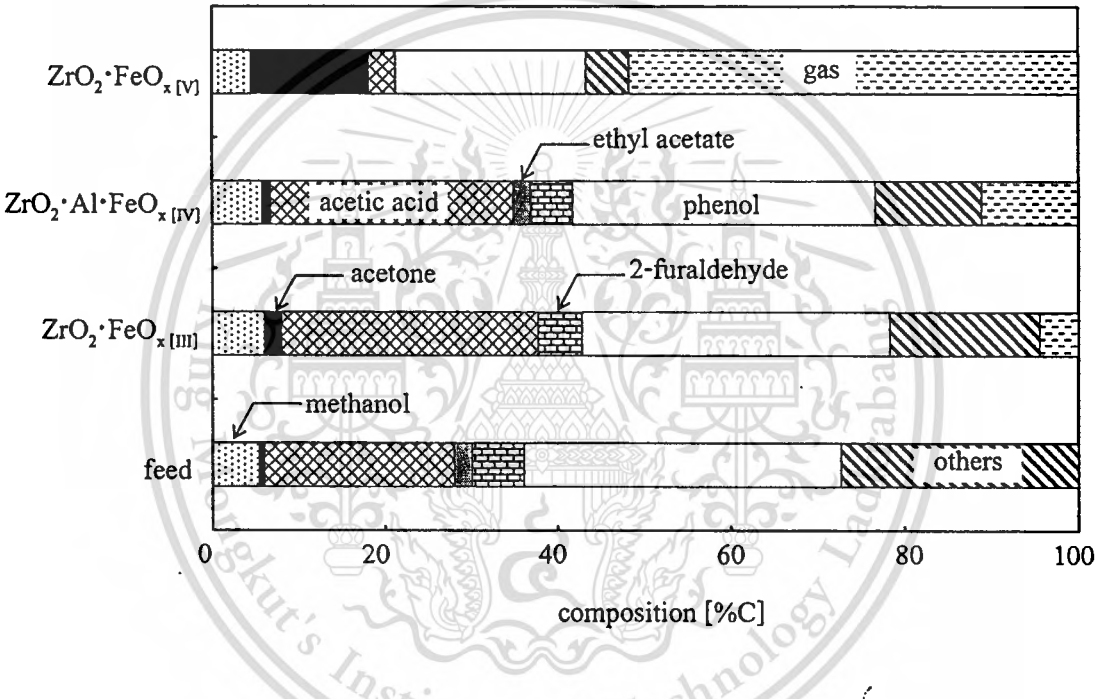

Figure 5.17 Effect of precursor salts on product distribution

5.2.4 Catalytic upgrading of dried sludge derived bio-oil over $ZrO_2 \cdot FeO_{x[V]}$

The liquid products obtained by pyrolysis of dried sludge contained aqueous and oil phases. In this study, these liquids were named as "DSO-aqueous" and "DSO-oil", respectively. The reaction test over the $ZrO_2 \cdot FeO_{x[V]}$ was performed separately for each phase.

Catalytic upgrading of aqueous phase

Figure 5.18 shows the effect of time factor on product yields at 513, 583, 593 and 643 K. The results show that the yield of "others" remarkably decreased with W/F while the yield of gas and coke increased. The simultaneous increase of gas and the decrease of others indicated that the others could be oxidized to produce CO_2 which was the final products of this reaction and the rate of oxidation increased when the reaction temperature increased. In the addition, the yield of coke was decreased as the temperature increased. This behavior showed the oxidation of carbon was accelerated at the higher temperature. The yield of methanol was slightly changed by the increasing of W/F and the temperature was not high enough for methanol decomposition in this temperature range. The decreasing of acetic acid as well as the increasing of acetone yields took place at the lower of W/F then the yield of acetone continuously decreased at higher of W/F. It can be supposed that the high productivity of acetone in this study resulting from the oxidation of acetic acid which was initial component in DSO-aqueous. The decreasing of acetone yield after reaching the maximum value was more pronounced at the higher temperature (T > 593 K). The highest yield of acetone was obtained at W/F was 2 h and reaction temperature was 593 K. This condition was used for determining the suitable condition of the DSO-aqueous reaction.

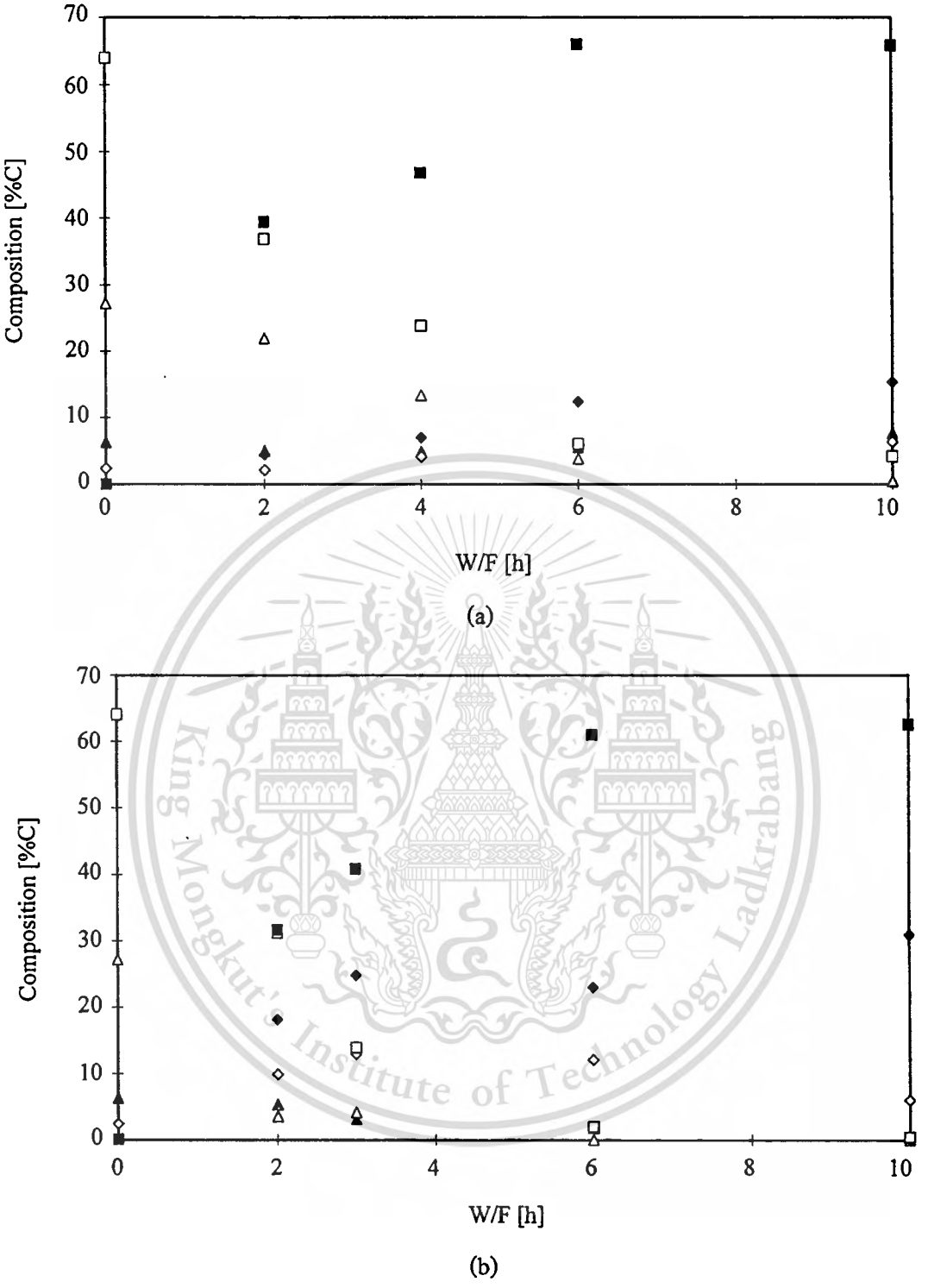

Figure 5.18 Effect of W/F on the product yields obtained from the reaction of DSO-aqueous at (a) 513 K (b) 583 K (c) 593 K and (d) 643 K (▲ : methanol, ◇ : acetone, △ : acetic acid, □ : others in liquid, ◆ : gas, ■ : residue)

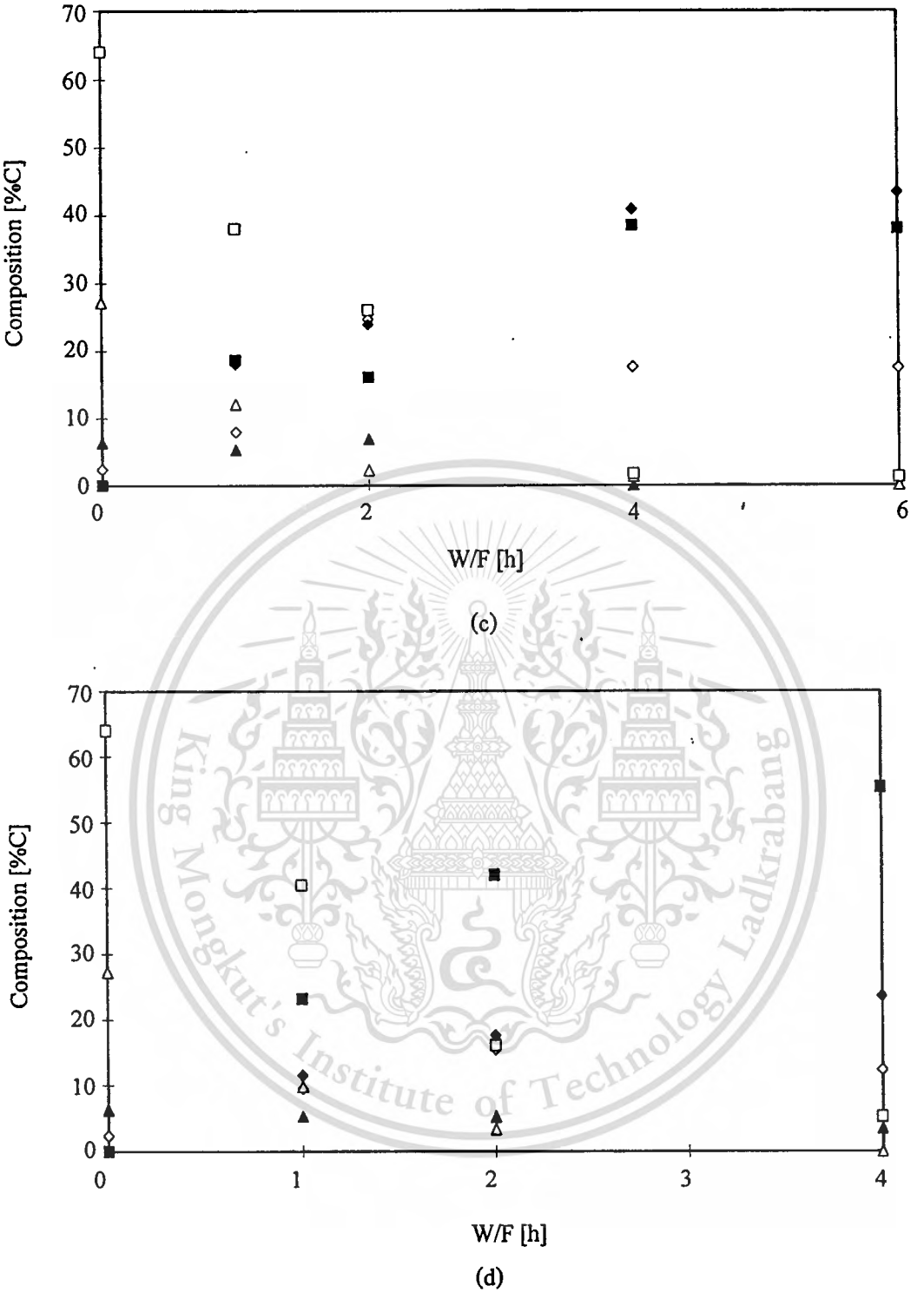

Figure 5.18 (cont.) Effect of W/F on the product yields obtained from the reaction of DSO-aqueous at (a) 513 K (b) 583 K (c) 593 K and (d) 643 K
(▲ : methanol, ◇ : acetone, △ : acetic acid, □ : others in liquid, ◆ : gas, ■ : residue)

Catalytic upgrading of oil phase

The reaction of DSO-oil was carried out in the temperature range of 593 - 723 K and W/F range of 0.25 – 8 h. Figure 5.19 shows the effect of W/F on the product yields at the difference of temperature. An increasing of coke with the W/F was observed in this temperature range. However, amount of coke decreased when the reaction temperature increased. For instance, the coke reduced from 45 %C to 38 %C when the reaction temperature increased from 593 K to 723 K at W/F of 6 h. It is implied that the increasing of temperature accelerated the oxidation rate of solid carbon to CO_2. High amount of phenol was obtained as the main product from the reaction of oil phase, whereas m-cresol and acetone were slightly produced. In addition, the yield of m-cresol was nearly constant for this range of reaction temperature. The results show that m-cresol was thermally stable and should be considered as one of the target products for recovery because it is a high value chemical. At lower temperature (593 K), the yield of some useful chemicals i.e. acetone and phenol reached the maximum at the W/F was 6 h and then remarkably decreased at higher W/F. The total liquid yield was gradually decreased by W/F whereas gaseous was simultaneously produced. This behavior was also found at the higher temperature (T = 723 K), however, the maximum yield of phenol was shifted to the lower of W/F. The highest yield of phenol (10 %C) was observed when W/F was 4 h. At the reaction temperature was 693 K, the useful chemical was continuously decreased when the W/F increased. Even though the high amount of phenol (19 %C) was obtained at W/F = 0.25 h the recovery of total useful chemicals was lower than those of the useful chemicals obtained from T = 593 K and W/F = 6 h. Furthermore, the unidentified chemical was much higher compared to the earlier condition. It could be concluded that the suitable condition for the reaction of DSO-oil was T = 593 K and W/F = 6 h. Under this condition, the 5.2 %C of acetone, 11.7 %C of phenol and 1.2 %C of m-cresol were produced.

The useful chemical obtained from the best condition from the reaction of DSO-oil and DSO-aqueous was shown in Table 5.9.

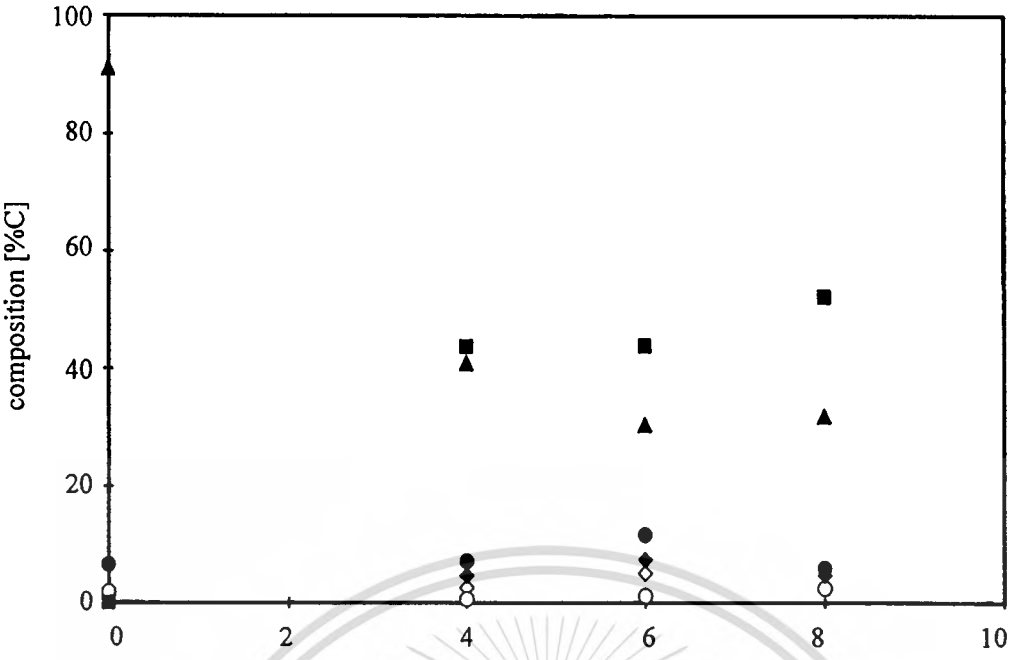

(a)

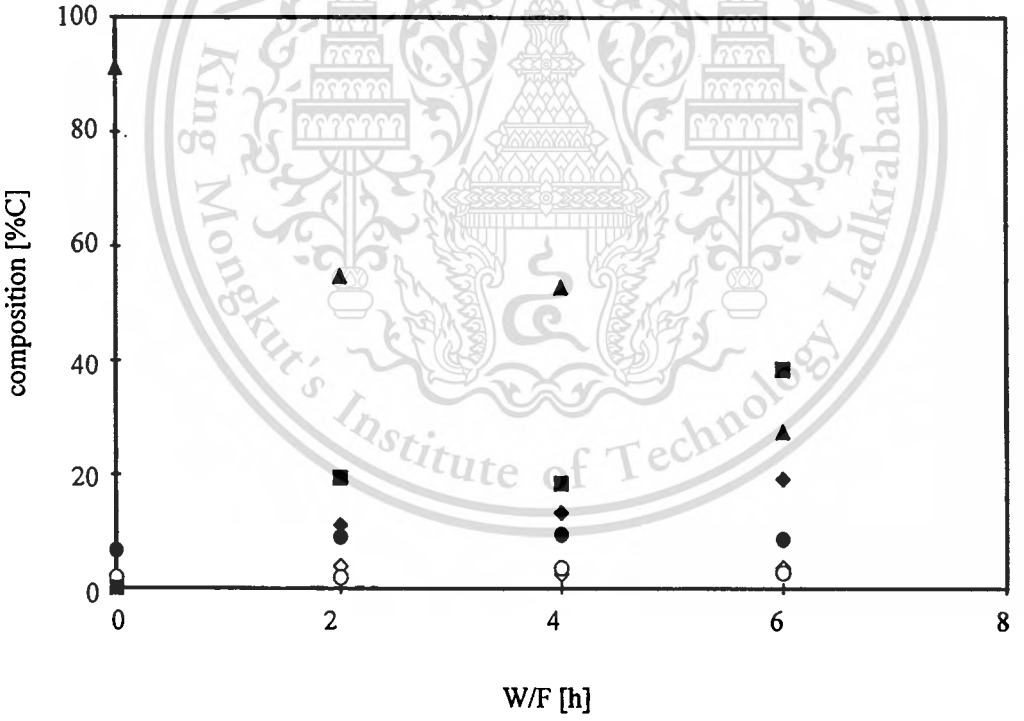

(b)

Figure 5.19 Effect of W/F on the product yields obtained from the reaction of DSO-oil at (a) 593 K (b) 693 K and (c) 723 K

(○ : m-cresol, ● : phenol, ◇ : acetone, ▲ : others in liquid, ◆ : gas, ■ : residue)

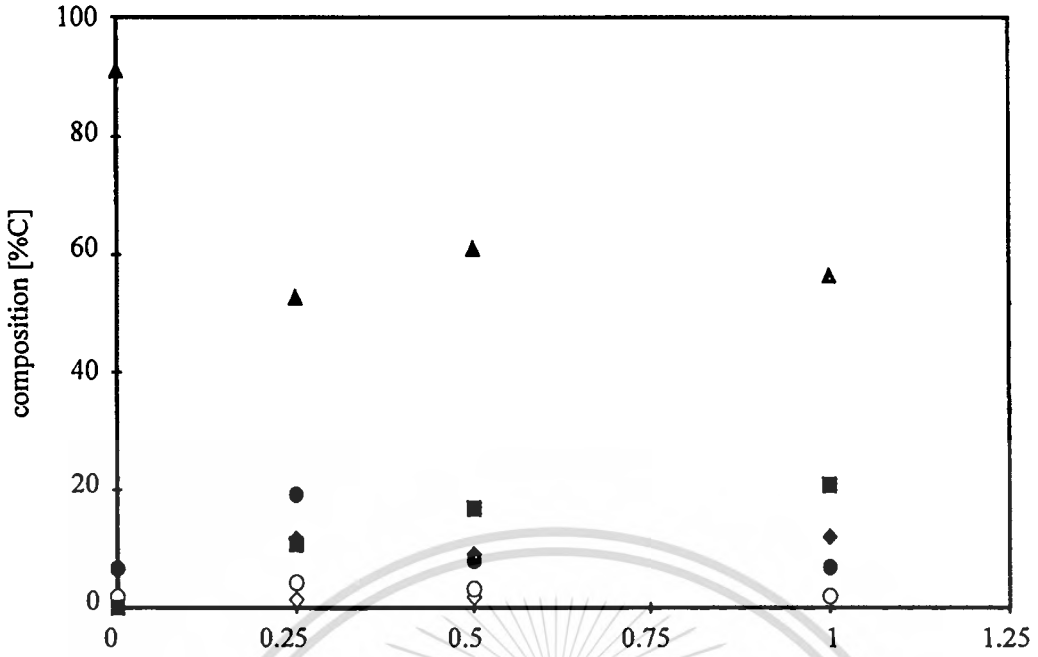

(c)

Figure 5.19 (cont.) Effect of W/F on the product yields obtained from the reaction of DSO-oil at (a) 593 K (b) 693 K and (c) 723 K
(○ : m-cresol, ● : phenol, ◇ : acetone, ▲ : others in liquid, ◆ : gas, ■ : residue)

Table 5.9 The useful chemical obtained from the best condition

component	%C recovery	
	DSO-oil	DSO-aqueous
Methanol	-	6.88
Acetone	5.15	24.71
Acetic acid	-	2.27
Phenol	11.74	-
m-cresol	1.23	-
others in liquid	30.56	26.11
gas	7.44	23.93
residue	43.88	16.1

5.3 Reaction of Model compound

The main components existing in the bio-oil were selected to study the individual reaction over zirconia supporting iron oxide catalyst. Acetic acid, acetone and methanol were selected as representative of carboxylic acids, ketones and alcohols, respectively. Based on the experimental results of each compound, the reaction pathways were proposed. The reaction undergoes under the plug flow behavior. The kinetic parameters (rate constant of reaction and activated energy) were calculated on the assumption of each reaction step was the first order reaction. The kinetic parameters for each reaction could be evaluated from the equation;

$$Rate = \frac{df_i}{d(W/F)} \tag{5.1}$$

The Arrhenius equation was applied to calculate the activation energy;

$$k = \exp\left(\frac{-E_a}{RT}\right) \tag{5.2}$$

5.3.1 Reaction of acetic acid

Acetic acid was selected as the model compound to represent the reactivity of the reaction of carboxylic acid over zirconia supporting iron oxide catalyst. Furthermore, acetic acid is one of the major components in bio-oil as well. Thus, the investigation on the reaction of acetic acid is necessary. The reaction of acetic acid over several types of catalyst was studied by many researchers. It has been reported that acetone was produced via the ketonization of acetic acid over several oxide catalysts [55,60],

$$2CH_3COOH \longrightarrow (CH_3)_2CO + H_2O + CO_2 \tag{5.3}$$

In the presence of water, steam reforming of acetic acid and acetone occurred as following reaction [60],

$$CH_3COOH + 2H_2O \longrightarrow 4H_2 + 2CO_2 \tag{5.4}$$

$$(CH_3)_2CO + 5H_2O \longrightarrow 8H_2 + 3CO_2 \tag{5.5}$$

Furthermore, at high reaction temperature the thermal decomposition of acetic acid and the Boudouard reaction occurred simultaneously [55],

$$CH_3COOH \text{ or } (CH_3)_2CO \longrightarrow C_2H_4, C_2H_6, C_3H_4, \text{coke}, \ldots \quad (5.6)$$

$$2CO \longrightarrow CO_2 + C \quad (5.7)$$

Figure 5.20 shows the effect of W/F on product distribution for the reaction of acetic acid over ZrO_2·$FeO_{x[V]}$ at the reaction temperature of 573, 623 and 673 K. The yield of acetone increased with increasing W/F to the maximum value and then gradually decreased with increasing W/F. The yield of CO_2 continuously increased with the increasing W/F. These results imply that acetone is an intermediate and CO_2 is the final product of the reaction.

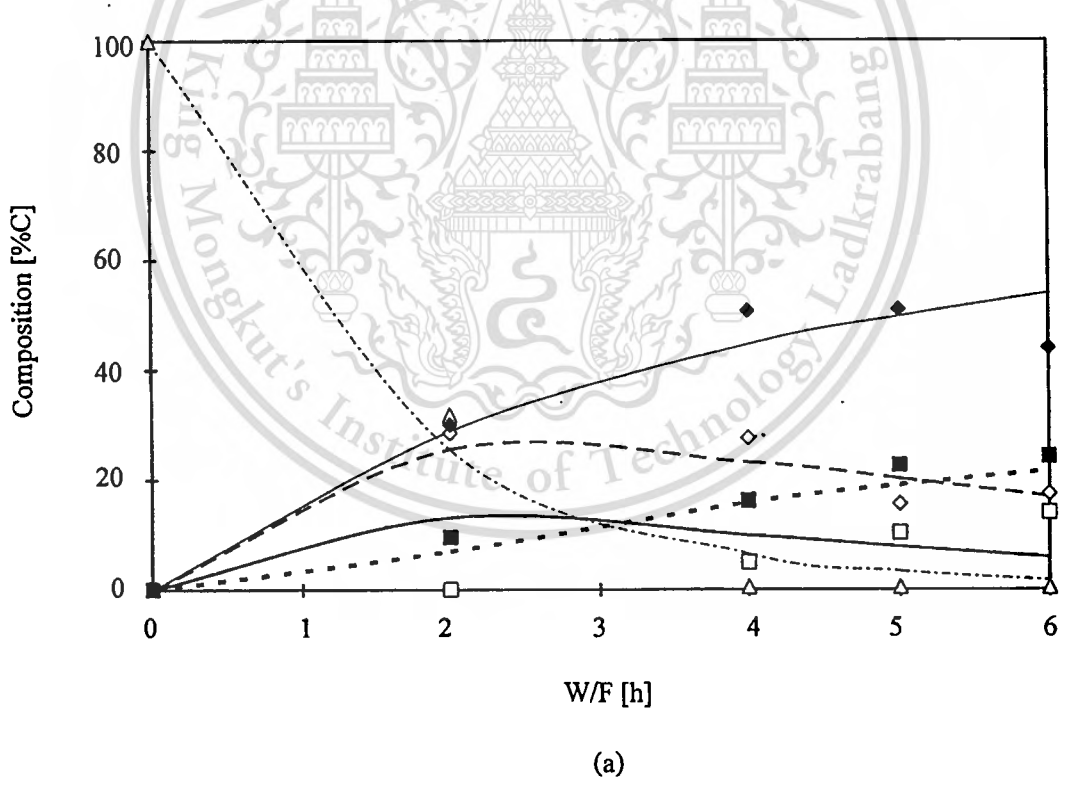

(a)

Figure 5.20 Effect of W/F on the product distribution of acetic acid at (a) 573 K (b) 623 K and (c) 673 K

(△ , ·····) : acetic acid, (◇ , - -) : acetone, (◆ , ——) : CO_2, (□ , ——) : HCs gas, (■ , ·····) : residue

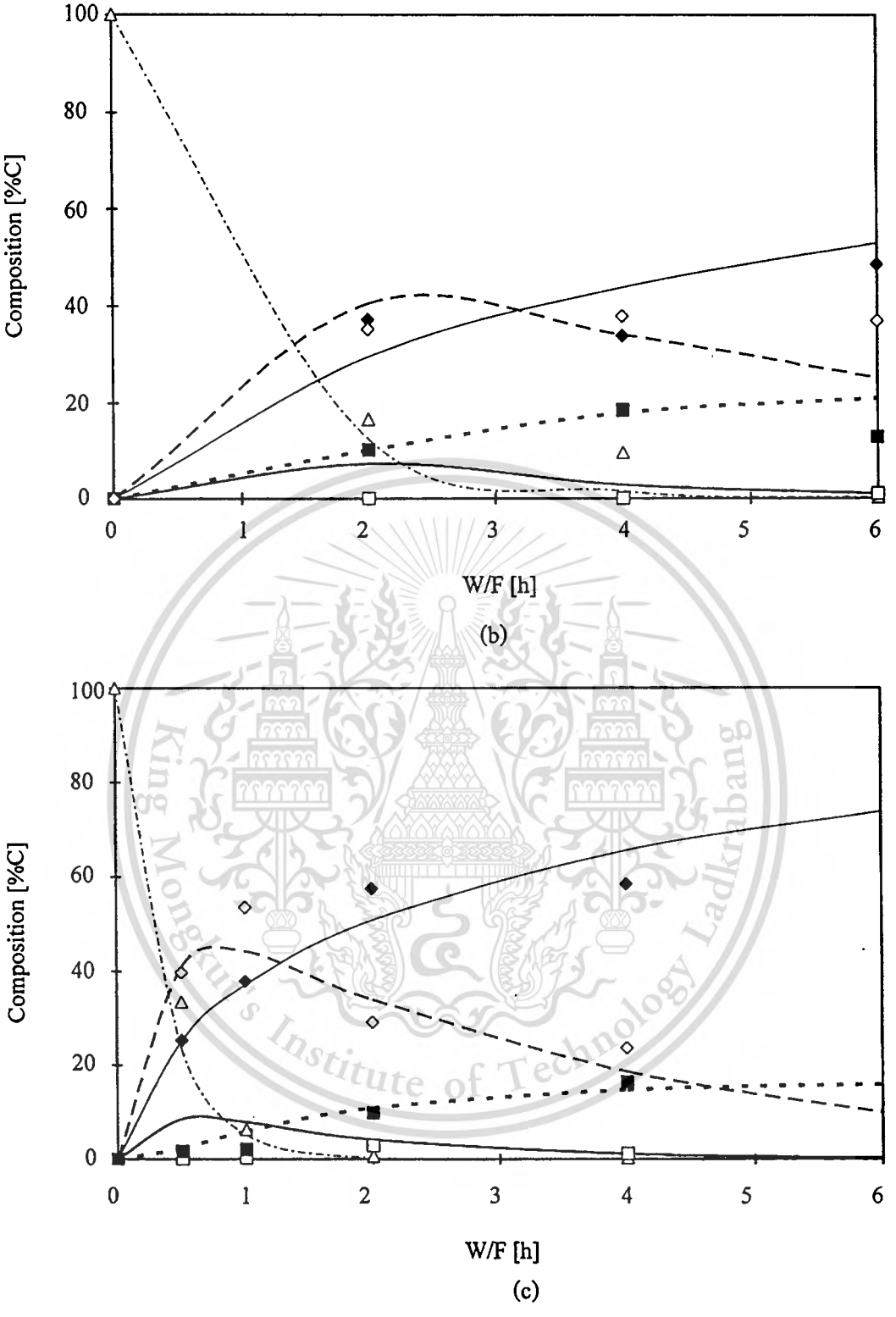

Figure 5.20 (cont.) Effect of W/F on the product distribution of acetic acid at (a) 573 K (b) 623 K and (c) 673 K

(△ , ·····) : acetic acid, (◇ , – –) : acetone, (◆ , ——) : CO_2, (□ , ——) : HCs gas, (■ , ·····) : residue

According to the experimental results and the reaction described previously (eq. 5.3 – 5.7), the reaction pathway of acetic acid was proposed as shown in Figure 5.21. The kinetic parameters estimated based on the proposed reaction pathway was listed in Table 5.10. The trend of product distribution as showed by line was compared with the experimental value in Figure 5.20. It is observed that the proposed pathway with its parameters was reasonably predicted the behavior of the reaction of acetic acid over the $ZrO_2 \cdot FeO_{x[V]}$ catalyst.

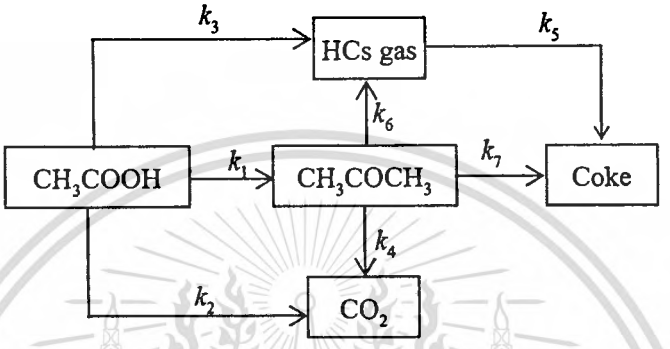

Figure 5.21 Reaction pathway of acetic acid

Table 5.10 Kinetics parameters for reaction of acetic acid

step	k_0 (s^{-1})	E_a (kJ/mol)
1	3×10^4	55.20
2	1.59×10^3	43.55
3	31.19	25.04
4	2.18	12.13
5	71.52	24.92
6	3.74	35.60
7	0.01	1.68

As the data showed in Table 5.10, the low activation energy of solid carbon formation step was observed implying that the reaction temperature had slight effect on the solid carbon formation. The highest activation energy for the formation of acetone indicated that this reaction was strongly sensitive to the temperature, however, the reaction was limited by the formation of gaseous product due to the relatively high activation energy of the CO_2 and HCs gas formation step (43.55 and 36.6 kJ/mol, respectively).

5.3.2 Reaction of acetone

Acetone was selected as the model compound to represent the reactivity of the reaction of carbonyl-containing group i.e. ketones and aldehydes. The main reactions of acetone in the presence of water were steam reforming and thermal decomposition of acetone itself according to reaction (5.5) and (5.6), respectively [55].

$$(CH_3)_2CO + 5H_2O \longrightarrow 8H_2 + 3CO_2 \quad (5.5)$$

$$(CH_3)_2CO \longrightarrow C_2H_4, C_2H_6, C_3H_4, \text{coke}, \ldots \quad (5.6)$$

Figure 5.22 shows the effect of W/F on product distribution of the reaction of acetone. CO_2 and hydrocarbon gas were mainly produced as well as coke formation. The yield of CO_2 increased with the increase of W/F. For all reaction temperature, the yield of HCs gas slightly increased with the increasing of W/F at the lower W/F. Contrarily, the yield of HCs gradually decreased at higher W/F. It implied that acetone decomposed into the lower molecule hydrocarbons and these hydrocarbons was further oxidized to CO_2. The decreasing of coke formation was observed as the reaction temperature increased, whereas CO_2 significantly increased with the increase temperature. The proposed reaction pathway and kinetic parameters of the reaction of acetone were obtained by the incorporation of the experimental data and the above equation. The reaction pathway shows in Figure 5.23 and kinetic parameter was listed in Table 5.11.

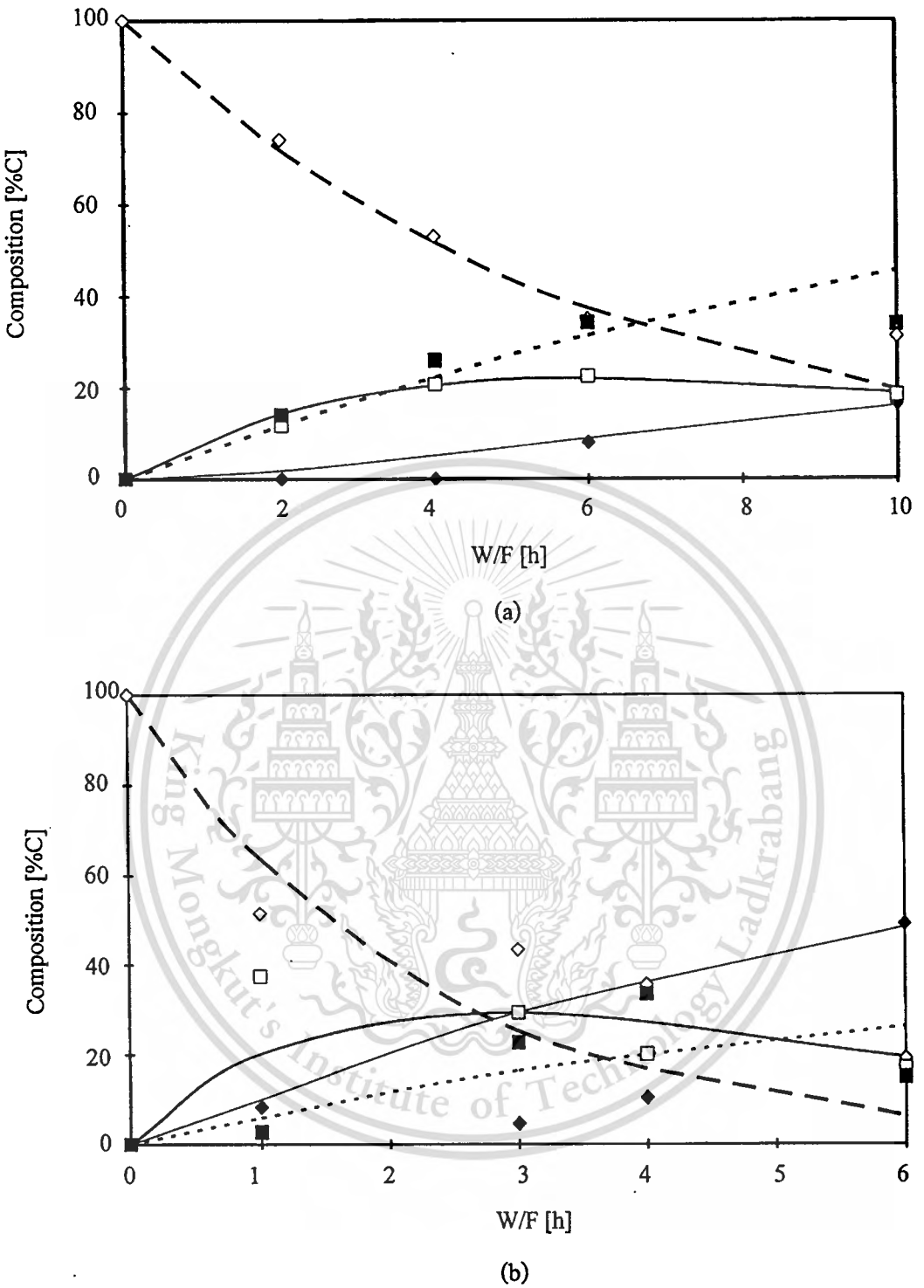

Figure 5.22 Effect of W/F on the product distribution of acetone at (a) 573 K (b) 623 K and (c) 673 K (◇ , — - : acetone), (◆ , —— : CO_2), (□ , —— : HCs gas, (■ , ····· : residue)

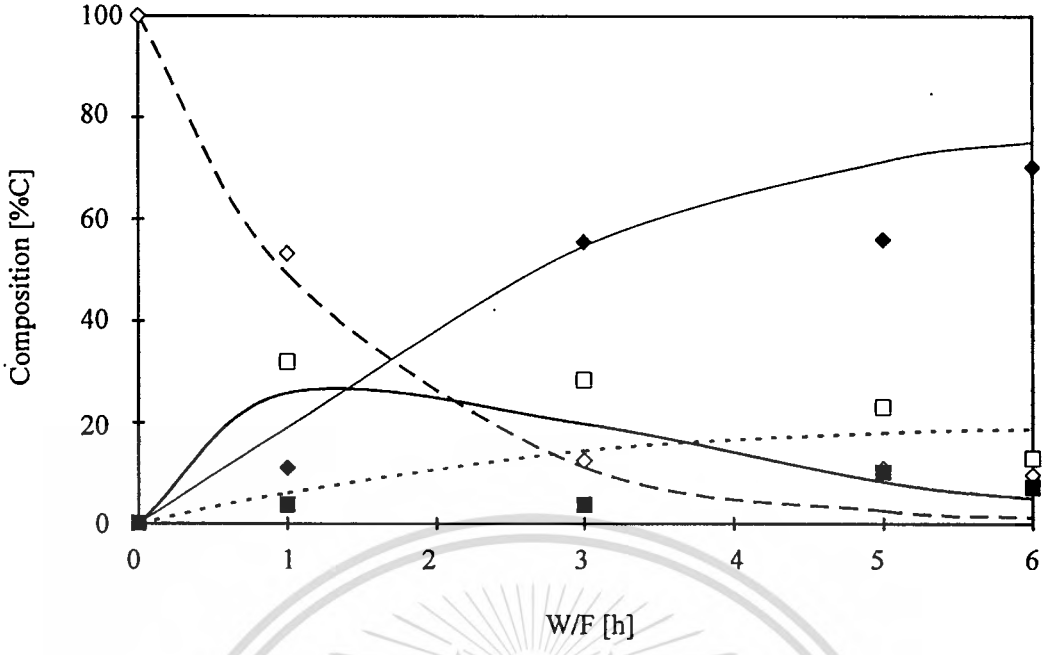

(c)

Figure 5.22 (Cont.) Effect of W/F on the product distribution of acetone at (a) 573 K (b) 623 K and (c) 673 K (◇ , — - : acetone), (◆ , —— : CO_2), (□ , —— : HCs gas, (■ , ····· : residue)

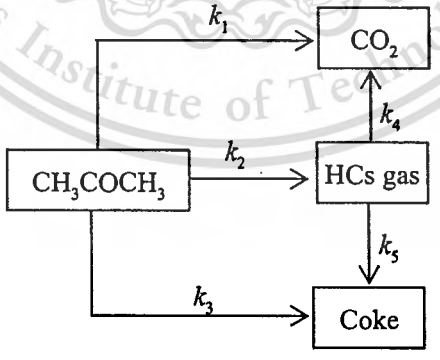

Figure 5.23 Reaction pathway of acetone

Table 5.11 Kinetics parameters for reaction of acetone

step	k_0 (s^{-1})	Ea (kJ/mol)
1	8.16×10^8	122.75
2	4.56×10^3	53.22
3	0.1	2.58
4	3.19×10^4	61.60
5	0.18	3.37

The highest activation energy of the CO_2 step (122.75 kJ/mol) indicating the steam reforming became more important as the increasing of the reaction temperature. Similarly to the reaction of acetic acid, the solid carbon formation step had less sensitivity to the reaction temperature due to the lowest reaction temperature.

5.3.3 Reaction of methanol

Methanol was selected as the model compound to represent the reactivity of the reaction of alcohol. The reaction of methanol itself has been widely investigated because it is an important alternative energy source [24]. Similarly to the reaction of acetone, the main reactions of methanol in the presence of water were steam reforming and thermal decomposition as the following reactions [24,61];

$$CH_3OH + H_2O \longrightarrow CO_2 + 3H_2 \quad (5.8)$$

$$CH_3OH \longrightarrow CO + 2H_2 \quad (5.9)$$

$$CO + H_2O \longrightarrow CO_2 + H_2 \quad (5.10)$$

Figure 5.24 shows effect of W/F on product distribution. Gaseous products i.e. CH_4 and CO_2 were produced. CO was not observed in this study indicating the produced CO probably reacted with steam via water-gas shift reaction to produce CO_2 (eq. 5.10). In the addition, the small amount of H_2 was detected (H_2 yield was not shown) implying that H_2 was used to reduce CH_3OH into CH_4. The reaction pathway of methanol decomposition over $ZrO_2 \cdot FeO_{x[V]}$ catalyst is shown in Figure 5.25 and estimated kinetic parameters is shown in Table 5.12.

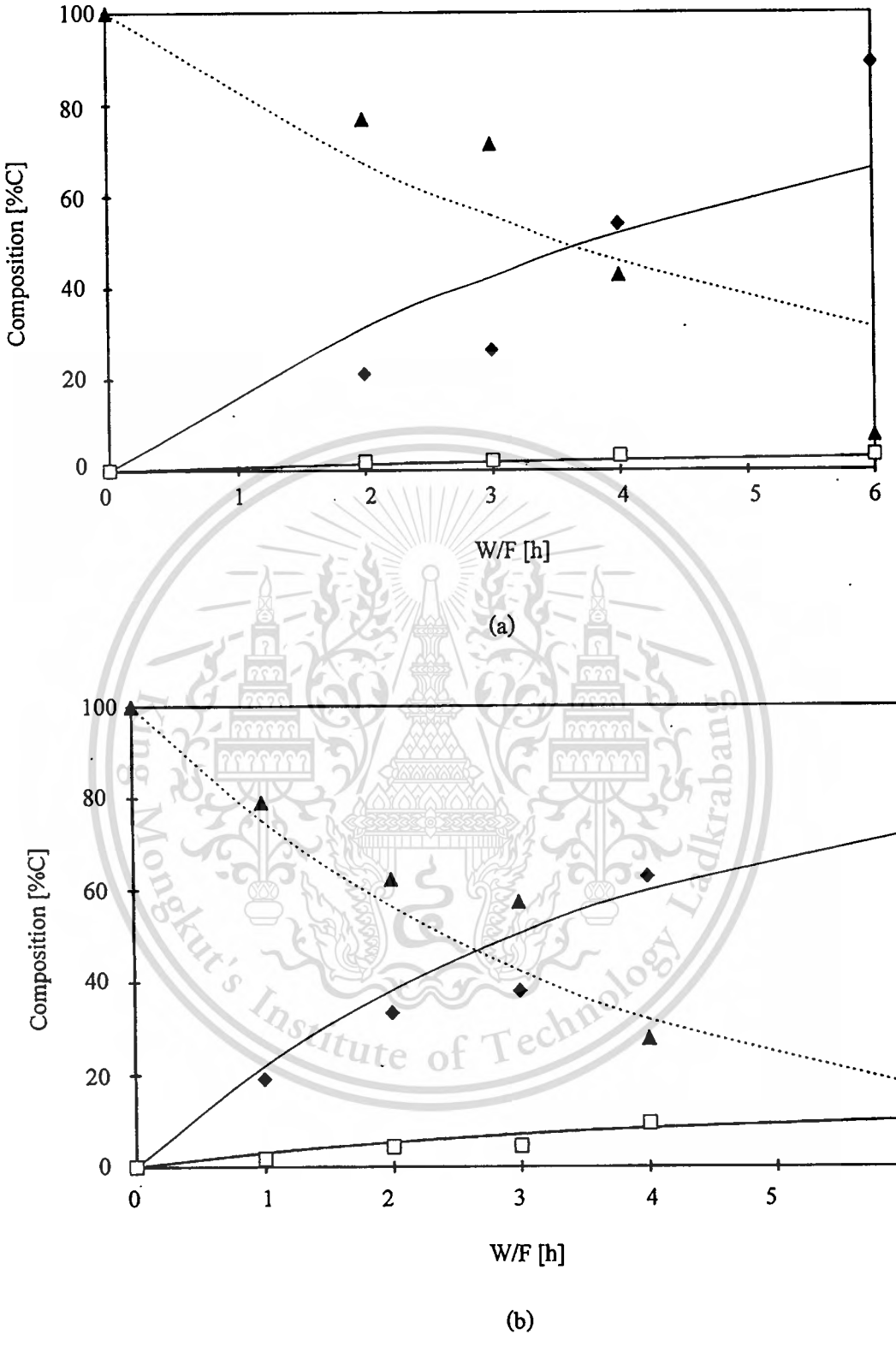

Figure 5.24 Effect of W/F on the product distribution of methanol at (a) 573 K (b) 623 K and (c) 673 K

(▲ , ------) : methanol, (◆ , —— : CO_2), (□ , —— : CH_4)

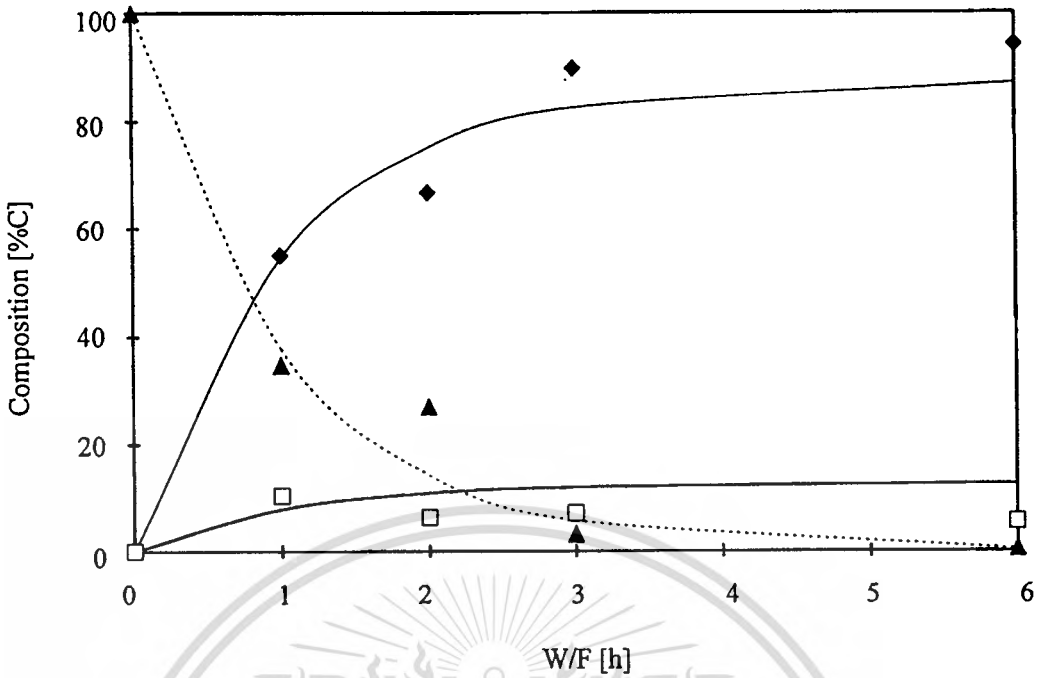

(c)

Figure 5.24 (Cont.) Effect of W/F on the product distribution of methanol at (a) 573 K (b) 623 K and (c) 673 K
(▲ , ------) : methanol, (◆ , —— : CO_2), (□ , —— : CH_4)

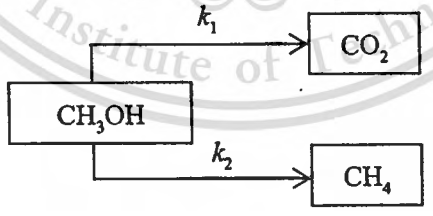

Figure 5.25 Reaction pathway of methanol

Table 5.12 Kinetics parameters for reaction of methanol

step	k_0 (s^{-1})	E_a (kJ/mol)
1	3.34×10^3	47.44
2	6.64×10^5	86.85

The activation energy of CH_4 formation step was larger than that of CO_2 formation step about 2 times indicating that the steam reforming of methanol was more sensitive to the reaction temperature. In the case of the reaction of methanol, no formation of solid carbon was observed due to the absent of C – C bond in the molecular structure of methanol.

5.4 Proposed reaction pathway of bio-oil and kinetics parameter estimation

It is known that the bio-oil is composed of several hydrocarbon compounds. Therefore, it is difficult to exactly predict the product distribution during the upgrading of bio-oil over $ZrO_2 \cdot FeO_{x[V]}$ catalyst. In section 5.3, the information on the reaction pathway with kinetic parameters of the main components of bio-oil i.e. methanol, acetone and acetic acid was obtained.

In this section, the reaction of aqueous phase of bio-oil obtained from pyrolysis of dried sludge was selected as model bio-oil. The reaction pathway of bio-oil was proposed base on the experimental data and the information obtained from the reaction of model compounds. As the reaction of model compounds, it was found that acetic acid mostly converted to acetone, CO_2 and coke. The large amount of CO_2 including some hydrocarbon gases and coke were produced when acetone was used as the feedstock. Methanol converted to CO_2 and CH_4 without coke formation. Therefore, the reaction pathway was proposed as shows in Figure 5.26.

Table 5.13 shows the pre-exponential factor (k_0) and activation energy (E_a) of the reaction of bio-oil which obtained from the plot of ln k_i versus 1/T by the least squares method. The experimental data and estimated results of product distribution of the reaction of bio-oil over $ZrO_2 \cdot FeO_{x[V]}$ catalyst is shown in Figure 5.27. The acceptable fit of the estimated and experimental results indicating that the simple first-order kinetics model was reliable to predict the conversion of bio-oil over $ZrO_2 \cdot FeO_{x[V]}$ catalyst.

The reaction scheme in Figure 5.26 suggests that the main reaction of the hydrocarbons in the bio-oil correspond to the steam reforming, ketonization, water-gas shift reaction and thermal cracking. Regarding the estimated activation energy, it was found that the activation energy varied in the wide range between 9 – 92 kJ/mol. The highest activation energy was observed for the formation of gaseous product from acetic acid (92 kJ/mol) this value was higher than that those obtained from the formation of acetone (85.62 kJ/mol). It is indicate that the reaction of acetic acid to gas becomes a dominant factor at the higher temperature and the acetone

production was limited. In the addition, at high temperature, the formation of solid carbon probably occurred due to the decomposition of acetic acid itself because the activation energy of step 4 was higher than step 7. The relatively low activation energy of the solid carbon formation from "others" was observed (9.35 kJ/mol) implying that most of hydrocarbons favorably formed to volatile products at high temperature.

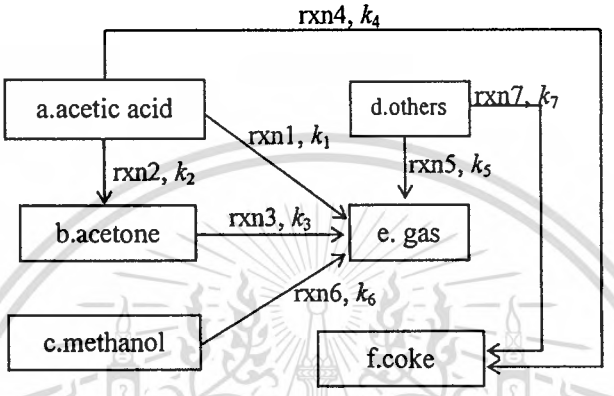

Figure 5.26 Proposed reaction pathway for the reaction of DSO-aqueous

Table 5.13 The kinetic parameters for the reaction of aqueous phase

Reaction	$k_0(s^{-1})$	Activation Energy E_a (kJ/mol)
1. acetic acid ⟶ gas	5.61×10^6	92.08
2. acetic acid ⟶ acetone	1.40×10^7	85.62
3. acetone ⟶ gas	2.36×10^3	55.01
4. acetic acid ⟶ coke	1.04×10^2	30.55
5. others ⟶ gas	4.04×10^1	26.57
6. methanol ⟶ gas	2.17×10^1	23.97
7. others ⟶ coke	2.55	9.35

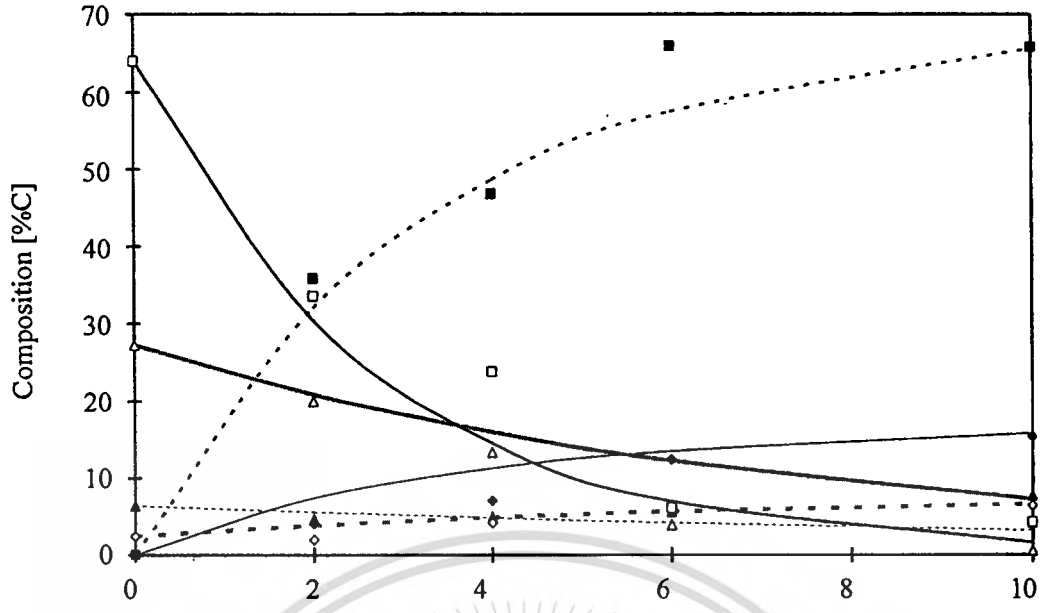

(a)

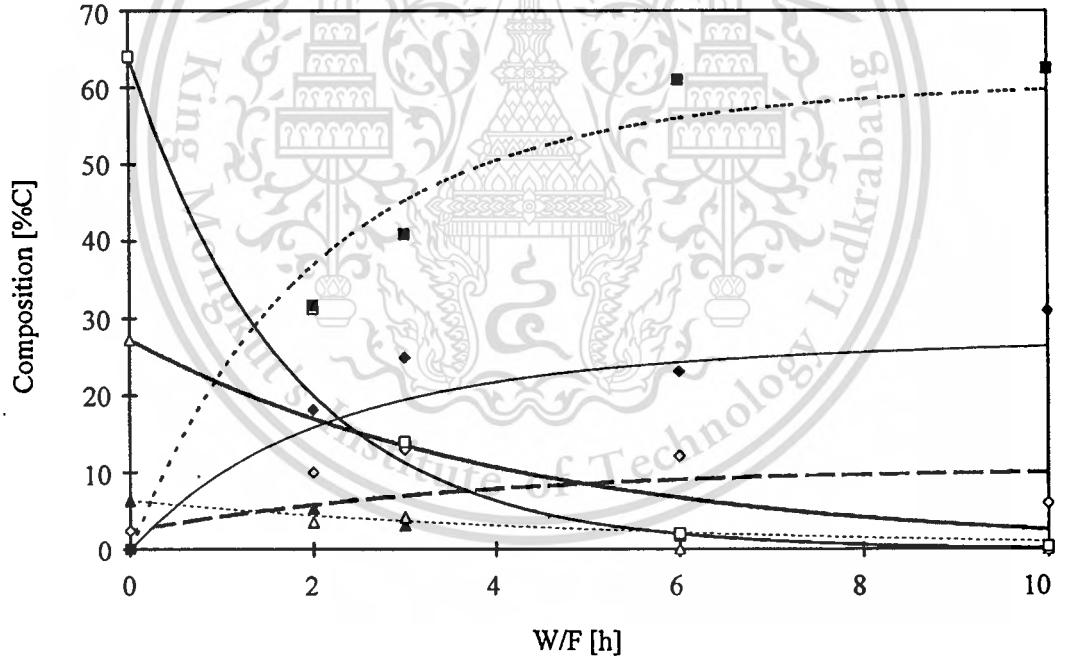

(b)

Figure 5.27 Effect of W/F on the product yields obtained from the reaction of aqueous phase at (a) 513 K (b) 583 K (c) 593 K and (d) 643 K

(▲ ,·····) : methanol, (◇ ,– –) : acetone, (△ ,——) : acetic acid,

(□ ,——) : others in liquid, (◆ ,——) : gas, (■ ,·····) : residue

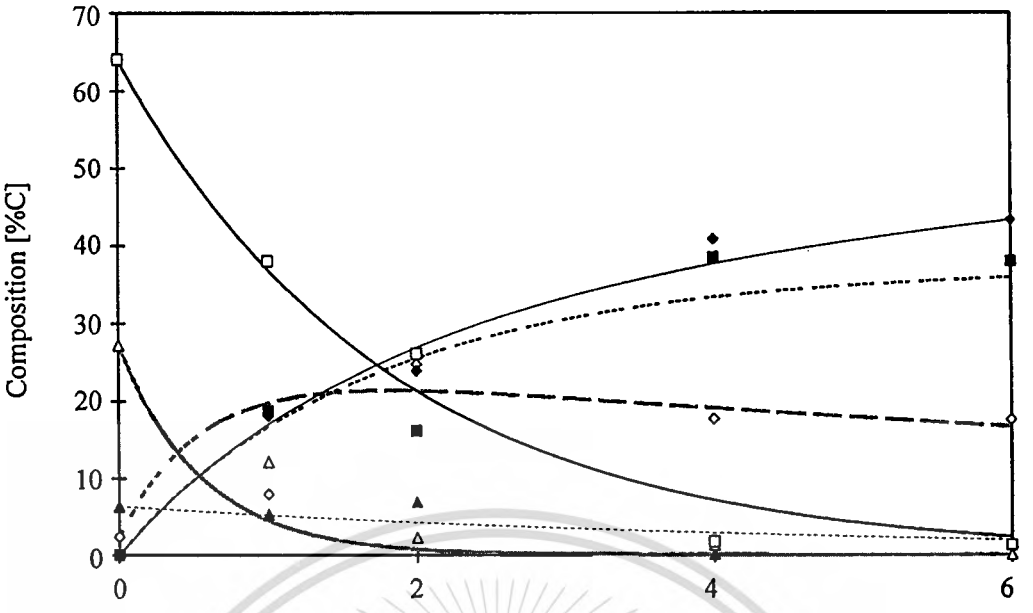

(c)

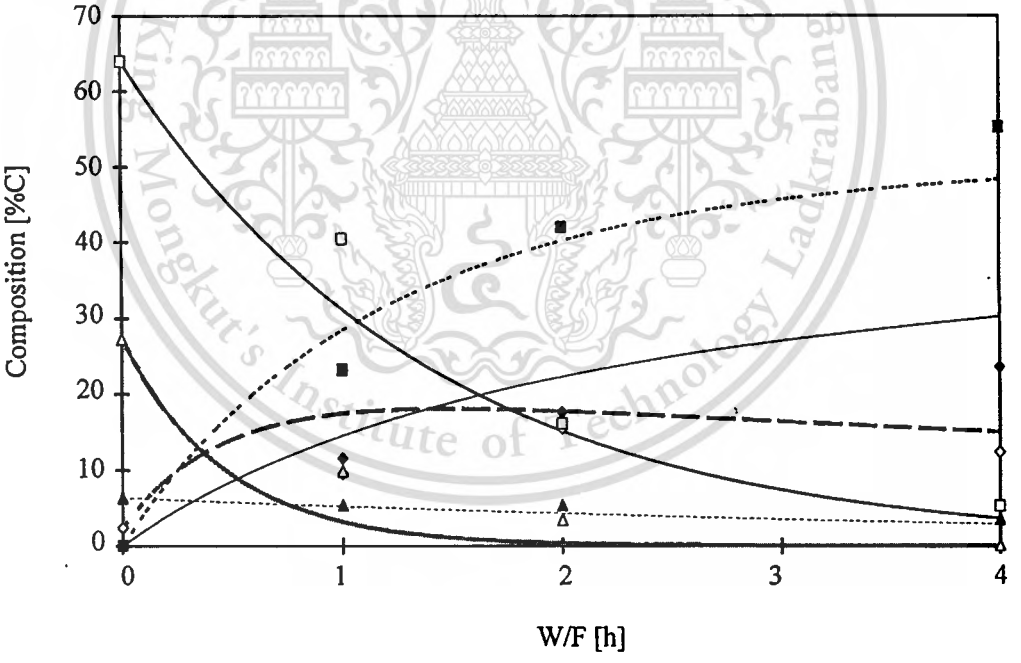

(d)

Figure 5.27 (cont.) Effect of W/F on the product yields obtained from the reaction of aqueous phase at (a) 513 K (b) 583 K (c) 593 K and (d) 643 K

(▲ , ·····) : methanol, (◇ , — -) : acetone, (△ , ——) : acetic acid,

(□ , ——) : others in liquid, (◆ , ——) : gas, (■ , ·····) : residue

Similar to the reaction of DMSO-aqueous, the product distribution from the reaction of palm shell derived bio-oil was evaluated. The experimental data in section 5.2.2 was used as the information to propose the reaction pathway. On the basis of the reaction pathway in Figure 5.28, the kinetic parameters were estimated as listed in Table 5.14. The product distribution was represented by curves in Figure 5.29. The result shows that the estimated values were in good agreement with the experimental values.

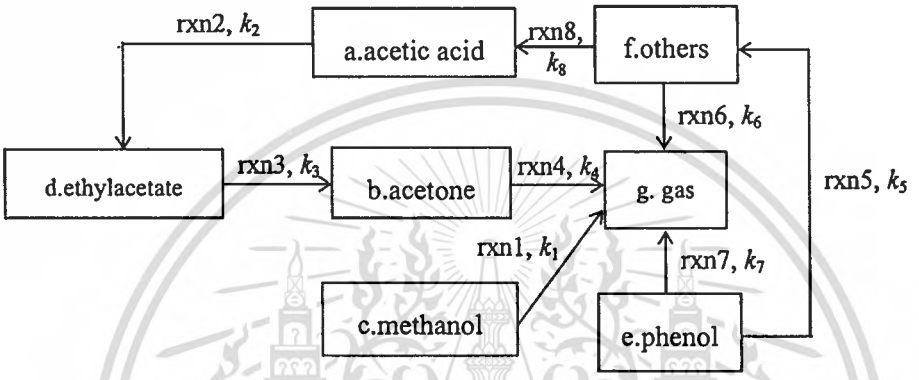

Figure 5.28 Proposed reaction pathway for the reaction of palm shell derived bio-oil

Table 5.14 The kinetic parameters for the reaction of palm shell derived bio-oil

Reaction	$k_0(s^{-1})$	Activation Energy E_a (kJ/mol)
1. methanol ⟶ gas	9.42×10^{-2}	3.03
2. acetic acid ⟶ ethylacetate	4.50×10^{3}	51.3
3. ethylacetate⟶ acetone	1.51×10^{2}	25.45
4. acetone ⟶ gas	2.24×10^{2}	25.57
5. phenol ⟶ others	3.33×10^{3}	70.19
6. others ⟶ gas	3.92×10^{2}	41.36
7. phenol ⟶ gas	7.05×10^{3}	63.88
8. others ⟶ acetic acid	2.42×10^{3}	46.49

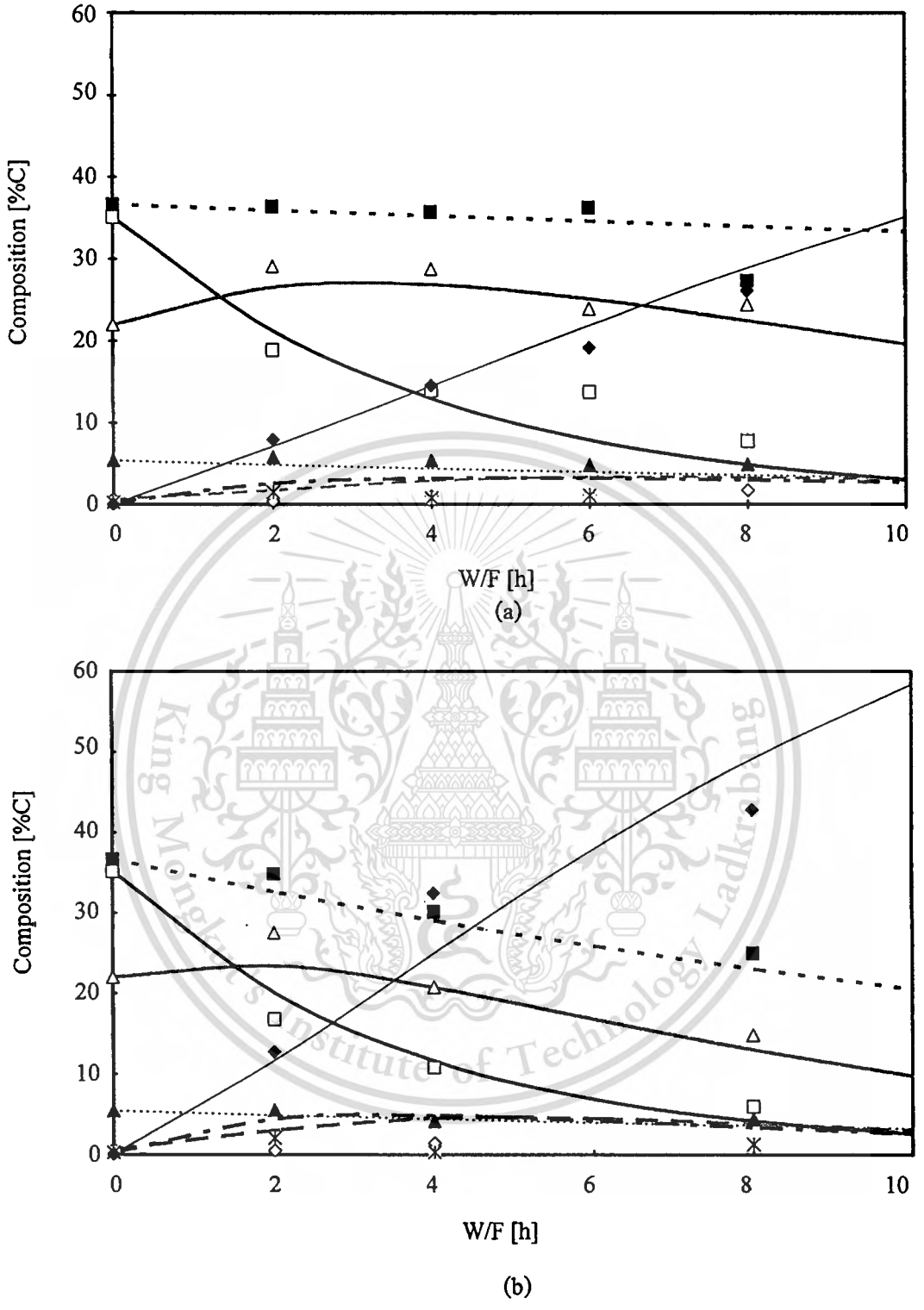

Figure 5.29 Effect of W/F on the product yields obtained from the reaction of palm shell derived bio-oil at (a) 623 K (b) 673 K (c) 723 K

(▲ ,·····) : methanol, (✳ , — ·) : ethylacetate, (△ , ▬) : acetic acid, (◇ , – –) : acetone, (■ ,·····) : phenol, (□ ,——) : others in liquid, (◆ ,——) : gas

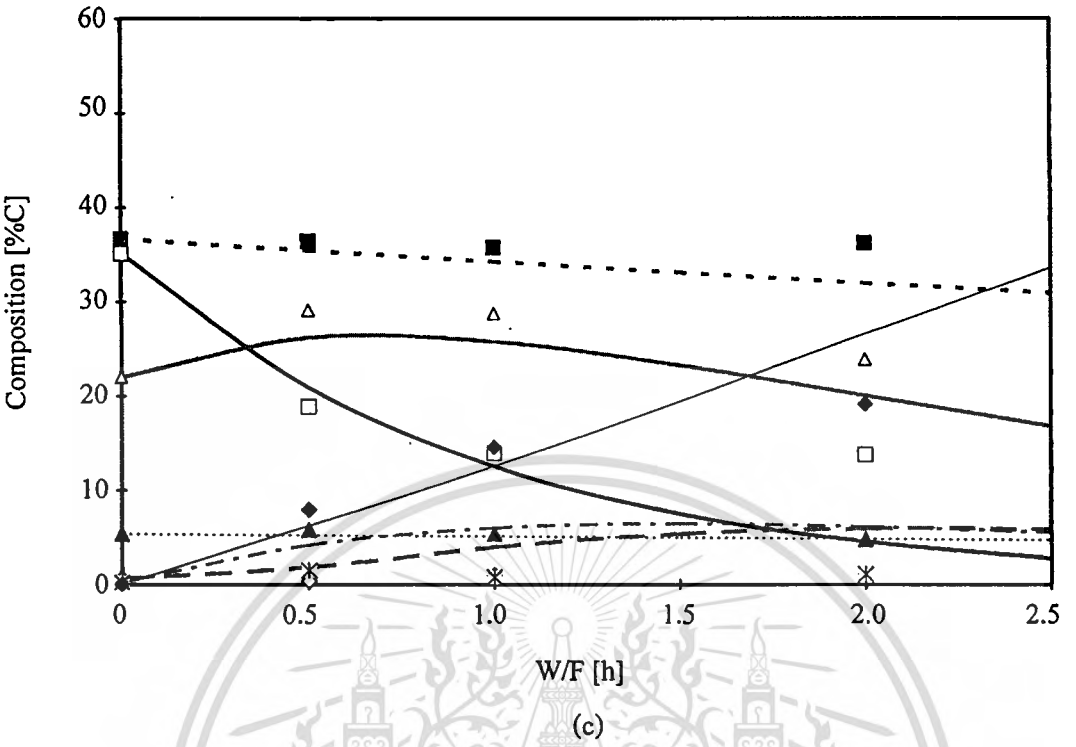

Figure 5.29 (cont.) Effect of W/F on the product yields obtained from the reaction of palm shell derived bio-oil at (a) 623 K (b) 673 K (c) 723 K

(▲ ,------) : methanol, (✳ , — ·) : ethylacetate, (△ , ___) : acetic acid,

(◇ , - -) : acetone, (■ ,·····) : phenol, (□ ,——) : others in liquid,

(◆ , ——) : gas

5.5 Catalyst deactivation

5.5.1 Temperature Program Oxidation

The experimental result in section 5.2.4 showed that large amount of carbon was deposited on the $ZrO_2 \cdot FeO_x$ catalyst when the catalyst was used to upgrade the dried sludge derived bio-oil. Generally, carbon deposition is one of the most important mechanism of the deactivation of catalyst. In this section temperature program oxidation technique was employed to characterize the carbon deposited on the $ZrO_2 \cdot FeO_x$ catalyst used in DSO upgrading. Figure 5.30 shows the CO_2 evolution curves obtained from the TPO analysis of the used FeOx and $ZrO_2 \cdot FeO_x$ catalysts. In the TPO curve of the used $ZrO_2 \cdot FeO_x$, two peaks of CO_2 were observed. The one in the low temperature region appeared at 543 K and reached the maximum around 573 K. The other one appearing in the high temperature region reached the maximum around 623 K. In the TPO curve of the used FeO_x, only one broaden peak appeared around 590 K. By comparison the two TPO profiles of the used $ZrO_2 \cdot FeO_x$ and the used FeO_x catalysts, we assigned the peak appeared in the higher temperature region (>593 K) to the CO_2 produced from oxidation of the carbon deposited on FeO_x surface and the peak appeared in the lower temperature region to the CO_2 produced from the carbon deposited on the ZrO_2 surface. In addition, the TPO profile of the used $ZrO_2 \cdot FeO_x$ catalyst showed that CO_2 completely evolved from the catalyst before the temperature reached 773 K. From the TPO study, we concluded that the regeneration of the used $ZrO_2 \cdot FeO_x$ catalyst has to be done at the temperature higher than 823 K.

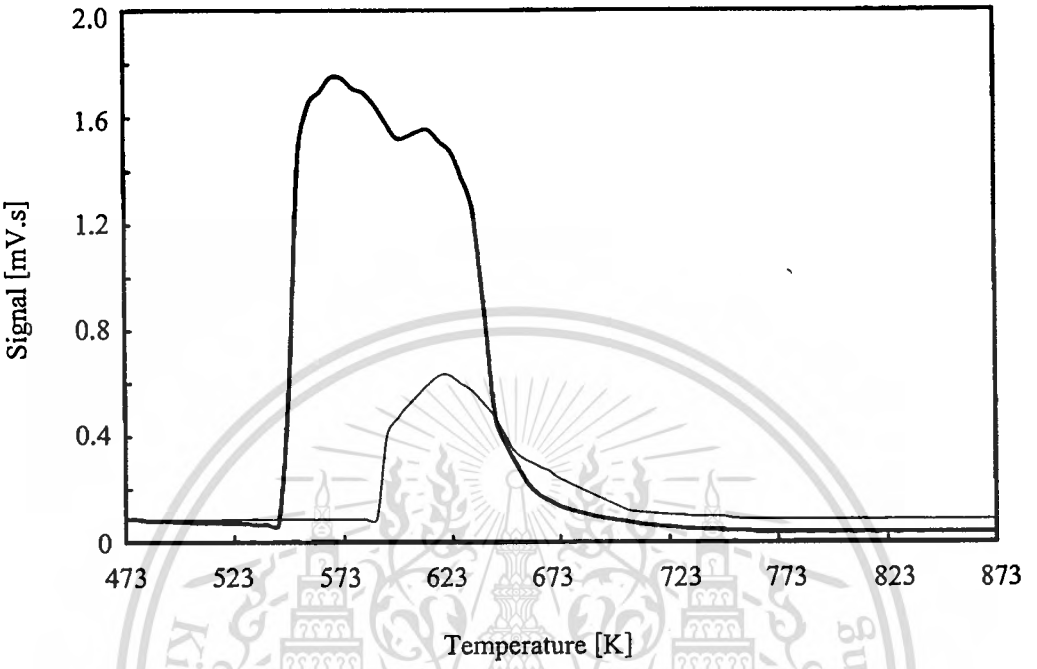

Figure 5.30 Temperature-programmed oxidation (TPO) of the deposited coke catalysts

(—— : ZrO_2·FeO_x, —— : FeO_x)

5.5.2 Characterization of deactivated catalysts

Figure 5.31 shows the XRD patterns of the $ZrO_2 \cdot FeO_{x[V]}$ catalyst taken prior to and after the upgrading of DSO-aqueous. Both the fresh and the used $ZrO_2 \cdot FeO_{x[V]}$ catalyst had similar XRD patterns corresponding to the hematite structure. This result implied that the structure of the $ZrO_2 \cdot FeO_{x[V]}$ catalyst were not changed due to the reaction with oil phase DSO.

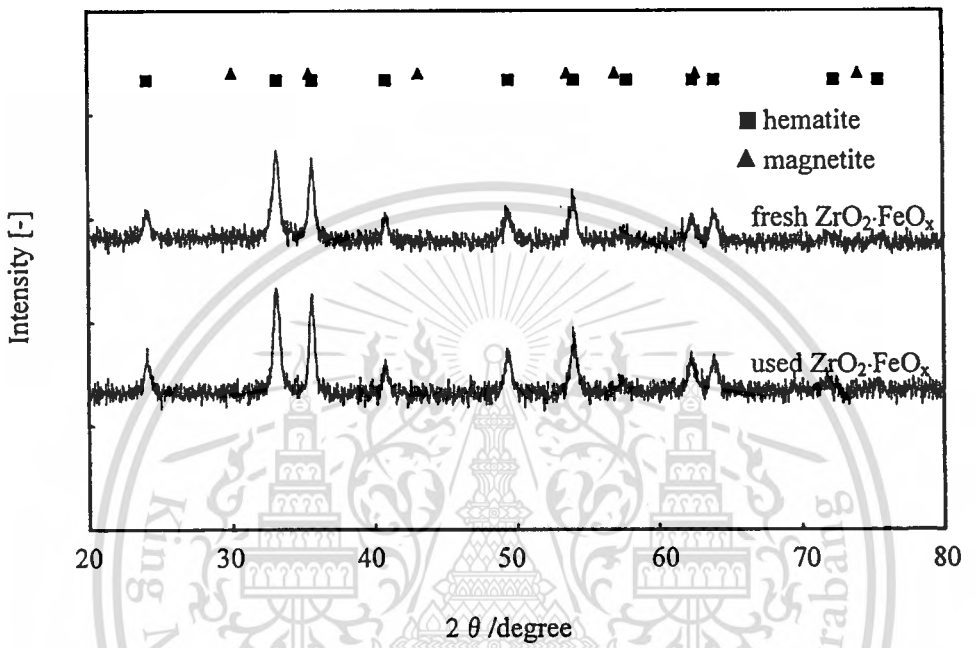

Figure 5.31 The XRD pattern of catalyst prior to and after reaction

In order to investigate effect of the reaction and the regeneration on physical properties of the $ZrO_2 \cdot FeO_{x[V]}$ catalyst, nitrogen adsorption by BET method was performed. The results including surface area (S_{BET}) and particle size are summarized in Table 5.15. The surface area of the catalyst decreased by 49.64% from 56.91 to 28.25 $m^2 \cdot g^{-1}$ after the catalyst was employed to the upgrading of DSO. Figure 5.32 showed that total pore volume of the catalyst significantly decreased after the reaction, especially the pore with small size of the radius of 0.5-3.5 nm. The surface area of the coked catalyst was partially recovered after the first regeneration cycle and this regeneration method could recover some of the small pores. However, the second cycle of the regeneration was not able to recover the small pores. Figure 5.33 (a) to (c) shows the TEM photographs of the fresh, the coked and the first cycle regenerated catalysts, respectively. The TEM result showed that the particle size became smaller due to the reaction and the regeneration. No agglomeration or coalescence was observed. According to the TPO, XRD and BET results, we concluded that the deactivation of the catalyst mainly caused by loss of surface area and pore plugging.

Table 5.15 Effect of reaction/regeneration cycle on properties of catalyst

catalyst	conditions	S_{area} ($m^2 g^{-1}$)	Particle size (nm)
$ZrO_2 \cdot FeO_{x[V]}$	Fresh	56.91	43.0
	Coked	28.25	33.86
	1st regenerated	31.65	28.1
	2nd regenerated	36.22	-

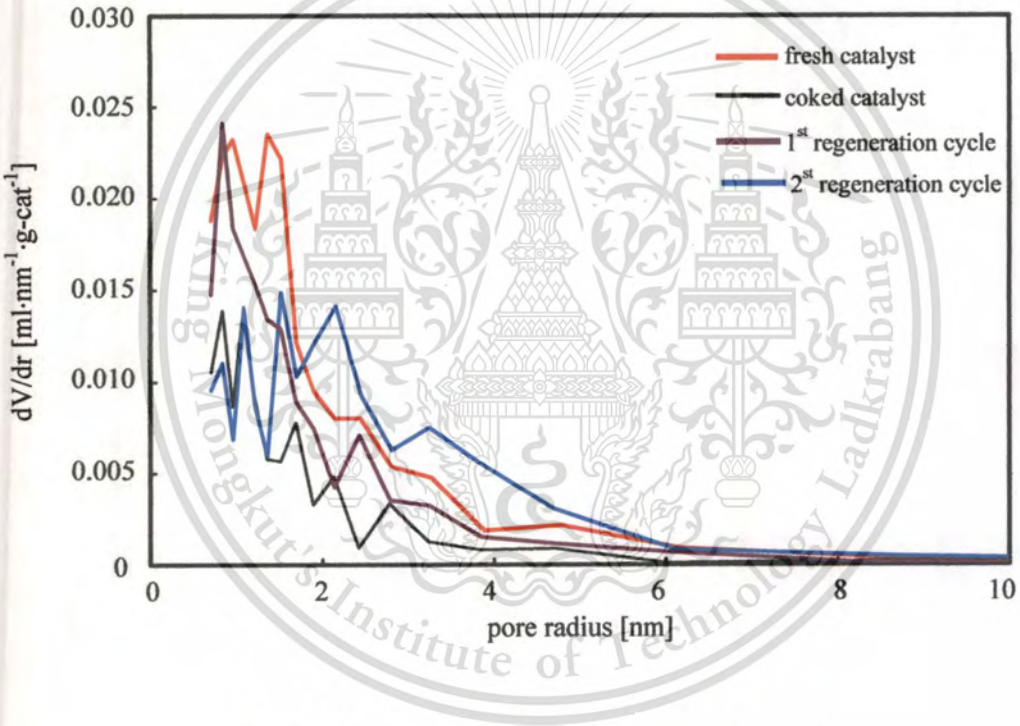

Figure 5.32 Pore size distribution of $ZrO_2FeO_{x[V]}$ catalysts

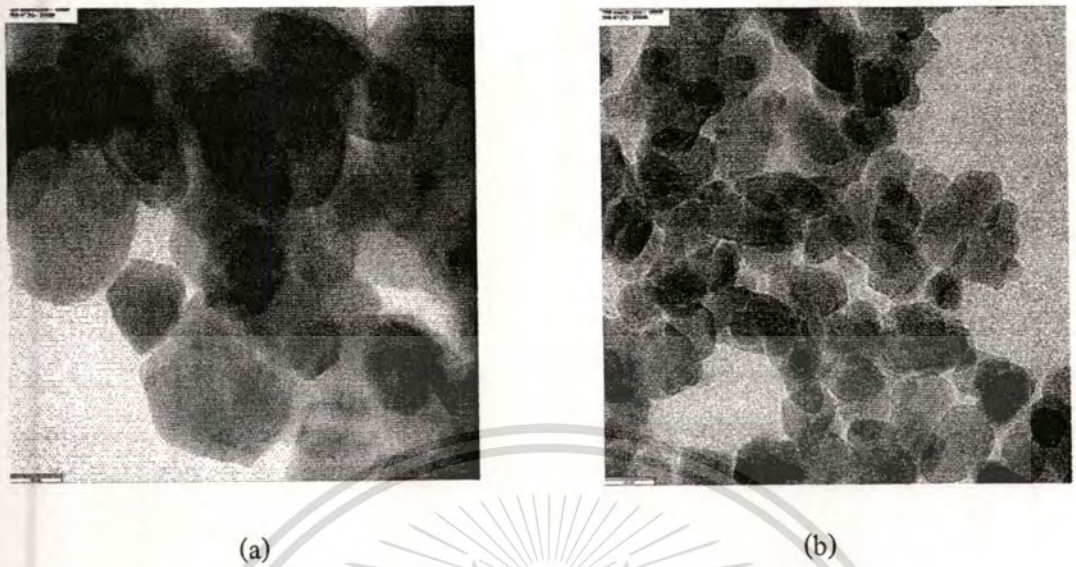

(a) (b)

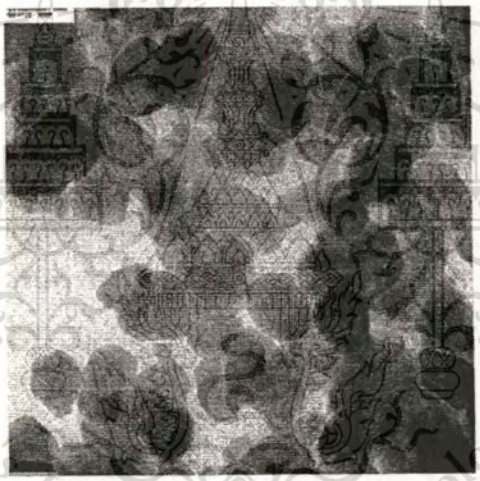

(c)

Figure 5.33 TEM micrograph of ZrO_2·FeO_x (a) prior to the reaction (b) after reaction (c) regenerated at 823 K

According to the TPO result, we decided the condition to regenerate the catalyst as follow; treating the catalyst with 21 %vol of O_2 at 823 K for 1 h. Figure 5.34 shows the product distribution of the upgrading of DSO aqueous phase when the fresh catalyst and the regenerated (1st cycle) catalyst were used. The yields of gas product and solid residue slightly increased while the yields of the target methanol and acetone slightly decreased.

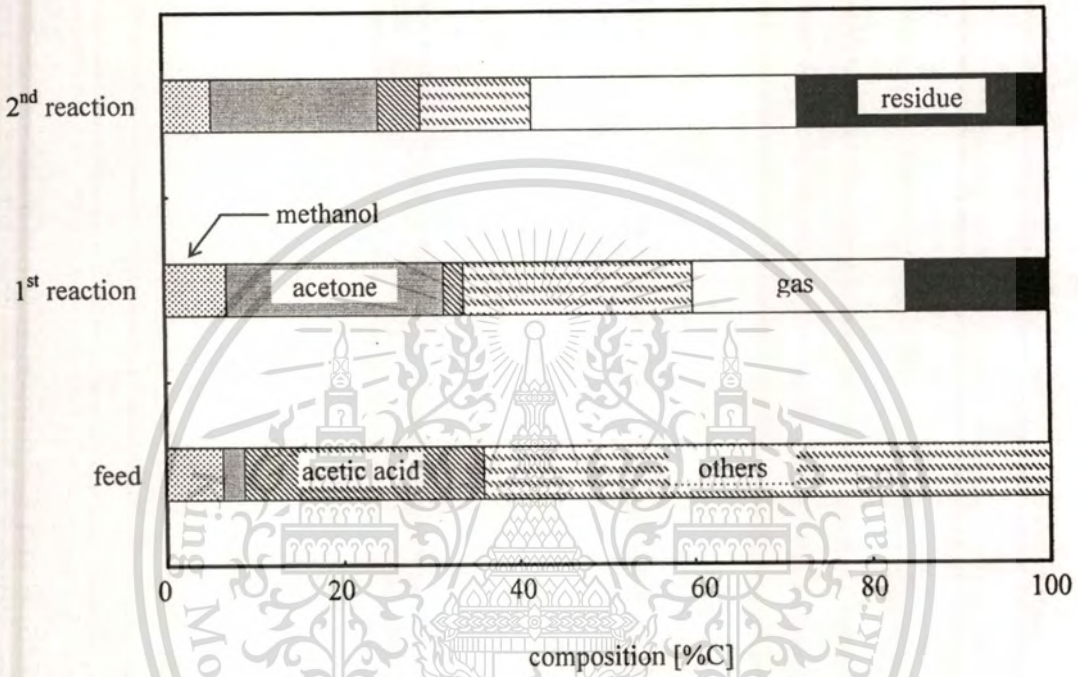

Figure 5.34 The distribution of product over the catalyst regenerated at 823 K in air flow (T = 593 K, W/F = 2 h)

5.6 Economic aspect

Figure 5.33 shows the energy flow diagram of the process for chemicals production from wastewater. The 24 tones/h of wastewater generated from the palm oil mill with the capacity of 40 tones of FFB and 2.4 tones of palm shell. Base on this value, the energy consumption and generation from each unit were calculated as listed in Table 5.16 – 5.17. The detail in the calculation was described in Appendix D.

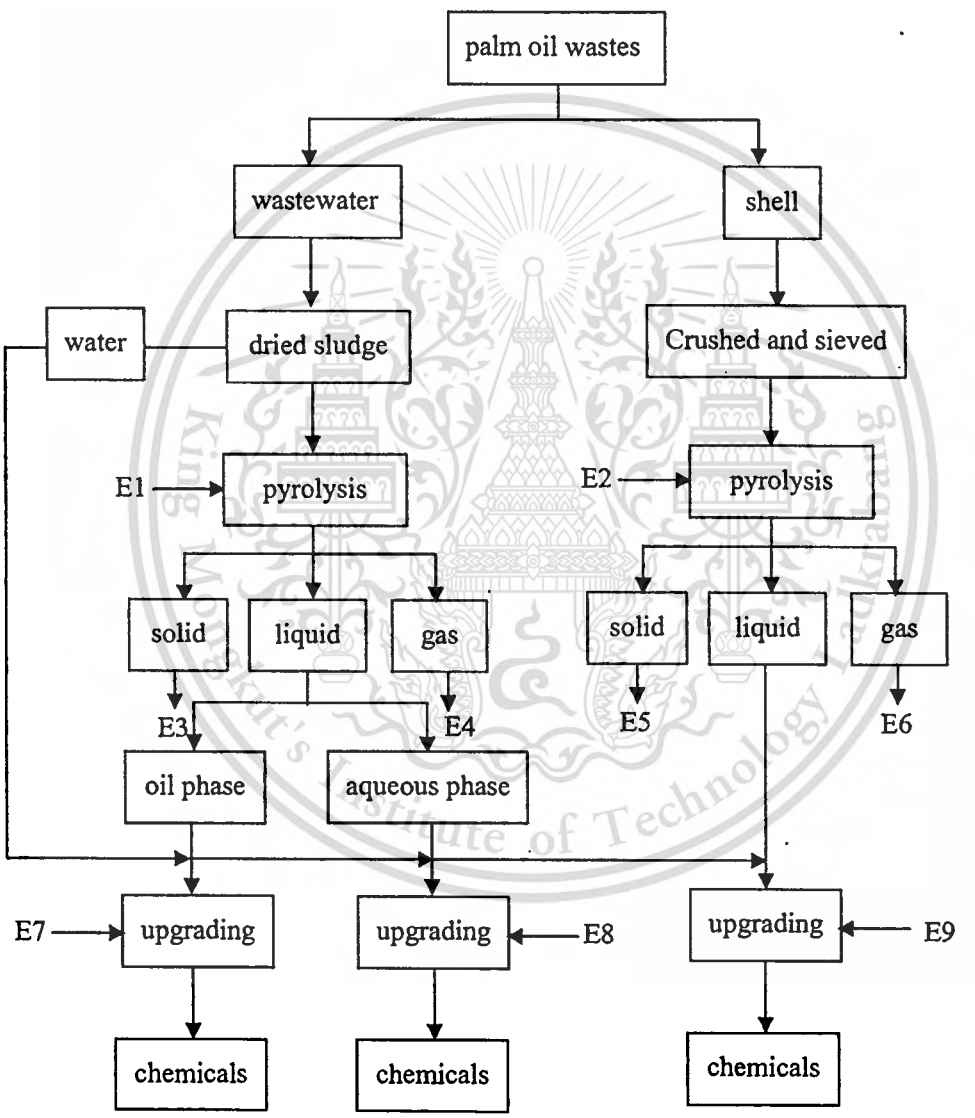

Figure 5.33 Energy flow diagram for chemical production from palm oil mill wastes

Table 5.16 Energy consumption for each step

step	Description	Energy	
		kJ/h	kW-h
E1	- Energy consumed for pyrolysis of dried sludge	2.7×10^6	750
	- Energy consumed for condensation of pyrolysis product	3,960	1.1
E2	- Energy consumed for pyrolysis of palm oil shell	8.58×10^5	238
	- Energy consumed for condensation of pyrolysis product	3,960	1.1
E7	- Energy consumed for upgrading of DSO-oil phase	1.83×10^7	5,083
	- Energy consumed for condensation of product	3,960	1.1
	- Energy for catalyst regeneration	1.65×10^6	460
E8	- Energy consumed for upgrading of DSO-aqueous phase	8.1×10^6	2,241
	- Energy consumed for condensation of product	3,960	1.1
	- Energy for catalyst regeneration	1×10^6	277
E9	- Energy consumed for upgrading of palm shell derived bio-oil	1.45×10^7	4,027
	- Energy consumed for condensation of product	3,960	1.1
	- Energy for catalyst regeneration	2.8×10^6	778
	Total energy consumption	5.0×10^7	13,868

Table 5.17 Energy generation for each step

Step	Description	Energy	
		kJ/h	kW-h
E3	Energy produced from char (dried sludge)	4.86×10^7	13,500
E4	Energy produced from gas pyrolysis (dried sludge)	1.67×10^7	4,638
E5	Energy produced from char (shell)	2.64×10^7	7,333
E6	Energy produced from gas pyrolysis (shell)	4.7×10^6	1,305
	Total energy generation	9.64×10^7	26,777

From the calculation of energy consumed, the basic data was obtained in order to design of the required equipment and the respective investment costs of the system was estimate as listed in Table 5.18.

Table 5.18 The investment and operating cost of the process

Description	Price (bath)
Investment cost	
- separation system	200,000
- Pyrolysis system	3,000,000
- Reaction of DSO-oil phase system	3,650,000
- Reaction of DSO-aqueous system	3,650,000
- Reaction of palm shell derived bio-oil system	3,650,000
- Distillation system	1,000,000
Total investment cost	15,150,000
Operating cost	
- Electricity (5.0×10^7 kJ/h)*	-
- Nitrogen (303 m^3/h)	3,636,000 bath/year
- Catalyst (30 ton/year)	60,000,000 bath/year
- Water (6,660 kg/h)*	-
Total operating cost	63,636,000

*could be recycle back from the process

Table 5.19 shows the outcome obtained from the process. It is interesting that when compared with the investment and operating cost (Table 5.17), this process seem worthwhile. However, some parameters may deviate from the experimental in lab scale when the process is operated in large scale. Furthermore, the continuity of the process and the life time of catalyst are necessary to improve.

Table 5.19 Price of palm oil wastes from palm oil mill

Chemical sources	Component	Productivity (kg/h)	Outcome (bath/year)
DSO- oil phase	acetone	32	11,776,000
	phenol	60	27,360,000
	m-cresol	9.2	7,875,200
DSO-aqueous phase	methanol	31	3,720,000
	acetone	66	24,288,000
	acetic acid	9.4	1,729,600
shell derived bio-oil	methanol	23.54	2,824,800
	acetic acid	176.58	32,490,720
	acetone	21.34	7,853,120
	phenol	414.96	189,221,760
			309,139,200

Chapter 6

Conclusions

A new method for utilization palm oil mill wastes was proposed. The process consisted of the pyrolysis step and the catalytic upgrading step. The palm oil mill wastes were pyrolysed to produce the oil which is the source of useful chemicals. This oil was upgraded over the zirconia supporting iron oxide catalyst. Prior to the pyrolysis, the thermal characteristic of wastes was studied by Themogavimetric Analysis (TGA) in order to determine the pyrolysis temperature.

The palm shell derived oil with 55%wt (ca 13%C) was obtained from the pyrolysis of palm shell at 773 K. The optimum condition for recovery useful chemicals from palm shell derived oil over $ZrO_2 \cdot Al \cdot FeO_x$ was the temperature of 623 K and W/F of 6 h. Under the optimum condition a mixture of methanol 6%C, acetic acid 24%C, acetone 3%C and phenol 36%C was obtained.

The liquid product obtained from the pyrolysis of dried sludge (DSO) at 773 K was separated into two layers. The upper layer with 15 %wt (ca 72.8 %C) was water-insoluble fraction (DSO-oil) and the lower layer with 30 %wt (ca 16 %C) was water soluble fraction (DSO-aqueous). The reaction of DSO was performed over the zirconia supporting iron oxide improved by using the nitrate salts as precursor.

The optimum condition for recovery useful chemicals from DSO-oil phase over $ZrO_2 \cdot FeO_x$ was the temperature of 593 K and W/F of 6 h. Acetone, phenol and m-cresol were the main products with 5, 12 and 1.2 %C, respectively. The optimum condition for recovery useful chemicals from DSO-aqueous phase over $ZrO_2 \cdot FeO_x$ was the temperature of 593 K and W/F of 2 h. Methanol, acetone and acetic acid were the main products with 7, 25 and 2.3 %C, respectively.

The results showed that the zirconia supporting iron oxide catalyst had high capability to recover useful chemicals from the pyrolysis oil. The activity of catalyst could be enhanced by increasing of surface area. The type of precursor salt played an important role on the catalytic property. Furthermore, the activity of catalyst was partially recovered by the oxidation with air at 823 K.

References

[1] **Palm oil stat. 2008.** [online].
Available : http://www.gapkiconference.org/download/Palm%20Stats%202008.pdf

[2] 1997. **Environmental Management Guideline for the Palm oil Industry.** [online].
Available : http://www.elaw.org/system/files/th.palm.oil.industry.guidelines.pdf

[3] Igwe J.C., Onyegbado C.C. "A review of Palm Oil Mill Effluent (POME) Water Treatment." **Global Journal of Environmental Research,** vol.1 (2), 2007. pp. 54 – 62

[4] Ahmad A.L., Ismail S. and Bhatia S. "Water Recycling from Palm Oil Mill Effluent (POME) using Membrane Technology." **Desalination,** vol. 157, 2003. pp. 87 – 95

[5] Najafpour G.D., Zinatizadeh A.A.L., Mohamed A.R., Isa M.H. and Nasrollahzadeh H. "High-Rate Anaerobic Digestion of Palm Oil Mill Effluent in an Upflow Anaerobic Sludge-Fixed Film Bioreactor." **Process Biochemistry,** vol. 41, 2006. pp. 370 – 379

[6] Paepatung N., Kullavanijaya P., Loapitinan O., Noppharatana A., Songkasiri W. and Chaiprasert P. "Assessment of Palm Oil Mill Effluent as Biogas Energy Source in Thailand." **33rd Congress on Science and Technology of Thailand,** Oct 2007, pp. 1 - 4

[7] Yacob S., Hassan M.A., Shirai Y., Wakisaka M. and Subash S. "Baseline Study of Methane Emission from Anaerobic Ponds of Palm Oil Mill Effluent Treatment." **Science of the Total Environment,** vol. 366, 2006. pp. 187 – 196

[8] Chan Y.J., Chong M.F., Law C.L. and Hassell D.G. "A Review on Anaerobic-Aerobic Treatment of Industrial and Municipal Wastewater." **Chemical Engineering Journal,** vol. 155, 2009. pp. 1 -18

[9] Wu T.Y., Mohammad A.W., Jahim J.Md. and Anuar N. "A holistic Approach to Managing Palm Oil Mill Effluent (POME) : Biotechnological Advance in the Sustainable Reuse of POME." **Biotechnology Advance,** vol. 27, 2009. pp. 40 - 52

[10] Tandukar M., Ohashi A. and Harada H. "Performance Comparison of a Pilot-Scale UASB and DHS System and Activated Sludge Process for the Treatment of Municipal wastewater." **Water Research,** vol. 41, 2007. pp. 2697 – 2705

References (cont.)

[11] Ahmad A.L., Ismail S. and Bhatia S. "Membrane Treatment for Palm Oil Mill Effluent : Effect of Transmembrane Pressure and Crossflow Velocity." **Desalination**, vol. 179, 2005. pp. 245 – 255

[12] Poh P.E., Fong M.F. "Development of Anaerobic Digestion Methods for Palm Oil Mill Effluent (POME) Treatment." **Bioresource Technology**, vol. 100, 1009. pp. 1 – 9

[13] Badal S., Loren I., Michael C. and Victor W.Y. "Cost-Effective Bioprocess Technologies for Production of Biofuels from Lignocellulosic Biomass." **UJNR Food & Agricultural Panel Proceedings**, Dec 2004. pp. 181 – 185

[14] Lindemann M.D., Kornegay E.T. and Moore R.J. "Digestibility and Feeding Value of Peanut Hulls for Swine." **Journal of Animal Science**, vol. 62, 1986. pp. 412 – 421

[15] Zhuang X., Yuan Z., Ma L., Wu C., Xu M., Xu J., Zhu S. and Qi W. "Kinetic Study of Hydrolysis of Xylan and Agricultural Wastes with Hot Liquid Water." **Biotechnology Advances**, vol. 27, 2009. pp. 578 – 582

[16] Aziz A.A., Husin M. and Mokhtar A. "Preparation of Cellulose from Oil Palm Empty Fruit Bunches via Ethanol Digestion : Effect of Acid and Alkali Catalysts." **Journal of Oil Palm Research**, vol. 14, No.1, June 2002. pp. 9 - 14

[17] Viera R.G.P., Filho G.R., Assunção R.M.N., Meireles C.S., Vieira J.G. and Oliveira G.S. "Synthesis and Characterization of Methylcellulose from Sugas Cane Bagasse Cellulose." **Carbohydrate Polymers**, vol. 67, 2007. pp. 182 – 189

[18] Mohan D., Pittman C.U. and Steele P.H. "Pyrolysis of Wood/Biomass for Bio-Oil : A Critical Review." **Energy & Fuels**, vol. 20, 2006, pp. 848 – 889

[19] Bridgewater A.V., Peacocke G.V.C. "Fast Pyrolysis Processes for Biomass." **Renewable and Sustainable Energy Reviews**, vol. 4, 2004. pp. 1 - 73

[20] Lyle F. Albright, Billy L. Crynes and William H. Corcoran, Editors. **Pyrolysis Theory and Industrial Practice**. New York : Academic Press. 1983.

[21] Yaman S. "Pyrolysis of Biomass to Produce Fuels and Chemical Feedstocks." **Energy Conversion and Management**, vol. 45, 2004. pp. 651 – 671

References (cont.)

[22] Valenzuela M.B., Jones C.W. and Agrawal P. K. "Batch Aqueous – Phase Reforming of Woody Biomass." **Energy & Fuels**, vol. 20, 2006. pp. 1744 – 1752

[23] Qi Z., Jie C. Tiejun W. and Ying X. "Review of Biomass Pyrolysis Oil Properties and Upgrading Research." **Energy Conversion and Management**, vol. 48, 2007. pp. 87 - 92

[24] Pinzari F., Patrono P. and Costantino U. "Methanol Reforming Reactions over Zn/TiO_2 Catalysts." **Catalysis Communications**, vol. 7, 2006. pp. 696 – 700

[25] Garcia L., French R., Czernik S. and Chornet E. "Catalytic Steam Reforming of Bio-Oils for the Production of Hydrogen : Effects of Catalyst Composition." **Applied Catalysis A: General**, vol. 201, 2000. pp. 225 – 239

[26] Cornell R.M., Schwertmann. **The Iron Oxides : Structure, Properties, Reactions, Occurrences and Uses.** 2nd ED. Weinheim : Wiley-VCH GmbH & Co.KGaA. 2003.

[27] Das P., Sreelatha T. and Ganesh A. "Bio Oil from Pyrolysis of Cashew Nut Shell-Characterisation and Related Properties" **Biomass and Bioenergy**, vol. 27, 2004. pp. 265 – 275

[28] Tsamba A.J., Yang W. and Blasiak W. "Pyrolysis Characteristics and Global Kinetics of Coconut and Cashew Nut Shells" **Fuel Processing Technology**, vol. 87, 2006. pp. 523 – 530

[29] Onay O. "Fast and Catalytic Pyrolysis of Pistacia Khinjuk Seed in a Wall-Swept Fixed Bed Reactor" **Fuel**, vol. 86, 2007. pp. 1452 - 1460

[30] Lede J., Broust F., Ndiaye F.T. and Ferrer M. "Properties of Bio-Oils Produced by Biomass Fast Pyrolysis in a Cyclone Reactor." **Fuel**, vol. 86, 2007. pp. 1800 - 1810

[31] Branca C., Giudicianni P. and Blasi C.D. "GC/MS Characterization of Liquids Generated from Low-Temperature Pyrolysis of Wood." **Ind. Eng. Chem. Res.**, vol.42, 2003. pp. 3109 – 3202

References (cont.)

[32] Yang H., Yan R., Chin T., Liang D.T., Chen H. and Chuguang Z. "Thermogravimetric Analysis-Fourier Transform Infrared Analysis of Palm Oil Waste Pyrolysis." **Energy & Fuels**, vol. 18, 2004. pp. 1814 – 1821

[33] Gua J., Lau A.C. "Kinetic Study on Pyrolytic Process of Oil-Palm Solid Waste using Two-Step Consecutive Reaction Model." **Biomass and Bioenergy**, vol. 20, 2001. pp. 223 – 233

[34] MD Kawser J., Nash A.F. "Oil Palm Shell as a Source of Phenol" **Journal of Oil Palm Research**, vol. 12, 2000. pp. 86 – 94

[35] Yan R., Yang H., Chin T., Liang D.T., Chen H. and Zheng C. "Influence of Temperature on the Distribution of Gaseous Products from Pyrolyzing Palm Oil Wastes." **Combustion and Flame**, vol. 142, 2005. pp. 24 - 32

[36] Islam M.N., Zailani R. and Ani F.N. "Pyrolytic Oil from Fluidised Bed Pyrolysis of Oil Palm Shell and its Characterisation." **Renewable Energy**, vol. 17, 1999. pp. 73 – 84

[37] Yang H., Yan R., Chen H., Lee D.H. and Zheng C. "Characteristics of Hemicellulose, Cellulose and Lignin Pyrolysis." **Fuel**, vol. 86, 2007. pp. 1781- 1788

[38] Jindaron C., Meeyoo V., Rirksomboon T., Kitiyana B. and Rangsunvigit P. "The Production of Bio-Oil by Oxidative Pyrolysis of Sewage Sludge in Rotating Fixed Bed Reactor." **Proceedings of the Joint International Conference on Sustainable Energy and Environment**, Dec 2004.

[39] Dominguez A., Menendez J.A., Inguanzo M. and Pis J.J. "Investigations into the Characteristics of Oils Produced from Microwave Pyrolysis of Sewage Sludge." **Fuel Processing Technology**, vol. 86, 2005. pp. 1007 - 1020

[40] Kaminsky W., Kummer A.B. "Fluidized Bed Pyrolysis of Digested Sewage Sludge." **Journal of Analytical and Applied Pyrolysis**, vol. 16, 1989. pp. 27 – 35

References (cont.)

[41] Sanchez M.E., Marinez O., Gomez X. and Moran A. "Pyrolysis of Mixtures of Sewage Sludge and Manure: A Comparison of the Results Obtained in the Laboratory (Semi-Pilot) and in a Pilot Plant." **Waste Management**, vol. 27, 2007. pp. 1328 – 1334

[42] Kim Y., Parker W. "A Technical and Economic Evaluation of the Pyrolysis of Sewage Sludge for the Production of Bio-Oil." **Bioresource Technology**, vol. 99, 2008. pp. 1409 – 1416

[43] Shen L., Zhang D.K. "An Expermental Study of Oil Recovery from Sewage Sludge by Low-Temperature Pyrolysis in a Fluidised-Bed." **Fuel**, vol. 82, 2003. pp. 465 – 472

[44] Vitolo S., Bresci B., Seggiani M. and Gallo M.G. "Catalytic Upgrading of Pyrolytic Oils over HZSM-5 Zeolite: Behaviour of the Catalyst when used in Repeated Upgrading – Regenerating Cycles." **Fuel**, vol. 80, 2001. pp.1 17 – 26

[45] Vitolo S., Seggiani M., Frediani P., Ambrosini G. and Politi L. "Catalytic Upgrading of Pyrolytic Oils to Fuel over Different Zeolites." **Fuel**, vol. 78, 1999. pp. 1147 – 1159

[46] Adam J., Antonakou E., Lappas A., Stocker M., Nilsen M.H., Bouzga A., Hustad J.E. and Øye G. "In situ Catalytic Upgrading of Biomass Derived Fast Pyrolysis Vapours in a fixed Bed Reactor using Mesoporous Materials." **Microporous and Mesoporous**, vol. 96, 2006. pp. 93 – 101

[47] Nokkosmaki M.I., Kuoppala E.T., Leppamaki E.A. and Krause A.O.I. "Catalytic Conversion of Biomass Pyrolysis Vapours with Zinc Oxide." **Journal of Analytical and Applied Pyrolysis**, vol. 55, 2000. pp. 119 – 131

[48] Basagiannis A.C., Verykios X.E. "Steam Reforming of the Aqueous Fraction of Bio-Oil over Structured Ru/MgO/Al_2O_3 Catalysts." **Catalysis Today**, vol. 127, 2007. pp. 256 – 264

References (cont.)

[49] Iojoju E.M., Domine M.E. Davidian T., Guilhaume N. and Mirodatos C. "Hydrogen Production by Sequential Cracking of Biomass-Derived Pyrolysis Oil over Noble Metal Catalysts Supported on Ceria – Zirconia." **Applied Catalysis A: General**, vol. 323, 2007. pp. 147 - 161

[50] Uddin Md. A., Tsuda H., Wu H. and Sasaoka E. "Catalytic Decomposition of Biomass Tars with Iron Oxide Catalysts." **Fuel**, vol. 87, 2008. pp.451 – 459

[51] Fumoto E., Tago T. Tsuji T. and Masuda T. "Recovery of Useful Hydrocarbons from Petroleum Residual Oil by Catalytic Cracking with Steam over Zirconia-Supporting Iron Oxide Catalyst." **Energy & Fuels**, vol. 18, 2004. pp. 1770 – 1774

[52] Fumoto E., Tago T. and Masuda T. "Production of Lighter Fuels by Cracking Petroleum Residual Oils with Steam over Zirconia-Supporting Iron Oxide Catalysts." **Energy & Fuels**, vol. 20, No.1, Jan 2006. pp. 1 – 6

[53] Fumoto E., Mizutani Y., Tago T. and Masuda T. "Production of Ketones from Sewage Sludge over Zirconia-Supporting Iron Oxide Catalysts in a Steam Atmosphere." **Applied Catalysis B: Environmental**, vol. 68, 2006. pp. 154 -159

[54] Masuda T., Kondo Y., Miwa M., Shimotori T., Mukai S.R., Hashimoto K., Takano M., Kawasaki S. and Yoshida. "Recovery of Useful Hydrocarbons from Oil Palm Waste using ZrO2 Supporting FeOOH Catalyst." **Chemical Engineering Science**, vol. 56, 2001. pp. 897 – 904

[55] Basagiannis A.C., Verykios X.E. "Reforming Reactions of Acetic acid on Nickel Catalysts over a Wide Temperature Range." **Applied Catalysis A: General**, vol. 308, 2006. pp. 182 - 193

[56] Adjaye J.D., Bakhshi N.N. "Catalytic Conversion of a Biomass-Derived Oil to Fuels and Chemicals I: Model Compound Studied and Reaction Pathways." **Biomass and Bioenergy**, vol. 8, No. 3, 1995. pp. 131 – 149

[57] Adjaye J.D., Bakhshi N.N. "Catalytic Conversion of a Biomass-Derived Oil to Fuels and Chemicals II: Chemical Kinetics, Parameter Estimation and Model Prediction." **Biomass and Bioenergy**, vol. 8, No. 4, 1995. pp. 265 – 277

References (cont.)

[58] Vijayaraghavan K., Ahmad D. and Bin Abdul Aziz M.E. "Aerobic Treatment of Palm Oil Mill Effluent." **Journal of Environmental Management,** vol. 82, 2007. pp.24 – 31

[59] Kahrizsangi R., Abbasi M.H. "Evaluation of Reliability of Coats-Redfern Method for Kinetic Analysis of Non-Isothermal TGA." **Transactions of Nonferrous Metals Society of China,** vol.18, 2008. pp. 217 – 221

[60] Takanabe K., Aika K., Inazu K. , Baba T., Seshan K. and Lefferts L. "Steam Reforming of Acetic acid as a Biomass Derived Oxygenate: Bifunctional Pathway for Hydrogen Formation over Pt/ZrO_2 Catalysts." **Journal of Catalysis,** vol. 243, 2006. pp. 263 - 269

[61] Patel S., Pant K.K. "Hydrogen Production by Oxidative Steam Reforming of Methanol using Ceria Promoted Copper – Alumina Catalysts." **Fuel Processing Technology,** vol. 88, 2007. pp. 825 - 832

Appendix

Appendix A

Component analyzed by GC-MS

Table A.1 Component of the bio oil obtained from the pyrolysis of palm oil shell at 500 °C

Component	Chemical formula	structure
Methanol	CH_4O	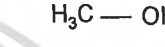
Acetone	$C_3H_6O_2$	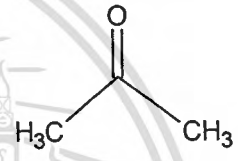
Acetic acid	$C_2H_4O_2$	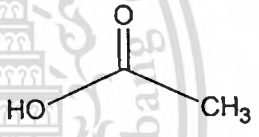
2-furaldehyde	$C_5H_4O_2$	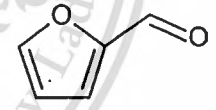
4-Ethyl 2-methoxy phenol	$C_9H_{12}O_2$	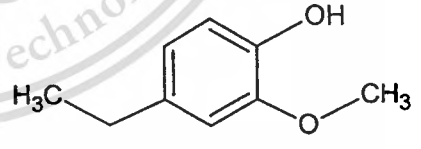
4-Methyl 2-methoxy phenol	$C_8H_{10}O_2$	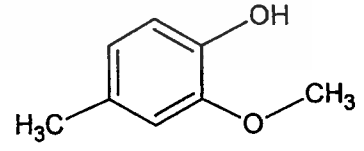
2-Methoxy phenol	$C_7H_8O_2$	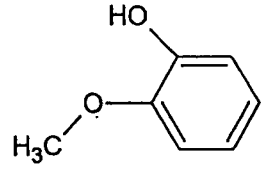

Table A.1 (cont.)Composition of the oil phase obtained from the pyrolysis of palm oil shell at 773 K

Component	Chemical formula	Chemical structure
2,6-Dimethoxy phenol	$C_8H_{10}O_3$	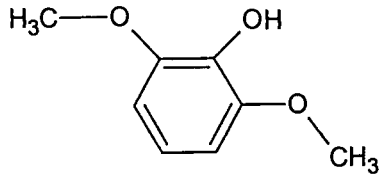
3-hydroxyl-4-methoxy-benzoic acid	$C_8H_8O_4$	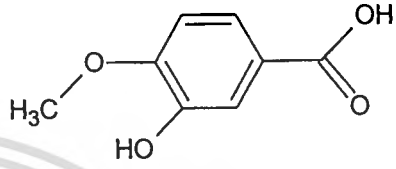
2,3,5-trimethyltoluene	$C_{10}H_{14}O_3$	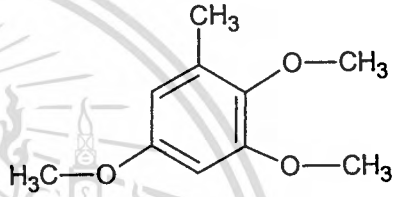
Dodecanotic acid	$C_{12}H_{24}O_2$	
4-hydroxy-3-methoxy-benzaldehyde	$C_8H_8O_3$	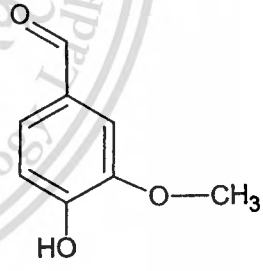
4-allyl-2,6-dimethoxyphenol	$C_{11}H_{14}O_3$	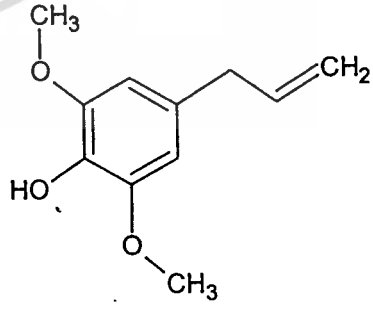
Phenol	C_6H_6O	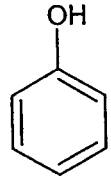

Table A.2 Composition of the raw wastewater

component	Chemical formula	Chemical structure
Pyridine	C_3H_6O	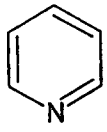
furan, 2,5-dimethyl	C_6H_8O	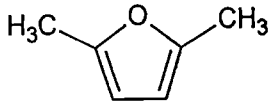
benzeneethanol	$C_8H_{10}O$	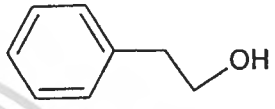
4-vinyl-2-methoxy-phenol	$C_9H_{10}O_2$	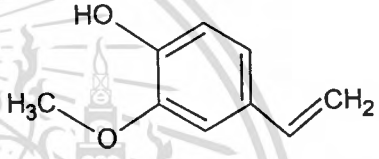
palmitic acid	$C_{16}H_{32}O_2$	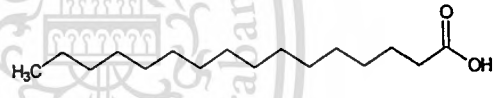
4-hydroxypyridine	C_5H_5NO	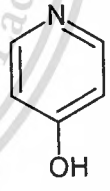
9-octadecenoic acid methyl ester	$C_{18}H_{34}O_2$	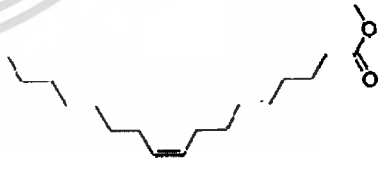
9,12-octadecadienoic acid methyl ester	$C_{18}H_{32}O_2$	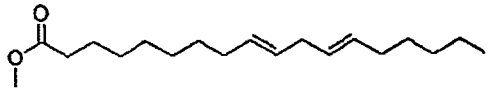

Table A.3 Component of the aqueous phase obtained from the pyrolysis of dried sludge at 773 K

component	Chemical formula	structure
Trimethylamine	C_3H_9NO	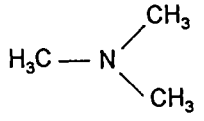
Methyl alcohol (methanol)	CH_4O	
Pyridine	C_5H_5N	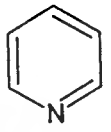
1-hydroxy-2-propanone	$C_3H_6O_2$	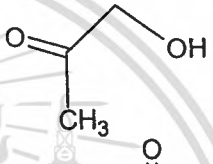
2-cyclopentanone	C_5H_8O	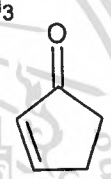
2-methyl-2-cyclopentanone	$C_6H_{11}O$	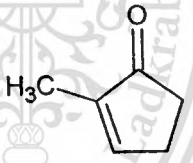
Acetic acid	$C_2H_4O_2$	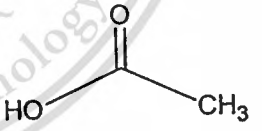
2-oxopropyl acetate	$C_5H_8O_3$	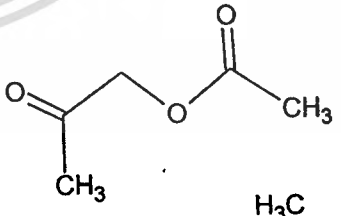
2,5-dimethyl-1,4-hexadiene	$C_{10}H_{18}$	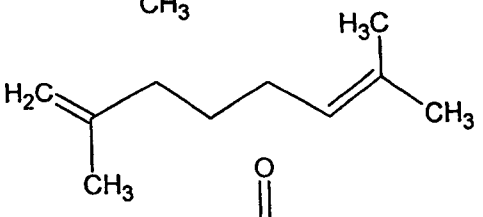
3-methyl-2-cyclopentenone	C_6H_8O	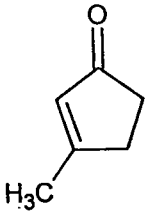

Table A.3 (Continue) Component of the aqueous phase obtained from the pyrolysis of dried sludge at 773 K

component	Chemical formula	structure
Propanoic acid	$C_3H_6O_2$	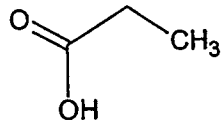
Butanoic acid	$C_4H_6O_2$	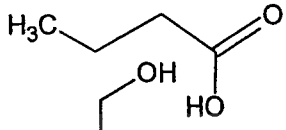
Furfuryl alcohol	$C_5H_6O_2$	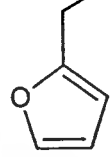
2(5H)-Furanone	$C_4H_4O_2$	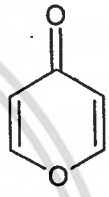
Acetamide	C_2H_5NO	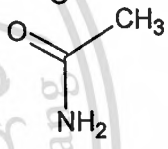
4-Pyrone	$C_5H_4O_2$	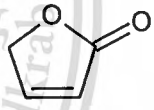
2-hydroxy-1-methylcyclopenten-3-one	$C_6H_8O_2$	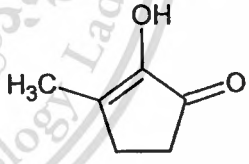
Phenol	C_6H_6O	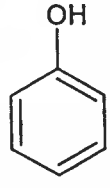
2-Pyrolidinone	C_4H_7NO	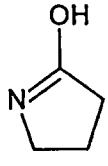
3-Pyridinol	C_5H_5NO	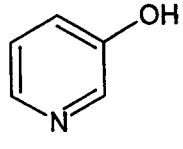

Table A.4 Component of the oil phase obtained from the pyrolysis of dried sludge at 773 K

component	Chemical formula	structure
Acetone	C_3H_6O	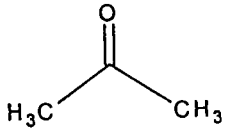
N-Pentadecane	$C_{15}H_{32}$	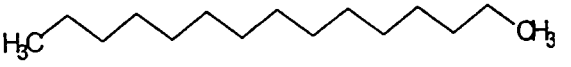
m-Cresol	C_7H_8O	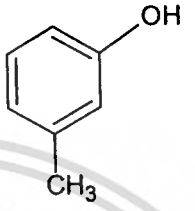
Phenol	C_6H_6O	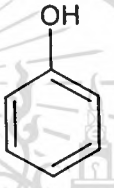
2-Tridecanone	$C_{13}H_{26}O$	
Myristonitrile	$C_{14}H_{27}N$	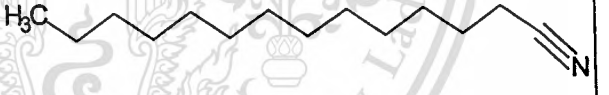

Appendix B

Raw data

Table B.1 Composition (%C) of liquid product obtained from the reaction of palm shell derived-oil over ZrO_2·Al·FeO_x at 623 K

component	W/F [h]			
	2	4	6	8
methanol	5.81	5.39	4.79	4.92
acetone	0.36	0.97	1.14	1.73
acetic acid	29.09	28.74	23.90	24.38
phenol	36.42	35.72	36.24	27.31
others in liquid	20.36	14.66	14.81	15.60
Gas	7.96	14.51	19.13	26.06
C balance (%C)	98	95	95	96

Table B.2 Composition (%C) of liquid product obtained from the reaction of palm shell derived-oil over ZrO_2·Al·FeO_x at 673 K

component	W/F [h]			
	2	4	8	12
methanol	5.47	4.12	4.38	0.23
acetone	0.50	1.42	5.72	0.88
acetic acid	27.60	20.76	14.85	0.19
phenol	34.88	30.14	25.00	3.86
others in liquid	24.29	15.19	11.61	0.86
Gas	12.74	32.48	42.82	94.21
C balance (%C)	98	96	95	94

Table B.3 Composition (%C) of liquid product obtained from the reaction of palm shell derived-oil over ZrO_2·Al·FeO_x at 723 K

component	W/F [h]		
	0.5	1	2
methanol	5.31	5.48	2.53
acetone	0.92	1.02	3.13
acetic acid	26.55	27.47	9.83
phenol	35.82	32.96	26.54
others in liquid	16.45	15.44	9.13
Gas	14.95	17.64	48.85
C balance (%C)	.96	98	94

Table B.4 Composition (%C) of aqueous phase of bio oil obtained from the reaction of dried sludge derived-oil over ZrO_2·FeO_x at 513 K

component	W/F [h]			
	2	4	6	10
methanol	5.04	4.89	5.59	7.67
acetone	2.14	4.13	6.05	6.37
acetic acid	21.98	13.35	3.87	0.53
others in liquid	36.93	23.81	6.06	4.21
gas	4.46	7.02	12.39	15.38
residue	39.45	46.81	66.03	65.84
C balance (%C)	105	107	100	99

Table B.5 Composition (%C) of aqueous phase of bio oil obtained from the reaction of dried sludge derived-oil over $ZrO_2 \cdot FeO_x$ at 583 K

component	W/F [h]			
	2	3	6	10
methanol	5.39	3.15	1.80	0.00
acetone	9.97	12.97	12.10	6.04
acetic acid	3.56	4.18	0.00	0.00
others in liquid	31.23	13.93	2.01	0.43
gas	18.16	24.90	23.08	31.00
residue	31.69	40.87	61.02	62.54
C balance (%C)	104	101	90	91

Table B.6 Composition (%C) of aqueous phase of bio oil obtained from the reaction of dried sludge derived-oil over $ZrO_2 \cdot FeO_x$ at 593 K

component	W/F [h]			
	1	2	4	6
methanol	5.24	6.89	0.00	0.00
acetone	7.91	24.71	17.63	17.49
acetic acid	12.10	2.27	1.31	0.00
others in liquid	38.03	26.11	1.73	1.23
gas	18.04	23.93	40.87	43.33
residue	18.67	16.10	38.47	37.95
C balance (%C)	104	95	100	92

Table B.7 Composition (%C) of aqueous phase of bio oil obtained from the reaction of dried sludge derived-oil over $ZrO_2 \cdot FeO_x$ at 643 K

component	W/F [h]		
	1	2	4
methanol	5.37	5.31	3.52
acetone	9.54	15.50	12.37
acetic acid	9.86	3.40	0.00
ethyl acetate	9.86	0.00	1.04
others in liquid	30.63	16.13	4.22
gas	11.56	17.65	23.56
residue	23.20	42.01	55.30
C balance (%C)	102	93	94

Table B.8 Composition (%C) of oil phase of bio oil obtained from the reaction of dried sludge derived-oil over $ZrO_2 \cdot FeO_x$ at 593 K

component	W/F [h]		
	4	6	8
acetone	2.65	5.15	2.51
phenol	7.21	11.74	5.99
m-cresol	0.65	1.23	2.52
others in liquid	40.95	30.56	31.96
gas	4.73	7.44	4.78
residue	43.81	43.88	52.23
C balance (%C)	107	95	106

Table B.9 Composition (%C) of oil phase of bio oil obtained from the reaction of dried sludge derived-oil over $ZrO_2 \cdot FeO_x$ at 693 K

component	W/F [h]		
	2	4	6
acetone	3.86	2.44	3.60
phenol	8.99	9.41	8.52
m-cresol	1.88	3.52	2.69
others in liquid	54.79	52.83	27.55
gas	11.05	13.37	19.20
residue	19.43	18.44	38.43
C balance (%C)	94	106	95

Table B.10 Composition (%C) of oil phase of bio oil obtained from the reaction of dried sludge derived-oil over $ZrO_2 \cdot FeO_x$ at 723 K

component	W/F [h]		
	0.25	0.5	1
acetone	1.42	1.83	1.98
phenol	19.17	7.89	6.81
m-cresol	4.25	3.20	1.97
others in liquid	52.73	61.11	56.37
gas	11.69	9.05	12.03
residue	10.75	16.93	20.84
C balance (%C)	105	98	100

Appendix C

C.1 Estimation of kinetic parameters for the decomposition of palm shell

A simple kinetics model was applied to estimate the kinetics parameters of palm shell decomposition according to the following reaction.

$$\text{Palm shell} \xrightarrow{k} \text{Char} + \text{Volatile} \tag{C.1}$$

The rate of decomposition which corresponds to the above reaction can be expressed by the eq. (C.2).

$$\frac{d\alpha}{dT} = kf(\alpha) \tag{C.2}$$

where

$$f(\alpha) = (1-\alpha)^n \tag{C.3}$$

$$k = A\exp(-E/RT) \tag{C.4}$$

The change in weight of sample was defined as the eq. (C.5).

$$\alpha = \frac{W_0 - W}{W_0 - W_\infty} \tag{C.5}$$

For constant heating rate, β ($\beta = dT/dt$), the eq. (C.2) can be re-arranged

$$\frac{d\alpha}{f(\alpha)} = \frac{k}{\beta}dt \tag{C.6}$$

The integration of eq. (C.6) is shown as below;

$$g(\alpha) = \int_0^\alpha \frac{d(\alpha)}{f(\alpha)} = \frac{A}{\beta}\int_{T_0}^{T} \exp(-E/RT)dt \tag{C.7}$$

Caots-Redfern method [59] was used to apply for integration of eq. (C.7)

$$\ln\left[\frac{g(\alpha)}{T^2}\right] = \ln\left\{\frac{AR}{\beta E}\left[1-\frac{2RT}{E}\right]\right\} - \frac{E}{RT} \tag{C.8}$$

Where

$$g(\alpha) = -\ln(1-\alpha) \qquad \text{if} \quad n = 1 \tag{C.9}$$

$$\text{And} \quad g(\alpha) = \frac{1-(1-\alpha)^{1-n}}{(1-n)} \qquad \text{if} \quad n \neq 1 \tag{C.10}$$

Therefore, a plot of $\ln\left[\frac{g(\alpha)}{T^2}\right]$ versus $\frac{1}{T}$ resulting in the straight line of slope

Activation energy (*E*a) and pre exponential factor (*A*) were calculated from the slope and interception.

C.2 Set of equation for estimation kinetic parameter of the reaction of DSO-aqueous

$$\frac{df_A}{d(W/F)} = -k_1 f_A - k_2 f_A - k_4 f_A \tag{C.11}$$

$$\frac{df_B}{d(W/F)} = -k_3 f_B + k_2 f_A \tag{C.12}$$

$$\frac{df_C}{d(W/F)} = -k_6 f_C \tag{C.13}$$

$$\frac{df_D}{d(W/F)} = -k_5 f_D - k_7 f_D \tag{C.14}$$

$$\frac{df_E}{d(W/F)} = k_1 f_A + k_3 f_B + k_5 f_D + k_6 f_C \tag{C.15}$$

$$\frac{df_F}{d(W/F)} = k_4 f_A + k_7 f_D \tag{C.16}$$

when : A : Acetic acid

B : Acetone

C : Methanol

D : Others

E : Gas

F : Coke

C.3 Set of equation for estimation kinetic parameter of the reaction of palm shell derived bio-oil

$$\frac{df_A}{d(W/F)} = -k_2 f_A + k_8 f_F \quad \text{(C.17)}$$

$$\frac{df_B}{d(W/F)} = -k_3 f_D - k_4 f_B \quad \text{(C.18)}$$

$$\frac{df_C}{d(W/F)} = -k_1 f_C \quad \text{(C.19)}$$

$$\frac{df_D}{d(W/F)} = k_2 f_A - k_3 f_D \quad \text{(C.20)}$$

$$\frac{df_E}{d(W/F)} = -k_7 f_E - k_5 f_E \quad \text{(C.21)}$$

$$\frac{df_F}{d(W/F)} = -k_6 f_F + k_5 f_E - k_8 f_F \quad \text{(C.22)}$$

$$\frac{df_G}{d(W/F)} = k_1 f_C + k_4 f_B + k_6 f_F + k_7 f_E \quad \text{(C.23)}$$

when : A : Acetic acid

B : Acetone

C : Methanol

D : Ethylacetate

E : Phenol

F : Others

G : gas

Appendix D

The energy calculation of the process for chemical production from POME

E1: Energy for dried sludge pyrolysis system

- Heat for pyrolysis of dried sludge

Data :	specific heat capacity of sample	1.212	$kJ \cdot kg^{-1} \cdot K^{-1}$
	Feed flow rate	4500	$kg \cdot h^{-1}$
	Heat capacity of N_2	1.1	$kJ \cdot kg^{-1} \cdot K^{-1}$
	Flow rate of N_2	150	$m^3 \cdot h^{-1}$
	Temperature raising	298 – 773	K

Energy balance

$$\frac{dE}{dt} = \sum_{i=1}^{n} F_{i0} H_{io} - \sum_{i=1}^{n} F_i H_i - \Delta H_{Rxn} + Q = 0$$

$$\sum_{i=1}^{n} F_{i0} H_{i0} - \sum_{i=1}^{n} F_i H_i = \dot{m} Cp \Delta T\big|_{N2} + \dot{m} Cp \Delta T\big|_{sample}$$

= 187.5 kg/h x 1.1 kJ/kg-K x (298-773) K + 4500 kg/h x 1.212 kJ/kg-K x (298-773) K

= -2.7×10^6 kJ/h

- Energy for condensation of condensable product

Data :	Heat capacity of gas product	2.3	$kJ \cdot kg^{-1} \cdot K^{-1}$
	Flow rate of carrier gas	150	$m^3 \cdot h^{-1}$
	Temperature of input cooling water	288	K
	Temperature of input cooling water	323	K

$$m_g c_g \Delta T = m_W c_W \Delta T$$

$$m_W = \frac{m_W c_g \Delta T}{c_W \Delta T}$$

= (139 x 2.3) x 485/(4.2 x 35)

= 1054 l/h

Water Pump with capacity 2.5 $m^3 \cdot h^{-1}$ (Power 0.11 kW)

Power of Refrigerator = 1000 W

Total power = 1100 W

Total energy for E1 = 2.76×10^6 kJ/h (767.7 kW)

E2: Energy for palm shell pyrolysis system

Similarly to E1, total energy for pyrolysis palm shell was calculated.

Total energy for E2 = 8.62×10^5 kJ/h

E3 : Energy generation from char (dried sludge)

Data :	Heating value of char	32.4	MJ/kg
	Productivity of char	1500	kg/h

Energy from char = 32.4 MJ/kg × 1500 kg/h = 4.86×10^7 kJ/h

E4 : Energy generation from gas (dried sludge)

Data :	Heating value of gas	18	kJ/kg
	Productivity of gas	930	kg/h

Energy from gas = 18 kJ/kg × 930 kg/h = 1.67×10^7 kJ/h

E5: Energy generation from char (palm shell)

Similarly to E3, energy generation from char (palm shell) was calculated.

Energy from char (palm shell) = 2.64×10^7 kJ/h

E6: Energy generation from gas (palm shell)

Similarly to E4, energy generation from gas (palm shell) was calculated.

Energy from gas (palm shell) = 4.7×10^6 kJ/h

E7 : Energy for upgrading of DSO - oil phase

- Reaction system

Data :		
	Feed flow rate	6,077.7 kg/h
	Heat capacity of water	Cp = 9.07R
	Latent heat of feed	2268 kJ/kg
	Heat capacity of steam	$Cp/R = 3.47+1.45x10^{-3}T+0.121T^{-2}$

$$Q_{total} = (Q_1 + Q_2 + Q_3)_R + Q_{N2}$$

$$\dot{Q} = \dot{m}\int_{298}^{373} CpdT + \dot{m}\int_{373}^{593} CpdT + \dot{m}L + \dot{m}\int_{298}^{593} CpdT\Big|_{N2}$$

$$= 1.83 \times 10^{7}\ \text{kJ/h}$$

- Cooling system

Water flow rate	1	m^3/h
Cp of N_2	1.1	kJ/kg-K
Cp of CO_2	1.17	kJ/kg-K
Temperature of input cooling water	288	K
Temperature of input cooling water	323	K

$$m_g c_g \Delta T = m_W c_W \Delta T$$

$$m_W = \frac{m_W c_g \Delta T}{c_W \Delta T}$$

$$= (139 \times 2.3) \times 485/(4.2 \times 35)$$

$$= 1054\ \text{l/h}$$

Water Pump with capacity 2.5 $m^3 \cdot h^{-1}$ (Power 0.11 kW)

Power of Refrigerator = 1000 W

Total power = 1100 W

- Regeneration system

Cp air	1.012	kJ/kg-K
Cp Fe_3O_4	0.652	kJ/kg-K

Energy for regeneration catalyst of oil phase

$$\dot{Q} = \dot{m} \int_{298}^{823} CpdT\Big|_{air} + \dot{m} \int_{298}^{823} CpdT\Big|_{cat}$$

$$= 9.37 \times 10^{4}\ (\text{air}) + 1.56 \times 10^{6}(\text{catalyst}) = 1.65 \times 10^{6}\ \text{kJ/h}$$

Energy for compressor = 3.6×10^{3} kJ/h

Total energy consumption for reaction of DSO - oil phase = 2×10^{7} kJ/h

E8 : Energy for upgrading of DSO - aqueous phase

Similarly to the oil phase, energy for reaction, cooling and regeneration systems were calculated.

Total energy consumption for reaction of DSO - aqueous = 9.1×10^{6} kJ/h

E9 : Energy for upgrading of palm shell derived bio-oil

Total energy consumption for reaction of palm shell derived bio-oil = 1.73×10^{7} kJ/h

Appendix E

Table E.1 The price of useful chemicals

chemicals	Prices (bath/kg)
Methanol	15
Acetone	46
Acetic acid	23
Phenol	57
m-cresol	107

Source : www.icispricing.com

Biography

Name	Ratanaporn Yuangsawad
Date of birth	11 August 1982
Place of birth	Chachoengsao, Thailand
Education	Bachelor of Engineering (Chemical Engineering), Department of Chemical Engineering, Faculty of Engineering, King Mongkut's Institute of Technology Ladkrabang, 2001-2005. Master of Engineering (Chemical Engineering), Department of Chemical Engineering, Faculty of Engineering, King Mongkut's Institute of Technology Ladkrabang, 2005-2007.

Academic works

Publications

- Duangkamol Na-Ranong, Ratanaporn Yuangsawad, Prakob Kitchaiya and Takashi Aida, "Application of Periodic Operation to Kinetic Study of NO-CO Reaction over Rh/Al_2O_3." *Chemical Engineering Journal*, 146 (2009) 275-286.
- Duangkamol Na-Ranong, Ratanporn Yuangsawad, Teruoki Tago, and Takao Masuda "Recovery of useful chemicals from oil palm shell-derived oil using zirconia supporting iron oxide catalysts" *Korean Journal of Chemical Engineering*, 25 (2008) 426-430.
- Takashi Aida, Takanori Yotsumoto, Kaori Kimura and Ratanaporn Yuangsawad "Effects of operating parameters on removal of low concentration carbon monoxide from hydrogen" *KAGAKU KOGAKU RONBUNSHU* , 34 (2008) 95-101.
- Ratanaporn Yuangsawad, Walirat Suksamai and Duangkamol Na-Ranong, "Improving of Zr-FeOx catalyst for recovering useful chemicals from palm shell derived bio-oil" *Thammasat International Journal of Science and Technology*, 13 (2009) 18-23
- รัตนาภร ยวงสวัสดิ์, ดวงกมล ณ ระนอง และ ประกอบ กิจไชยา, "จลนพลศาสตร์เบื้องต้นของปฏิกิริยาระหว่างคาร์บอนมอนอกไซด์กับไนตริกออกไซด์โดยใช้ตัวเร่งปฏิกิริยาโรเดียมบนอะลูมินา" *วิศวสารลาดกระบัง*, ปีที่ 22 ฉบับที่ 3, กันยายน 2548, หน้า 7- 12.

Conferences

- Ratanaporn Yuangsawad, Walairat Suksamai and Duangkamol Na-Ranong, "Catalytic decomposition of model compounds over zirconia supporting iron oxide catalyst" *RSCE-SOMCHE 2008 proceeding*, 779 – 785.
- Duangkamol Na-Ranong, Ratanaporn Yuangsawad, Teruoki Tago, and Takao Masuda, "Recovery of useful chemicals from oil palm shell-derived oil using zirconia supporting iron oxide catalysts" *The 11th Korea-Japan Symposium on Catalysis,* 21-23 May 2007, Seoul, Korea.
- Na-Ranong Duangkamol, Yuangsawad Ratanaporn, Fumoto Eri, Satoshi Funai, Teruoki Tago and Masuda Takao, "Recovery of useful chemicals from palm wastes using iron oxide based catalysts" *The 99th Symposium on Catalysis*, 28 – 29 April 2007, Kobe, Japan
- Ratanaporn Yuangsawad, Duangkamol Na-Ranong, Walairat Suksamai, Prakob Kitchaiya, Teruoki Tago and Takao Masuda "Improving of Zr-FeO_x Catalyst for Recovering Useful Chemicals from Palm Shell Derived Bio-Oil" *The 1nd Thammasat University International Conference on Chemical, Environmental and Energy Engineering*, 4 March 2008, Bangkok, Thailand.
- Ratanaporn Yuangsawad, Walairat Suksamai and Duangkamol Na-Ranong, "The possibility of the useful chemicals production from sewage sludge derived oil" *The 2nd Thammasat University International Conference on Chemical, Environmental and Energy Engineering*, 3 – 4 March 2009, Bangkok, Thailand.
- Makoto Takahashi, Duangkamol Na-Ranong, Ratanaporn Yuangsawad and Takashi Aida "Cyclic concentration forcing of NO–CO–O2 reaction over supported noble metal catalysts" *5th International conference on unsteady-state processes in catalysis (USPC-5)*, 22 -25 November 2006, Osaka, Japan.
- Takanori Yotsumoto, Kaori Kimura, Ratanaporn Yuangsawad and Takashi Aida, "Effect of H2 on CO oxidation over Pt/Al2O3 in SMB reactor" *5th International conference on unsteady-state processes in catalysis (USPC-5)*, 22 -25 November 2006, Osaka, Japan.
- Kaori Kimura, Takanori Yotsumoto, Ratanaporn Yuangsawad and Takashi Aida, "Transient Response Analysis for CO Oxidation over Pt/Al2O3 at Low Temperature" *5th International conference on unsteady-state processes in catalysis (USPC-5)*, 22 -25 November 2006, Osaka, Japan.

- Maneewan Tonpoo, Manita Prasongjareon, Ratanaporn Yuangsawad and Duangkamol Na-Ranong, "Recovery of dl-limonene from used tires by pyrolysis" *The 19th Thailand Chemical Engineering and Applied Chemistry Conference*, 26 – 27 October 2009, Kanjanaburi, Thailand.
- Ratanaporn Yuangsawad and Duangkamol Na-Ranong, "Kinetics decomposition of model compounds presented in biomass derived oil over $ZrO_2 \cdot FeO_x$" *The 18th Thailand Chemical Engineering and Applied Chemistry Conference*, 20- 21 October 2008, Chonburi, Thailand.
- รัตนาภร ยวงสวัสดิ์ และ ดวงกมล ณ ระนอง "การปรับปรุงคุณภาพผลิตภัณฑ์เหลวที่ได้จากการไพโรไลซิสกะลาปาล์มน้ำมันโดยใช้ตัวเร่งปฏิกิริยา Zr-FeO_x" *การประชุมวิชาการวิศวกรรมเคมีและเคมีประยุกต์แห่งประเทศไทย ครั้งที่ 17*, 29 – 30 ตุลาคม 2550, เชียงใหม่, ประเทศไทย.
- รัตนาภร ยวงสวัสดิ์, ดวงกมล ณ ระนอง, Takanori Yotsumoto, Kaori Kimura and Takashi Aida, "ปฏิกิริยาออกซิเดชันของคาร์บอนมอนอกไซด์โดยใช้เครื่องปฏิกรณ์แบบเบดเคลื่อนที่จำลอง" *การประชุมวิชาการวิศวกรรมเคมีและเคมีประยุกต์แห่งประเทศไทย ครั้งที่ 16*, 26 – 27 ตุลาคม 2549, กรุงเทพฯ, ประเทศไทย.